SCHIFFMILLER, RICHARD

RESONANCE RAMAN STUDIES OF BACTERIORHODOPSIN ANALOGS AND RELATED SYSTEMS

City University of New York PH.D. 1980

RESONANCE RAMAN STUDIES OF BACTERIORHODOPSIN ANALOGS AND RELATED SYSTEMS

by

RICHARD SCHIFFMILLER

A dissertation submitted to the Graduate Faculty in Physics in partial fulfillment of the requirements for the degree of Doctor of Philosophy,
The City University of New York

1980

The manuscript has been read and accepted for the Graduate Faculty in Physics in satisfaction of the dissertation requirement for the degree of Doctor of Philosophy.

Sept. 8, 1980
date

Robert Callender
Chairman of Examining Committee

Sept 8, 1980
date

Francis Martinez
Executive Officer

Supervisory Committee

The City University of New York

Abstract

RESONANCE RAMAN STUDIES OF BACTERIORHODOPSIN ANALOGS AND RELATED SYSTEMS

by

Richard Schiffmiller

Adviser: Professor Robert H. Callender

In order to better understand the protein-chromophore interactions in bacteriorhodopsin, five retinal analogs - 10,14-dimethyl, 14-methyl, 10-methyl, 5,6-dihydro, and 13-desmethyl - have been regenerated with the opsin apoprotein from the purple membrane of Halobacterium Halobium to form artificial bacteriorhodopsin pigments. These were studied spectroscopically at liquid nitrogen temperatures using resonance Raman scattering techniques. A line appearing at 1010 cm^{-1} is assigned to a methyl vibration, while the 1300 cm^{-1} vibration is assigned to an interaction mode of adjacent methyl groups. The color of the analog pigments is shown to be due to the degree of π-electron delocalization on the polyene chain of the retinal chromophore. Both 10,14-dimethyl and 14-methyl bacteriorhodopsin are shown to have their chromophores linked to the protein by unproton-

ated Schiff bases, unlike the other analogs, and their blue-shifted absorption maxima are explained in terms of that observation. It is found that the shift in frequency of the C=C stretching vibration correlates linearly with the absorption maxima of the various analogs, as predicted by π-electron delocalization theory. Moreover, for the first time, the frequency of the C=N stretching vibration is correlated with the extent of delocalization in each analog.

The environment-sensitive lines of the 5,6-dihydro chromophore are shown to be affected less by the protein binding site than those of the other retinals, thus supporting a model which suggests the existence of a counter-ion in the bacterio-opsin protein near the chromophore's ionone ring.

Deuteration of the analogs with deuterium oxide reveals a very small shift in the 13-desmethyl $C=NH^+$ frequency, and possible implications of this are discussed.

The double beam pump/probe technique is used to obtain the resonance Raman spectrum of the first intermediate of the bacteriorhodopsin photocycle, known as "K". From the significant differences between the fingerprint region vibrations of bacteriorhodopsin and K, we conclude that a trans-cis isomerization has occurred in the photoinduced formation of K. Furthermore, the deuterated spectrum of K confirms that the Schiff base of K is protonated, which

argues against a model that proposes that proton tunnelling is the primary event in bacteriorhodopsin photoexcitation.

Finally, resonance Raman spectra of a homologous series of cyanine dyes, diQ - C_n - (2m+1), are presented. These dyes represent an extreme degree of π-electron delocalization and the lack of a shift in the key lines in their spectra with increasing polyene chain length confirms that a change in delocalization is responsible for Raman line shifts in polyene systems.

ACKNOWLEDGEMENTS

I would like to express my deepest gratitude and appreciation to Professor Robert Callender for his guidance, inspiration, patience, and scholarship.

This work would not have been possible without the invaluable contributions made by my colleagues, Doctors Bea Aton, Apostolos Doukas, David Narva, Jayanti Pande, and Tatsuo Suzuki.

My parents and brothers have always been a source of support and encouragement to me and I thank them for it.

Finally, I would like to thank my wife, Shari, and my daughters, Chana and Bracha, for their patience and tolerance over the years.

TABLE OF CONTENTS

LIST OF TABLES

LIST OF FIGURES

INTRODUCTION

Resonance Raman spectroscopy is a valuable investigative tool for examining the vibrational and electronic structure of molecules. In the Raman effect, incident monochromatic radiation (usually produced by a laser) on a sample is scattered and its frequency is shifted by amounts corresponding to the normal mode frequencies of the material. Thus, the technique is complementary to infrared absorption in that it measures vibrational, torsional, and bending frequencies. However, it has some important advantages:

(1) measurements of sample normal modes corresponding to frequencies of 5 cm^{-1} to 4000 cm^{-1} are possible with one apparatus and at the same time;

(2) more information on selection rules is available from the experiment (in isotropic material, symmetric and asymmetric modes can be distinguished by depolarization rules); and

(3) water has a small Raman cross-section and therefore generally does not give a troublesome background spectrum.

In a resonance Raman experiment, the frequency of the laser that generates the Raman scattering is selected to be in or near the electronic absorption band of a chromophoric group. This results in a resonance enhancement of the scattering from just those vibrations that are coupled

to the electronic excitation. Resonance Raman spectroscopy is therefore particularly well-suited for studies of biological macromolecules since (1) sample concentrations can be as low as 10^{-6} M, (2) sample volumes as small as a few microliters are practical, and (3) scattering from the non-resonant parts of the polypeptide or from surrounding liquids will not complicate the spectrum, since the Raman cross-section for the molecule in resonance with the laser beam is several orders of magnitude larger than the cross-section for any molecules that are off resonance (Callender and Honig, 1977). Thus, complicated preparation procedures are not needed. Indeed, in situ experiments are possible.

In recent years, resonance Raman studies on visual pigments and bacteriorhodopsin have been particularly interesting and productive. Theoretical studies have been undertaken in an attempt to interpret the complicated Raman spectra in the hope of better understanding the visual photochemistry which the spectra represent. In this work, we present the resonance Raman spectra of a series of organically synthesized analogs of retinal, the light-sensitive moiety (chromophore) found in the visual pigments and bacteriorhodopsin, both in solution (as aldehydes and protonated Schiff bases) and regenerated with the apoprotein bacterio-opsin (thereby forming a pigment). By a careful analysis of the line patterns, we will propose

several line assignments and discuss possible explanations of the relative frequencies of various vibrations. We have also been able to regenerate an analog chromophore with the apoprotein opsin, found in the retina of all vertebrates, thereby forming an artificial visual pigment. The spectrum of this compound sheds some light on the controversial primary event in visual excitation. In addition, the resonance Raman spectrum of the photoproduct formed within picoseconds of irradiation of bacteriorhodopsin, known as the "K" intermediate, is presented here and analyzed. Finally, included in this work are Raman studies of a homologous series of cyanine dyes whose linear conjugation system provides insight into the structure and characteristics of the polyene chains in the visual pigments.

The first section of this work includes (a) a short description of the Raman and resonance Raman effects, (b) a review of the purple membrane protein system from the bacterium Halobacterium halobium and its physiological role as a photosynthetic pigment, (c) a review of the bovine rhodopsin system and a discussion of the primary event in vision, (d) a synopsis of the information obtained from studies of analogs of retinal, and (e) a discussion of cyanine dyes and the relationship between their structure and that of the visual pigments.

In the second section, we analyze the photolability problems inherent in these studies and the techniques used

to overcome them. A detailed description of the sample preparations and purifications and the experimental conditions of the Raman measurements is also included. The concluding part contains the data taken and a discussion of the information contained in those spectra.

SECTION I

Raman Effect

When monochromatic radiation of frequency ν_0 is scattered by a molecule, most of the photons emerge from the scattering site with the same energy that they had upon entering. This effect, known as Rayleigh scattering, is due to the molecular electrons being set into oscillation by the light relative to the heavier nucleus, thereby inducing an oscillating dipole in the molecule. The polarized molecule then scatters photons in all directions at the laser frequency.

A second, much weaker, phenomenon occurs simultaneously with the elastic scattering just described. It was first seen experimentally by Raman and Krishnan in 1928 but had been predicted by Smekal five years earlier (Raman and Krishnan, 1928; Smekal, 1923). In this Raman effect, the photon either loses energy to (Stokes scattering) or gains energy from (anti-Stokes scattering) the molecule. The energy of scattered light is either $h\nu_o - h\nu_1$ or $h\nu_o + h\nu_1$ where $h\nu_1$ corresponds to the vibrational energy of a particular mode of the molecule. This type of scattering process arises from the fact that the electrons are coupled to the nuclei as well as to the incident laser field so that the vibrational frequency of the nuclei is superimposed upon the electronic motions. Thus the molecular electrons are oscillating to some degree at

the laser frequency plus and minus the vibrational frequencies, again creating an oscillating dipole moment. The Stokes bands of a Raman spectrum, although roughly 10^{-5} - 10^{-7} as intense as a Rayleigh line, are considerably stronger than anti-Stokes bands, owing to the greater population of molecules in the ground vibrational state as compared to the excited level (Boltzmann distribution).

We can see then that the Raman effect is complementary to infrared absorption spectroscopy, in that both measure molecular vibrational frequencies. However, the intensity of an infrared band is proportional to the change in the dipole moment as atoms pass through their equilibrium positions, whereas Raman intensity is governed by the change in molecular polarizability as atoms pass through their equilibrium positions.

When the incident radiation lies on or near a particular absorption band of the molecule, the Raman scattered light increases considerably in intensity. This resonance Raman effect, as well as the off-resonance effect, have been the subject of a considerable amount of theoretical work in the past 50 years.

In 1934, Placzek published a semi-classical analysis of the Raman effect, treating the molecule quantum mechanically and the radiation field classically (Placzek, 1934;

see also Van Vleck, 1929; Albrecht, 1961; Tang and Albrecht, 1970; Peticolas et al., 1970). The matrix elements of the scattering tensor for the transition from the m^{th} to the n^{th} vibrational level are given by

$$(\alpha_{\rho\sigma})_{mn} = \frac{1}{h} \sum_{r} \left[\frac{\langle r|M_\rho|n\rangle\langle m|M_\sigma|r\rangle}{\nu_{rm} - \nu_L} + \frac{\langle m|M_\rho|r\rangle\langle r|M_\sigma|n\rangle}{\nu_{rn} + \nu_L} \right] \quad (1)$$

where h is Planck's constant, the subscripts ρ and σ refer to a two-dimensional cartesian coordinate system fixed in the molecule, and m, r, and n are the initial, intermediate, and final energy states, respectively. M_ρ and M_σ are the scalar components of the dipole moments defined by $M = \sum_j e_j \vec{r}_j$, where $\vec{r}_j$ is the position vector of the j^{th} electron. ν_L is the laser frequency and $\nu_{rm} = (E_r - E_m)/h$. The summation is carried out over all intermediate vibrational states in all electronic manifolds. Figure 1 gives a schematic drawing of the excitation of the electrons to an excited state. It is important to keep in mind, however, that the transition to a virtual state need not conform to energy conservation restrictions.

The total intensity of the light scattered through a solid angle of 4π steradians, after averaging over all molecular orientations, is given by

Figure 1

A schematic drawing of the production of a Stokes scattered Raman line. The laser frequency is ν_L. $|m\rangle$, $|n\rangle$ and $|r\rangle$ represent the initial, final, and an intermediate state, respectively. Dashed lines indicate virtual transitions.

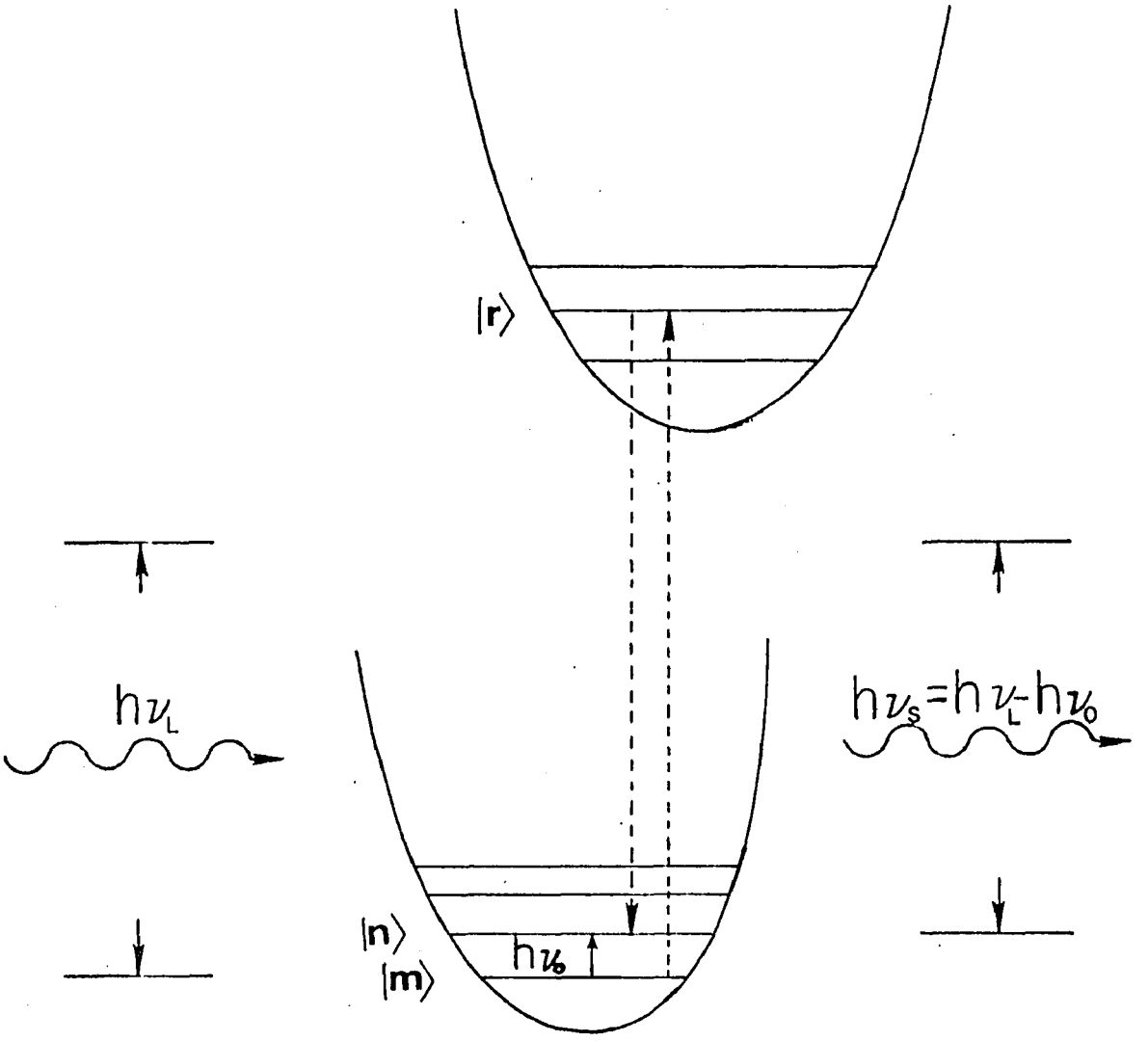
|r⟩
hν_L
hν_s=hν_L-hν_0
|n⟩
|m⟩
hν_0

$$I_{mn} = \frac{2^7 \pi^5}{3^2 c^4} I_o \left(\nu_L + \nu_{mn}\right)^4 \sum_{\rho,\sigma} \left|\alpha_{\rho\sigma}\right|^2_{mn} \qquad (2)$$

The quartic frequency term dominates the intensity dispersion when the incident radiation is far from an electronic absorption energy (off-resonance). As the laser frequency approaches the energy of an absorption transition however, the $1/(\nu_{rm} - \nu_L)$ term in the polarizability expression becomes most important. In that case, the summation over all electronic states can be dropped and the sum over the vibrational states is restricted to the manifold of the electronic state in resonance with the laser. A term related to the bandwidth of the energy level is usually added to the denominator to keep the polarizability tensor finite. Equation 1 then becomes

$$\left(\alpha_{\rho\sigma}\right)_{mn} = \frac{1}{h} \sum_K \frac{\langle K|M_\rho|n\rangle\langle m|M_\sigma|K\rangle}{\nu_{Km} - \nu_L + i\Gamma} \qquad (3)$$

where Γ is the bandwidth and K is some vibrational level.

The Zeroth-order Born-Oppenheimer approximation is now introduced. Every state is separated into a vibrational part, depending upon the nuclear coordinates (Q) only, and an electronic part, depending upon electronic (ξ) and nuclear coordinates. Our notation becomes

$$|m\rangle \equiv |g\rangle|g i\rangle \; ; \quad |n\rangle \equiv |g\rangle|g j\rangle \; ; \; |r\rangle \equiv |e\rangle|e v\rangle \qquad (4)$$

where g is the ground electronic state, e is some excited electronic state, and i, j, and v are the initial, final, and virtual vibrational states. Equation 1 now becomes

$$(\alpha_{\rho\sigma})_{gi,gj} = \frac{1}{h}\left[\frac{\langle ev|\langle e|M_\rho|g\rangle|gj\rangle\langle gi|\langle g|M_\sigma|e\rangle|ev\rangle}{\nu_{ev,gi} - \nu_L}\right.$$

$$\left. + \frac{\langle gi|\langle g|M_\rho|e\rangle|ev\rangle\langle ev|\langle e|M_\sigma|g\rangle|gj\rangle}{\nu_{ev,gj} + \nu_L}\right] \qquad (5)$$

The integration of the nuclear coordinates can be performed if the Q dependence of the electronic transition moment were determined. Two methods provide this information. The first is by expanding the electronic transition moment in a Taylor series about the equilibrium geometry as a function of the normal coordinates Q:

$$\langle e|M_\rho|g\rangle \equiv (M_\rho)_{eg} = (M_\rho)^\circ_{eg} + \sum_\alpha Q_\alpha \frac{\partial}{\partial Q_\alpha}(M_\rho)^\circ_{eg} + \ldots \qquad (6)$$

where the superscript $^\circ$ means evaluation at the equilibrium nuclear configuration and Q_α is the displacement of the α^{th} normal mode.

The second technique involves expanding by use of first order perturbation theory. If H is the electronic Hamiltonian, then $(\partial H/\partial Q_\alpha)\, Q_\alpha$ is the perturbing operator. This Herzberg-Teller expansion of the transition moment yields

$$(M_\rho)_{eg} = (M_\rho)^\circ_{eg} + \sum_{\substack{s \\ s \neq e}} \lambda_{es}(Q)\,(M_\rho)^\circ_{gs} \tag{7}$$

where $\lambda_{es}(Q) = \sum_\alpha \frac{Q_\alpha \cdot \epsilon^\alpha_{es}}{E_e - E_s}$. ϵ^α_{es} is a perturbation energy per unit displacement of the α^{th} mode due to the mixing of equilibrium configuration electronic states $|e\rangle$ and $|s\rangle$ under vibrational perturbation. By inserting (7) into (5), we arrive at Albrecht's expression for the polarizability tensor.

$$(\alpha_{\rho\sigma})_{gi,gj} = A + B + C \tag{8}$$

where

$$A = \frac{1}{h} \sum_{e,v} \left(\frac{1}{\nu_{ev,gi} - \nu_L} + \frac{1}{\nu_{ev,gj} + \nu_L} \right) \left[(M_\rho)^\circ_{ge} (M_\sigma)^\circ_{ge} \times \langle gi|ev\rangle\langle ev|gj\rangle \right] \tag{8a}$$

$$B = \frac{1}{h} \left(\frac{1}{\nu_{ev,gi} - \nu_L} \right) \sum_{\substack{s,\alpha \\ s \neq e}} \frac{\epsilon^\alpha_{es}}{E_e - E_s} \left[(M_\rho)^\circ_{ge} (M_\sigma)^\circ_{gs} \langle gj|ev\rangle \times \langle ev|Q_\alpha|gi\rangle + (M_\sigma)^\circ_{ge} (M_\rho)^\circ_{gs} \langle gi|ev\rangle\langle ev|Q_\alpha|gj\rangle \right] \tag{8b}$$

$$C = \frac{1}{h} \sum_{e,v} \left(\frac{1}{\nu_{ev,gj} + \nu_L} \right) \sum_{s,\alpha} \frac{\epsilon^{\alpha}_{es}}{E_e - E_s} \left[(M_g)^{\circ}_{ge} (M_\sigma)^{\circ}_{gs} \langle gi | ev \rangle \right.$$

$$\left. \times \langle ev | Q_\alpha | gj \rangle + (M_\sigma)^{\circ}_{ge} (M_g)^{\circ}_{gs} \langle gj | ev \rangle \langle ev | Q_\alpha | gi \rangle \right] \qquad (8c)$$

In the resonance case, Tang and Albrecht (1970) have shown that an expansion of the A term in powers of $\frac{\nu_{ev,gi} - \nu_{eg}}{\nu_{eg} - \nu_L}$ results in the following approximation:

$$A \approx \left(\frac{2}{h^2} \right) (M_g)^{\circ}_{ge} (M_\sigma)^{\circ}_{ge} \langle e^{\circ} | \epsilon_\alpha | e^{\circ} \rangle \langle i | Q_\alpha | j \rangle$$

$$\times \left(\nu_e^2 + \nu_L^2 \right) / \left(\nu_e^2 - \nu_o^2 \right)^2 \qquad (9a)$$

A similar expansion was performed for the B term, yielding:

$$B \approx \frac{4}{h^2} \sum_{s} \sum_{\alpha} (M_g)^{\circ}_{ge} (M_\sigma)^{\circ}_{gs} \langle i | Q_\alpha | j \rangle \langle e | \epsilon_\alpha | s \rangle$$

$$\times \frac{\nu_e \nu_s + \nu_o^2}{\left(\nu_e^2 - \nu_s^2 \right) \left(\nu_e^2 - \nu_L^2 \right)} \qquad (9b)$$

Using the frequency dependencies, Doukas, Aton and Callender measured the relative contributions of these terms in the resonance case for all-trans retinal and they found that the A term clearly dominates (Doukas et al., 1978a). It is reasonable to expect the same result for the visual pigments. Previously, Inagaki et al. (1974) reached the same conclusion for β-carotene.

As can be seen from equation (8a), the contribution of the A term to the Raman intensity will depend upon the vibrational overlap integrals (known as Franck-Condon factors) in the numerator of the equation. A vibrational mode will be strongly enhanced if the distortion of the molecule in the excited electronic state corresponds closely with the vibrational coordinates. Hence, vibrations will be resonantly enhanced if electronic excitation alters the bonding of nuclei whose motions are important in that vibrational mode.

Analysis of the vibrational modes that appear in a Raman spectrum can be handled in several ways. One method is to directly evaluate the Franck-Condon factors between the ground and excited states, and this technique has been considered in some detail by Karplus and Warshel (Warshel and Karplus, 1972, 1973; Warshel, 1973).

A second approach is based on finding common features among some bonds or groups in the Raman spectra of different molecules (for example, see Callender and Honig, 1977). There is, however, a caveat: the frequency of a particular group or bond vibration may be influenced by coupling with nearby modes and so comparisons of groups in different environments must be done carefully. In this work, comparisons among the Raman spectra of model chromophores, the visual pigment analogs, and the visual pigments have been made.

Bacteriorhodopsin

Halobacterium halobium is one of a number of halophilic bacteria that enjoys life in a highly saline environment (for a general review, see Stoeckenius et al., 1979; Henderson, 1977). When the oxygen supply to the organism is cut off, it synthesizes purple patches on its normally red membrane. By lowering the ambient salt concentration from 4.3 M (the growth concentration), one can fragment the cells and then isolate the purple membranes by sucrose density gradient centrifugation. The detailed procedure for preparing H. halobium and separating out the purple membrane is now standard (Oesterhelt and Stoeckenius, 1974; Becher and Cassim, 1975).

The bacterium itself is rod-shaped, about .5 μm in diameter and 5 μm long. It grows optimally in a 25% (wt/vol) salt solution (Larsen, 1967). The purple patches can account for up to 50% of its red membrane under anaerobic conditions. Light stimulates the synthesis of these blotches (Stoeckenius and Kunau, 1968). X-ray studies have shown that the purple membrane is a locally differentiated but nevertheless contiguous part of the cell membrane (Blaurock and Stoeckenius, 1971). The red color of the oxygenated bacterium is due to the presence of C_{50} carotenoid bacterioruberin, which probably functions as a shield against the ultraviolet rays of the sun (Kelly and Liaaen-Jensen, 1967). The purple color of the synthesized patches

is caused by a retinal chromophore linked to the membrane's polypeptide structure (Oesterhelt and Stoeckenius, 1971). Because a similar chromophore is found in the visual pigment rhodopsin, the purple membrane has acquired the name bacteriorhodopsin.

Through a series of experiments using freeze-fracture techniques, X-ray diffraction and electron microscopy studies, Stoeckenius, Henderson and co-workers have characterized in detail the structure and orientation of the protein in bacteriorhodopsin (Blaurock and Stoeckenius, 1971; Henderson, 1975). Each purple membrane patch consists of a rigid, highly ordered, two-dimensional hexagonal lattice structure of about 10^5 molecules with a 63-Å cell dimension. The protein molecules are arranged as trimers clustered about a symmetry axis in the unit cell. A hexagonal arrangement is considered to be the most efficient way to closely pack helical molecules with regard to space. The protein molecules (termed bacterio-opsin) consist of 248 amino acids with a molecular weight of 26,000 daltons and are arranged in 7 α-helical segments that span the width of the membrane. Four of the helices are virtually perpendicular to the plane of the membrane, while three are tilted at angles no more than 27° from the perpendicular position (Henderson and Unwin, 1975). This latter fact may make the membrane more permeable to ions. Recently, the amino acid sequence of bacterio-opsin

has been determined, with minor variations between published reports (Ovchinnikov et al., 1977, 1979; Khorana et al., 1979).

Retinal (vitamin A) is the chromophore in bacteriorhodopsin. It is covalently linked via a Schiff base to the ϵ-amino group of a lysine residue (Oesterhelt and Stoeckenius, 1971). Resonance Raman studies have indicated that the Schiff base is protonated (Lewis et al., 1974; Mendelsohn, 1976). The sequence data of Ovchinnikov et al. identify the lysine as lys 41 and place the Schiff base in a non-helical loop occurring 1.5 turns before the end of the second transmembrane segment counting from the NH_2 end (ouside) of the polypeptide chain (Ovchinnikov et al., 1979).

The retinal chromophore exists in two forms in the purple membrane, as evidenced from absorption spectra. The bacteriorhodopsin light-adapted form (BR^{LA}), absorbing at 568 nm, and the dark-adapted form (BR^{DA}, λmax = 558nm) have been the subject of a good deal of experiments aimed at determining their respective conformations (Oesterhelt and Hess, 1973; Oesterhelt et al., 1973; Pettei et al., 1977; Aton et al., 1977, 1979). Chemical extraction studies as well as resonance Raman work and other non-destructive spectroscopic techniques indicate that BR^{LA} contains all-trans retinal as its chromophoric unit, while

BR^{DA} contains a 1:1 mixture of all-trans and 13-cis retinal (Sperling et al., 1977; Ohno et al., 1977; Maeda et al., 1977). These isomeric structures of retinal are shown in Figure 2.

When the light adapted form of purple membrane absorbs a photon, it goes through a series of intermediate stages before cyclically returning to its original form. See Figure 3. The first product of this photoreaction, called K, is formed on a picosecond time scale photochemically, while the whole cycle is completed thermally in about 10 msec. (Lozier et al., 1975). Associated with the absorption of light is the pumping of a proton across the cell membrane which is used in ATP phosphorylation and for other energy related cell functions (Oesterhelt and Stoeckenius, 1973; Oesterhelt, 1972; Danon and Stoeckenius, 1974). Most biological pumps are multicomponent systems with complex structure (Stoeckenius et al., 1979). Bacteriorhodopsin is a notable exception. A detailed understanding of the structure of the intermediates in the BR cycle would contribute a great deal towards the understanding of membraneous pumps.

Oesterhelt and Stoeckenius (1973) showed that one of the thermal intermediates of the light-driven cycle is stable in ether and salt or at low temperature. Now known as the "M" intermediate, it has been confirmed that M is unprotonated (Aton et al., 1977), and this fact accounts

Figure 2

Conformations of various isomers of retinal (X=O), its Schiff base (X=N), and its protonated Schiff base ($X=NH^+$). (a) all-trans; (b) 13-cis; (c) 9-cis; (d) 11-cis, 12-s-trans; (e) 11-cis, 12-s-cis. Arrows indicate flexible bonds whose equilibrium configuration is not planar (from Callender and Honig, 1977).

a.

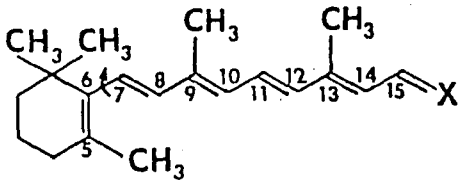
CH3 CH3
CH3
CH3
6
7
8
9
10
11
12
13
14
15
X
5
CH3

b.

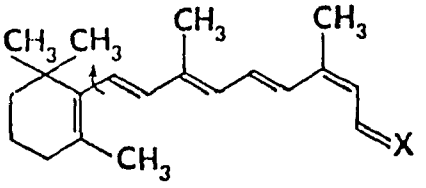
CH3 CH3
CH3
CH3
X
CH3

c.

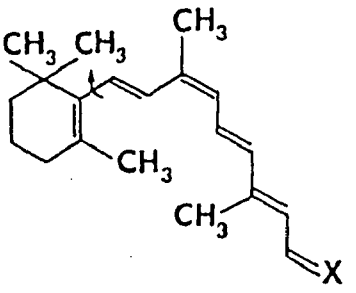
CH3 CH3
CH3
CH3
CH3
X

d.

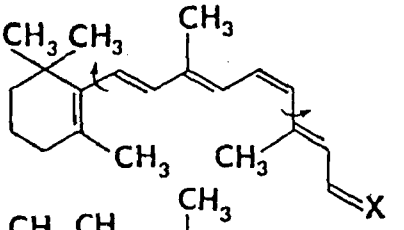
CH3 CH3
CH3
CH3
CH3
X

e.

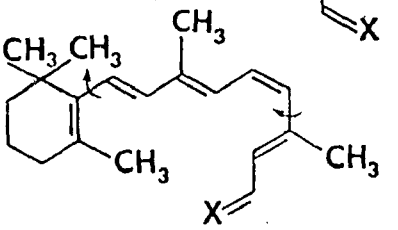
CH3 CH3
CH3
CH3
CH3
X

Figure 3

Photoreaction cycle of the purple membrane protein of Halobacterium Halobium. Bold face numbers give the absorption maxima of the intermediates. Wavy lines indicate photoreactions, solid lines indicate thermal (dark) reactions. Times of formation of the intermediates are given along the arrows.

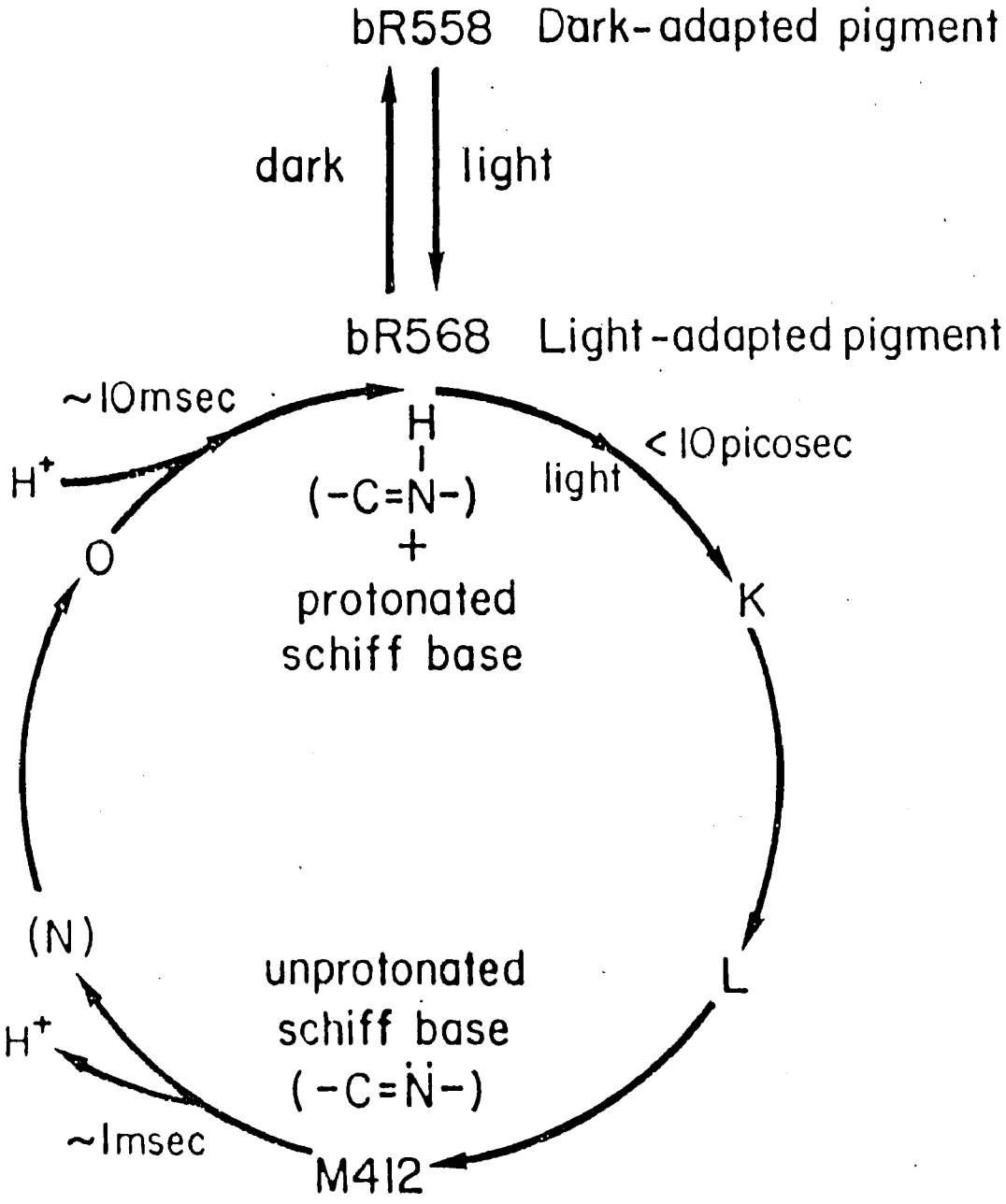
bR558 Dark-adapted pigment
dark
light
bR568 Light-adapted pigment
~10msec
H+
O
H
(-C=N-)
+
protonated
schiff base
light
< 10picosec
K
L
(N)
H+
unprotonated
schiff base
(-C=N-)
~1msec
M412

for the large blue-shift in its absorption (λmax=412 nm). After being warmed up, the unprotonated species cycles back to the protonated parent pigment form, giving evidence of proton release and uptake in the photocycle of bacteriorhodopsin (Lozier et al., 1975; Oesterhelt and Stoeckenius, 1973). The intermediate immediately preceding M in the photocycle is L_{550} and investigation by resonance Raman techniques has shown that its Schiff base is protonated (Marcus and Lewis, 1977; Campion et al., 1977; Narva and Callender, 1980).

In order to determine the isomeric conformation of L and M, the chromophore was chemically extracted using a variety of solvents and then analyzed by high performance liquid chromotography (Pettei et al., 1977; Tsuda and Ebrey, 1980; Tsuda et al., 1980). The results were that M contains 13-cis retinal as a chromophore. The extinction coefficient of L is not known precisely enough to deconvolute the components of the chromophore extracted from a mixture of L, M, and BR^{LA}, but Tsuda et al. suggest that L also has only 13-cis retinal as its chromophore. This would imply that a trans-cis isomerization occurred between the initial incidence of radiation and the formation of L. Resonance Raman data tend to support the conclusion of Tsuda et al. Additional evidence for major conformational changes during the photocycle has recently been found through a detailed study of volumetric fluctuations

in bacteriorhodopsin (Parson and Ort, 1980) and from a thermodynamic analysis of the isomerization model for the pump cycle (Schulten and Schulten, 1980). The intermediates L and M have been observed to revert back to BR^{LA} upon stimulation by light (Hurley et al., 1978; Honig and Ottolenghi, 1980), indicating another branch of the photocycle where photoisomerization plays a major role.

The primary event in the bacteriorhodopsin photocycle, leading to the formation of K, has been a subject of great controversy in recent years. Various models have been proposed (see the next section), and the ones receiving the most attention have been the proton translocation model (Applebury et al., 1978) and the trans-cis isomerization model (Rosenfeld et al., 1977; Hurley et al., 1977; Honig et al., 1979). Applebury et al. (1978) have measured the rise time of K from precursor (called J) as being 11 psec and have observed this time to slow down to 18 psec. for deuterated purple membrane. They infer from the data a proton sensitive mechanism for the K formation, namely translocation. Ippen et al. (1978) claim to have measured the rise of K in $1 \pm 1/2$ psec. and that it is stable for more than 50 psec. Honig has recently suggested an explanation of the data consistent with both models (Honig et al., 1979; Honig and Ottolenghi, 1980). Light excites the parent pigment into an excited state, called I. A trans-cis isomerization then occurs, forming the perturbed

ground state chromophore J in 1 psec. This is followed by a ground state relaxation of the protein, characterized by proton translocation and the rise of K in 11 psec. Confirmation of the trans-cis isomerization model for the bacteriorhodopsin primary event will be presented in this work.

A far less controversial subject is the role that the bacteriorhodopsin photocycle plays in the proton pumping ability of the purple membrane. The protonation and deprotonation of the Schiff base is generally considered to be an important part of the proton pumping process (Lewis et al., 1974; Stoeckenius et al., 1979). Other donor and acceptor groups exist, however, for protons. Tyrosine has been observed to become reversibly protonated during the $L \longrightarrow M$ transition (Bogomolni et al., 1978; Oesterhelt and Hess, 1973; Hess et al., 1979). This may mean that formation of a tyrosine ion is a prerequisite for deprotonation of the Schiff base. Support for this comes from chemical modification studies which show that the efficiency of the proton pump is controlled by protein-protein interactions and not from lipid-protein interactions, which are weak (Stoeckenius et al., 1980). Thus the protein residues are significant contributors to the pumping process. Honig and Ottolenghi (1980) suggest that one should consider not only light induced changes in the accessibility of the chromophore to the outside, but also the possibility that photoisomerization of the chromophore reduces its pK, and thus

triggers the proton release. Acceptor groups in the protein, which are accessible to the outside of the cell, accept and subsequently release the protons. This model would also explain the unidirectional flow of protons, as the Schiff base in this scheme functions as a gate. There is some evidence, though, that the pump scheme may be more complex than one of simple proton transport. Lanyi suggests that an additional pump in a second retinal protein of bacteriorhodopsin, absorbing at 588 nm, affects the outward transport of sodium cations and that the proton uptake may be a passive flux in response to the primary sodium extrusion (Lanyi, 1980; Lindley et al., 1979). At any rate, a great deal has been learned about the purple membrane's pumping function and this will contribute a great deal towards the understanding of membraneous pumps.

Rhodopsin

The visual pigments are located in the retina of the eye, on sites known as rods and cones because of their external shape. The rod consists of an inner segment that contains the nucleus and mitochondria and an outer segment (ROS) attached by a number of small fibrils. The length of the outer segment is 10 - 50 μm and the diameter is 1.6 μm. Rhodopsin is located in the outer segment, in the membrane of the disks that fill that area. The number of disks in the outer segment varies from one species to another, but is typically 500 - 2000. Low angle X-ray diffraction studies suggest a disk thickness of 150 Å and an

interdisk spacing of 300 Å (Blasie et al., 1965; Robertson, 1966). The most extensively studied visual system is that of bovine rhodopsin. Other vertebrates' rhodopsins share the general properties of bovine rhodopsin (Hubbard et al., 1959; Abrahamson and Fager, 1973).

Rhodopsin is a glycoprotein of molecular weight 36,000 daltons consisting of 11-cis retinal covalently bound to the ϵ-amino acid of a lysine residue of the protein opsin (Wald, 1968; Hubbard and Kropf, 1958; Kropf and Hubbard, 1958). The protein contains a single polypeptide chain. Resonance Raman studies have shown that the linkage is via a protonated Schiff base (Lewis et al., 1973; Oseroff and Callender, 1974). Composition studies have shown that 40% of the dry weight of the outer segment is lipid, mostly phospholipids, and 60% is protein, mostly rhodopsin (Papermaster and Dryer, 1974). Rough calculations based on the molecular weight and the dry weight of rhodopsin in the ROS suggest that the packing density of rhodopsin is extremely high (Bridges, 1970). Yet, the molecules have considerable freedom of rotational (Brown, 1972; Cone, 1972) and translational (Poo and Cone, 1974) motion, depending upon temperature (Blasie and Worthington, 1969; Worthington, 1971), and hence behave like a two-dimensional liquid. Studies of energy transfer between dye-labelled sites of rhodopsin have suggested that the molecule is ellipsoidal and at least 75 Å long; with hydrophilic and hydrophobic ends

(Wu and Stryer, 1972). Given the length of the molecule, rhodopsin probably spans the disk membrane.

Absorption of a photon isomerizes the chromophore and initiates production of a series of intermediates leading to the detachment of the chromophore from the protein (Wald, 1968). This process is called "bleaching", because pigments absorb in the visible range while the final products, retinal and opsin, absorb in the ultraviolet. As shown in Figure 4, the first intermediate in the bleaching sequence is bathorhodopsin (Yoshizawa and Wald, 1963), which is formed photochemically from rhodopsin in less than 6 psec. (Busch et al., 1972; Monger et al., 1979). This intermediate can also absorb a photon and revert back to rhodopsin or form a pigment called isorhodopsin, containing the 9-cis isomer of retinal as a chromophore (Fig. 2) and following the same bleaching sequence (Yoshizawa and Wald, 1963). Bathorhodopsin also decays thermally through the intermediates shown in Fig. 4.

Resonance Raman studies indicate that the Schiff base linkage remains protonated through the metarhodopsin I intermediate, and that the proton is released during the meta I-meta II conversion (Oseroff and Callender, 1974; Doukas et al., 1978b; Aton et al., 1980). This proton is correlated with neural activity. The exact mechanism by which an electric potential is established and a signal is sent to the brain remains uncertain.

Figure 4

The bleaching sequence of rhodopsin. Rhodopsin and isorhodopsin are placed lowest in the figure to indicate that they have lower free energy than their common photoproducts. Numbers in parentheses give absorption maxima, left-side numbers give the time of formation of the intermediates, and right-side numbers give the temperatures below which the intermediates are stable.

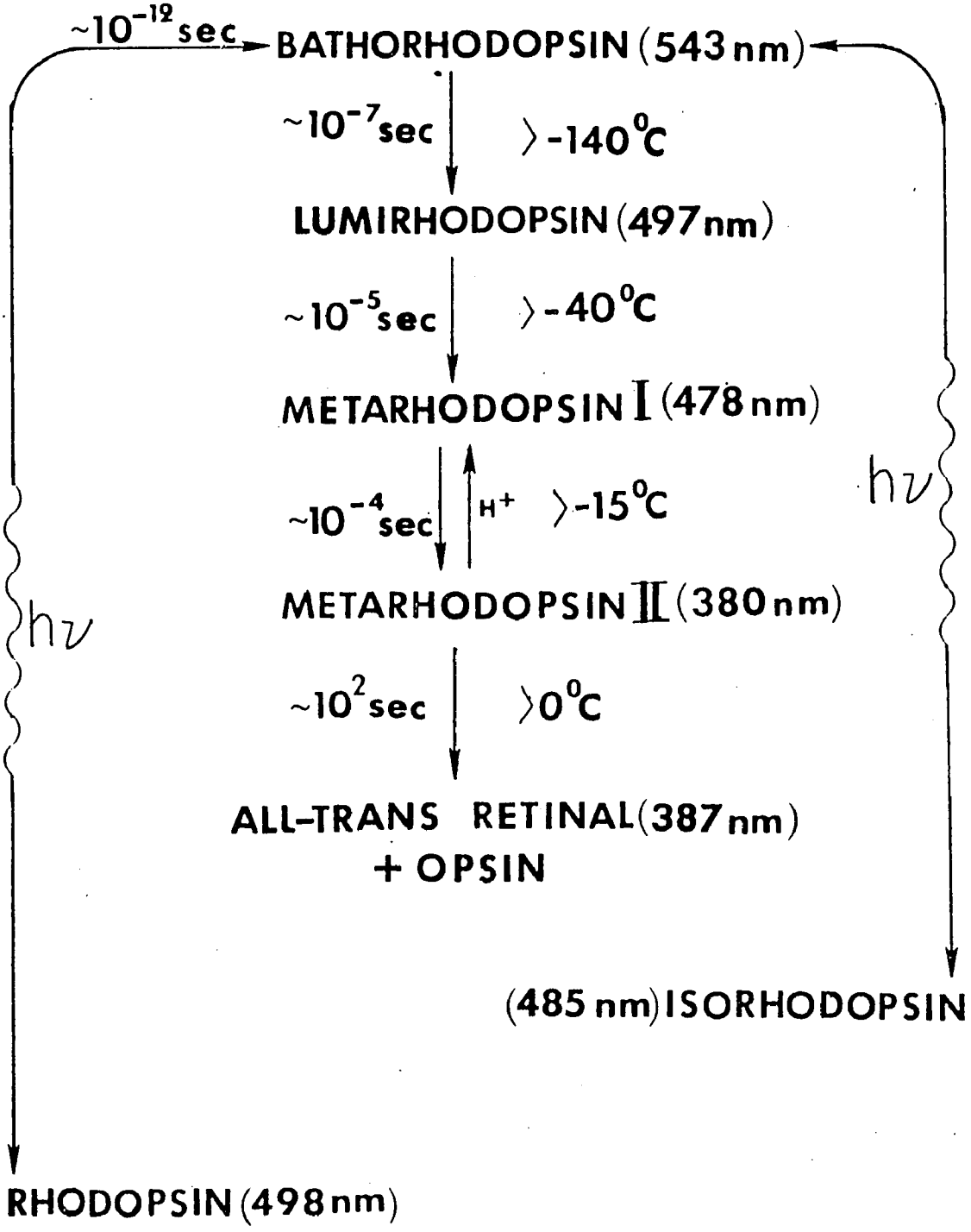
~10^-12 sec
BATHORHODOPSIN (543 nm)
~10^-7 sec
> -140°C
LUMIRHODOPSIN (497 nm)
~10^-5 sec
> -40°C
METARHODOPSIN I (478 nm)
~10^-4 sec
H+
> -15°C
METARHODOPSIN II (380 nm)
~10^2 sec
> 0°C
ALL-TRANS RETINAL (387 nm)
+ OPSIN
hν
hν
(485 nm) ISORHODOPSIN
RHODOPSIN (498 nm)

A great deal of controversy has arisen recently concerning the primary photochemical event in vision. It was originally suggested by Wald, Hubbard, and Kropf in their pioneering work that rhodopsin undergoes a photochemically induced cis-trans isomerization about the 11-12 double bond to an all-trans conformation (Hubbard and Kropf, 1958; Yoshizawa and Wald, 1963; Hubbard et al., 1965; Wald, 1968). They based this claim on the fact that at liquid nitrogen temperatures, a photostationary equilibrium exists between rhodopsin (11-cis), isorhodopsin (9-cis), and bathorhodopsin. Thus, both rhodopsin and isorhodopsin have the same photoproduct. The most plausible conformation for bathorhodopsin, then, would be all-trans. This assertion received confirmation when Doukas et al. (1978b) determined, from resonance Raman spectra, that metarhodopsin I was the all-trans conformation. However, direct Raman studies on bathorhodopsin revealed that the chromophore was in a twisted form of all-trans retinal, termed "transoid" (Callender and Honig, 1977; Aton et al., 1980; Eyring et al., 1980). A model for the primary event in vision, suggested by Honig et al. (1979), proposes that a cis-trans isomerization of the retinal chromophore of rhodopsin occurs which breaks a salt bridge formed by the Schiff base proton and a counterion embedded in the protein. The separation of charge causes the red-shift that is observed in the primary photoproduct of visual pigments.

Torsional motion about the 11-12 double bond and twisted single bonds cause the strained transoid conformation. The isomerization is completed by the metarhodopsin I stage, which is close to the true all-trans conformation.

One of the major arguments that has been advanced against the cis-trans isomerization model is that a molecule the size of retinal cannot isomerize at low temperatures, particularly in less than 6 psec. With regard to isomerization times, Honig et al. have shown with the equation $1/2I\,\omega^2 = 1/2kT$ (in which I is the relevant moment of inertia and ω is an angular frequency) that molecules the size of retinal, if not subject to a barrier, would have a rotation period at room temperature of this order. Moreover, so long as there is no barrier to the process, isomerization will be temperature independent and can occur in subpicosecond times under the influence of a driving force such as the gradient of a barrierless potential energy surface. Such a surface has been proposed by Honig et al. for the excited state of visual pigments (Hurley et al., 1977; Rosenfeld et al., 1977; Honig et al., 1979). In addition, photoisomerization at temperatures as low as 4K from rhodopsin (11-cis) to isorhodopsin (9-cis) has been clearly demonstrated (Aton et al., 1978). Thus it would appear that the active site has been so designed to facilitate rapid geometric rearrangements of the large retinal molecule.

Another model for the primary event in vision has been suggested by Rentzepis and co-workers which involves proton translocation as the rate-limiting step in the formation of bathorhodopsin, and relegates cis-trans isomerization to a secondary event (Peters et al., 1977). Their model is based on an observed transient absorption that appears in less than the 6-psec. resolution time of their apparatus at all temperatures. The transient state decays to the bathorhodopsin ground state via a temperature-dependent process that is resolvable below 20 K and is slowed down by deuterium exchange. They claim that they are observing a proton tunneling process which is involved in the formation of bathorhodopsin and that a likely candidate for the translocating charge is the Schiff base proton. In their scheme, cis-trans isomerization is a consequence, not a cause, of proton tunneling. Honig et al. (1979) incorporated the proton translocation data into their isomerization model, albeit as a secondary event. They assert that the transient alluded to above is a ground state precursor of bathorhodopsin, called batho', which is formed in less than 6 psec. at all temperatures. The formation of batho' involves a photoisomerization with the concomitant charge separation. The second, deuterium-dependent process observed by the Rentzepis group is a ground state relaxation of the protein to accommodate the isomerized chromophore and may take from less than 6 psec. to 36 psec., depending

on the temperature. This relaxation gives rise to the transient, and involves translocation of a proton in the protein.

Other models for the primary event have been proposed. One suggests that isomerization of the chromophore is a concerted rotation about two double bonds, the 11-12 and 15-16, in a "bicycle pedal" motion (Warshel, 1976). This model, however, predicts that the energy of bathorhodopsin is only 5 Kcal. above that of rhodopsin, which would admit the possibility of thermal initiation of the primary event-seeing in the dark. Additionally, it predicts an efficient photochemical path from isorhodopsin to rhodopsin and allows the reverse process. Neither reaction is known to occur since it is well established that both interconversions occur only via bathorhodopsin as a common photointermediate (Yoshizawa and Wald, 1963). A group in the Netherlands has proposed proton transfer from the methyl group at position 5 to a protein heteroatom as the primary process in vision (Fransen et al., 1976). This would entail a shifting of double bonds along the polyene chain with the formation of a "retro" compound. The formation of a retro compound would change the C=N bond to a single bond, which should cause a significant blue-shift in the absorption, since the protonated nitrogen is no longer conjugated to the chain (Rosenfeld et al., 1977). A red-shift, however, is observed for bathorhodopsin. Additionally, the fre-

quency of the C=N stretching mode would be expected to downshift, but resonance Raman experiments do not reveal any shift (Aton et al., 1980). Yet another model suggests that light initiates a reorientation of charge in the chromophore that leads to proton transfer in a vibrationally excited region of the retinal ground state (Lewis, 1978). This scheme implies that proton transfer precedes repopulation of the rhodopsin ground state, whereas Honig et al. (1979) have shown that ground state repopulation is the faster process. Thus, after careful comparison with all the experimental evidence (Green et al., 1977, Monger et al., 1979; Honig et al., 1979), only the cis-trans isomerization and proton translocation models remain viable. In this work, additional experimental verification of an isomerization as the primary photochemical event in rhodopsin and bacteriorhodopsin will be presented.

Use of Analogs

During the past few years, various analogs of different isomers of retinal have been synthesized and have proven to be a major source of information for the study of the purple membrane - visual pigment systems. Some of the problems which the analogs can help clarify are the following:

a) Selectivity of the binding site. For example, under physiological conditions, only the 13-cis and all-trans isomers of retinal bind to bacterio-opsin to form the pigment, while 9-cis and 11-cis retinal do not (Oesterhelt and

Schuhmann, 1974).

b) Protein shielding. Various reagents that react with retinal and its analogs in solution are inert when the chromophore is in its protein binding site (Honig and Ebrey, 1974).

c) Protein-chromophore interaction. For example, the injection of β-ionone into opsin has been shown to inhibit the regeneration of rhodopsin, implying the existence of a strong affinity of opsin for β-ionone (Matsumoto and Yoshizawa, 1975).

d) Chromophoric conformation in the protein binding site.

e) Pigment photosensitivity. It is quite high in rhodopsin (quantum yield 0.67) (Dartnall, 1972; Hubbard and Kropf, 1958) and lower in bacteriorhodopsin (0.3) (Becher and Ebrey, 1977) and in analogs such as 13-desmethyl rhodopsin (0.25) (Nelson et al., 1970).

f) Assignment of lines in Raman spectra.

Since the photochemical properties of the bound chromophore differ from those of free retinal (or P.S.B. of retinal) (see, for example, Honig and Ebrey, 1974), and since the bleaching sequence must involve changes in the conformation of opsin (Yoshizawa and Wald, 1963), it is thought that retinal fits into its binding site and that its interactions with this binding site control the pathways of isomerization and the subsequent changes in the

opsin structure (Ebrey et al., 1975). Thus, obtaining adequate solutions to the above-mentioned problems is crucial for a thorough understanding of the photochemistry of these pigments.

The types of analogs of retinal used to tackle these problems may be divided into three categories:

1) Changed length (either longer or shorter) of the polyene chain;
2) Isotopically substituted atoms;
3) Modified compounds with features such as added or removed methyl groups, shortened or lengthened conjugated chains, or bridges linking atoms that are not joined in "natural" retinal.

In this work, we have used compounds from the third group, as will be discussed extensively in Section III.

Because the chromophore in rhodopsin is easily dissociated from the protein by irradiation, recombination of opsin with an artificial retinal was attempted as early as 1968 (Blatz et al., 1968). It was not until 1974, however, that Oesterhelt and co-workers demonstrated that bacteriorhodopsin would also "bleach" when subjected to intense light for several hours in the presence of hydroxylamine (Oesterhelt et al., 1974). By now, the regeneration procedures for both rhodopsin and bacteriorhodopsin are standard (Oesterhelt and Schuhmann, 1974; Tokunaga and Ebrey, 1978). However, until this time, a great deal more work

with artificial compounds has been done on rhodopsin and its intermediates than on the purple membrane pigments. What follows is a short summary of some of the information gleaned from retinal-analog studies.

Selectivity

It was shown by Wald in his pioneering work that the rhodopsin binding site could accommodate either 11-cis or 9-cis retinal, but not the all-trans or 13-cis isomers (Yoshizawa and Wald, 1963; Wald, 1968). Which compounds can be bound to the protein and which cannot reflect on the geometry of the binding site and on the steric interactions that occur therein. It has been shown that 9-desmethyl (Blatz et al., 1969), 13-desmethyl (Nelson et al., 1970), 9,13-desmethyl (Blatz et al., 1969), 5,6-dihydro (Blatz et al., 1970), and 5,6 epoxide retinal (Azuma et al., 1973; see also Lewin and Thompson, 1967) all form pigments; these modifications do not interfere with pigment formation. Moreover, 14-methyl retinal not only formed a pigment, but the absorption, CD, and photosensitivity of that 14-methyl rhodopsin were very similar to that of native rhodopsin (Chan et al., 1974; Ebrey et al., 1975)! On the other hand, compounds with a changed length of the polyene side chain, such as C_{22} or C_{17}, do not form pigments, as evidenced by the lack of any change in the absorption spectrum (Blatz et al., 1969). Also, removing the ionone ring entirely impeded the chain from binding to opsin.

The situation is somewhat different in bacteriorhodopsin. The chromophores that form pigments in rhodopsin (as 11-cis and 9-cis isomers) also bind to the protein in the purple membrane (as all-trans and 13-cis isomers), but in addition, the shortened and lengthened retinals also form BR pigments (Tokunaga et al., 1977; Tokunaga et al., 1980; and this work). This implies that the binding site in the purple membrane has less stringent requirements on its chromophore (with respect to binding) than does rhodopsin's. It should be pointed out, however, that although the C_{15}, C_{17}, and C_{22} analogs all bind to bacterio-opsin, the C_{22} is unstable to hydroxylamine and the C_{15} pigment decomposes in the presence of hydroxylamine more rapidly than the C_{17}. These facts indicate the relative "looseness" of the protein's bond to these analogs.

Interestingly, although under physiological conditions bacterio-opsin binds only with the all-trans and 13-cis isomers of retinal, it has been shown that at low pH at $3^{o}C$ and under irradiation by red light, the 9-cis and 11-cis isomers can also form pigments, which absorb at 495 nm and 560 nm, respectively (Maeda et al., 1980). The accommodation of these isomers increases with increasing solvent polarity (Denny and Liu, 1977). Thus it has been suggested that changes in protein conformation due to variances in charge distribution may account for the expanded

space in the binding site needed to allow the inhabitation of 9-cis and 11-cis retinal (Maeda et al., 1980).

Shielding

The chromophore in bacteriorhodopsin is "protected" in the binding site from foreign compounds. Thus, BR does not react with hydroxylamine in the dark (Oesterhelt, 1971), and one can determine if a particular analog chromophore is shielded equally well by the protein by adding NH_2OH in the dark and monitoring to see if bleaching occurs. It has been observed by Oesterhelt and co-workers that the M intermediate is affected by hydroxylamine in the dark (Oesterhelt et al., 1974), which indicates that some movement in the chromophore and/or protein has occurred which exposed the retinal. Experiments with a spin-labelled derivative of retinal regenerated with bacterio-opsin (absorbing at 480 nm) have shown this analog to be less accessible to ascorbic acid (a hydrophilic agent) than when in solution (Stoeckenius et al., 1979). This has been interpreted as indicating that the hydrophobic end of the chromophore (namely, the ionone ring) is held in the binding site in a rigid conformation.

Protein-Chromophore Interactions

Ovchinnikov has recently reported that longer polyene chains (such as C_{22} retinal) have a greater ability to inhibit regeneration of the purple membrane protein than do shorter ones (such as C_{15} or C_{17}) (Ovchinnikov et

al., 1979). This would imply that there is some interaction occurring between the protein binding site and the polyene chain in the purple membrane.

Cassim and his colleagues have been able to produce a brown bacteriorhodopsin membrane by growing H. halobium in the presence of nicotine (Muccio and Cassim, 1979; Cassim, 1980). The brown pigment, a precursor of the purple form, consists of a 3:1 ratio of purple BR mixed with cytochrome b-561. They find no interaction whatsoever between the two species in the membrane, but they do detect a strong in-plane monomeric interaction between retinal and bacterio-opsin, in addition to excitonic interactions among the retinyl chromophores. These couplings are presumably also present in the purple membrane, since the cytochrome component has no effect on them.

The proton pumping ability of the membrane is certainly a result of protein-chromophore interactions. Changes in the π-electron structure of the β-ionone ring have been shown to have no effect on the pumping mechanism, however. Both 5,6-dihydro retinal (Nakanishi et al., 1980) and retinal$_2$ (Tokunaga and Ebrey, 1978; Tokunaga et al., 1977) (containing, respectively, one fewer and one more double bond in the ring than retinal) have the ability to pump protons when regenerated with bacterio-opsin. In addition, from a systematic study of 5,6-dihydro retinal and other dihydro analogs, Honig, Nakanishi, and coworkers

have proposed the existence of a counterion in the protein located near the β-ionone ring which affects the spectroscopic properties of the chromophores. They supported their conclusions by synthesizing retinals with bromine atoms replacing various methyl groups on the chain and showing that the resulting absorption shifts could be explained by the presence of a point-charge near the ring (Nakanishi et al., 1980). From electron microscopy studies on 9- and 13-bromo bacteriorhodopsins, Henderson has suggested that the chromophore is located near the surface of the membrane in the region between helices B, C, and G, and that the ionone ring may be close to the negative charge of Asp 96 (R. Henderson, unpublished data). The latter could very well be the point-charge of Nakanishi et al.'s (1980) model.

Conformation in the Binding Site

It has been know for several years that 11-cis retinal suffers a steric hindrance between the C-10 hydrogen and the 13-methyl group and will twist about its 12-s bond in order to relieve that hindrance (Patel, 1969; Honig and Ebrey, 1974). Since rhodopsin contains that isomer of retinal as its chromophore, the question that has been asked is whether the conformation is 12-s-cis or 12-s-trans (the former would relieve the strain - see Fig. 2). To solve the mystery, 14-methyl retinal was synthesized in the 11-cis isomeric configuration (Chan et al., 1974). It is

virtually impossible, because of the extreme steric hindrance between the 14-methyl group and the chain, for this molecule to assume a 12-s-cis form. By comparing the absorption maximum of the analog in solution with those of 11-cis retinal and all-trans retinal, it was shown that 11-cis retinal exists in 12-s-cis form in solution (Chan et al., 1974; Ebrey et al., 1975). In the pigment, however, 11-cis 14-methyl rhodopsin and 11-cis rhodopsin have very similar absorptions, CD spectra, and photosensitivities (Ebrey et al., 1975). These facts argue strongly for 11-cis retinal to be the 12-s-trans configuration in rhodopsin.

Photosensitivity

The photosensitivity of rhodopsin is quite large. The quantum yield has been measured to be about 0.67 (Hubbard and Kropf, 1958; Dartnall, 1972). When 13-desmethyl retinal was combined with opsin to form a pigment the photosensitivity dropped to about 40% of its value in natural rhodopsin even though their absorption spectra were similar (Blatz et al., 1969; Nelson et al., 1970; Kropf et al., 1973). Since the 11-cis isomer of 13-desmethyl retinal does not experience any steric hindrance which would cause it to twist about its 12-s-bond, it has been suggested (Nelson et al., 1970) that the high sensitivity of rhodopsin is due in part to its twisted 12-s-bond. The relatively low quantum yield of BR could also be understood in

these terms, since its chromophore does not experience such a twist. In addition, there may very well be less of a Van der Waal's interaction between the chromophore and protein in 13-desmethyl rhodopsin which might also contribute to the reduced sensitivity.

The blue membrane formed by regenerating retinal$_2$ with bacterio-opsin has a photosensitivity which is roughly 20% that of the purple membrane at liquid nitrogen temperatures (Tokunaga and Ebrey, 1978). While the quantum yield of bacteriorhodopsin does not change with temperature (Hurley et al., 1977; Iwasa et al., 1980), that of the blue membrane does, increasing with rising temperature. Isorhodopsin also has a temperature-dependent quantum efficiency for isomerization, while rhodopsin does not (Hurley et al., 1977). Studies with other analogs (Kropf et al., 1973) seem to confirm the pattern: natural pigments have temperature independent quantum yields while those of artificial pigments are temperature dependent. Two suggested explanations of this phenomenon are a) the conformation of the retinal analogs in the binding site is different from the chromophoric conformation in the natural pigments, just as isorhodopsin has a different conformation of its chromophore from rhodopsin (9-cis compared with 11-cis retinal), or b) the protein changes its shape to accommodate the artificial chromophore. Either of these could account for the temperature dependence of the analogs' quantum yields (Tokunaga and Ebrey, 1978).

Raman Spectral Assignments

The resonance Raman spectra of the visual pigments are potentially rich in information but unfortunately, the information is, in general, difficult to extract. One approach that has met with success in identifying the normal modes causing various spectral lines is that of substituting isotopically enriched atoms on the retinal molecule and observing the shifts in vibrational frequencies that result. Oseroff and Callender (1974) used this technique to unambiguously assign the 1655 cm^{-1} line in rhodopsin to a $C=NH^{+}$ stretching vibration. Recently, Mathies and co-workers (Eyring et al., 1980) substituted deuterium for various hydrogens on the polymethine chain in order to determine the cause of the anomalous lines in bathorhodopsin, located at 860, 880, and 925 cm^{-1}. These lines do not appear in any other pigment intermediates or model chromophores. They concluded that these modes were due to hydrogen out-of-plane vibrations, and were intensified by the twisted all-trans conformation of bathorhodopsin. Other groups have made line assignments by substituting butyl groups for methyls, and N^{15} for N^{14} in the retinal molecule (Cookingham and Lewis, 1978). We use analogs in this work to study the normal modes of bacteriorhodopsin.

Analog studies are unquestionably fruitful sources of information on the visual pigments, and as the organic

chemists are able to synthesize more diverse additions to, and substitutions and deletions in, the retinal chromophore, more and more knowledge will become available.

Cyanine Dyes

Polymethine dyes are linear, odd-numbered, conjugated molecules, as opposed to the even-numbered type of linear polyenes. This fact can radically change electronic and vibrational structure. For example, a symmetric cyanine dye such as $(CH_3)_2N-(CH=CH)_n-CH = N^+(CH_3)_2$ forms a resonance structure with $(CH_3)_2N^+ = CH-(CH=CH)_n-N(CH_3)_2$. Thus, there are no essential single and double bonds as there are in simple polyenes. The same is true for the oxanol dyes, such as $O=CH-(CH=CH)_n-O^-$. The absorption maxima of these molecules range from the near UV to the IR, and it has been observed that they shift by as much as 100 nm for each additional ethylenic bond (Brooker, 1942). It is expected from π-electron theory that these dyes exhibit a high degree of π-electron delocalization because of the superposition of the resonance structures in the ground and excited states (Suzuki, 1967). A simple calculation (Kuhn, 1949) using an infinite square well potential as an approximation of the constant interatomic potential caused by the extreme π-electron delocalization is contained in the Appendix. The monotonically increasing red-shift with increased chain length is shown to follow directly from this approximation.

The constant bathochromic shift observed in the cyanines stands in contradistinction to the shifts seen in the polyenes. In carotenoids and vitamin A-type molecules, the π-electrons are not completely delocalized; there is considerable single bond - double bond alternation. These polyenes display an asymptotic behavior with generally weaker dependence of λmax on chain length. The polyenes tend to be blue-shifted in their absorption maxima from the cyanines of the same chain length (Honig et al., 1976). Calculations which incorporate a varying potential due to bond alternation along the chain accurately depict the asymptotic behavior of the red-shift of polyenes as the chain length increases (Kuhn, 1949; Salem, 1966).

Absorption bandwidths of cyanines are relatively narrow (2000 cm^{-1}) and do not vary with λmax. Polyenes, on the other hand, exhibit broad bandwidths (6000 cm^{-1}) and they seem to vary with changed λmax (Hubbard and Kropf, 1965; Blatz, 1972). The amount of bond alternation affects the width of the absorption bands. If a given electronic transition causes a large displacement of the equilibrium nuclear configuration along a particular normal coordinate, a vibrational progression due to that normal mode will appear in the spectrum: the larger the displacement, the greater the extent of vibrational broadening. In polyenes, the first excited state is one of little bond alternation (Suzuki, 1967). Thus excitation of carotenoids and

vitamin A molecule involves a large displacement of the equilibrium nuclear configuration and a correspondingly broadened absorption band. In the cyanines, bond alternation is already indistinct in the ground state and so excitation results in only small displacements in the equilibrium nuclear configuration and little vibrational broadening (Greenberg et al., 1975).

From an understanding of the delocalization properties of cyanine dyes, Honig and coworkers were able to explain the experimentally observed wavelength dependence of the red-shift in λmax upon changing a visual pigment from a vitamin A_1-based compound to a vitamin A_2-based molecule (Honig et al., 1976; Ebrey and Honig, 1977). The change essentially involves lengthening the conjugated polyene chain by adding an extra double bond between the C-4 and C-5 positions. The pigments absorbing toward the red show cyanine-like behavior and have decreased bond alternation in their conjugated chains. Thus, as with a cyanine dye, they exhibit large wavelength shifts in going from A_1 to A_2 chromophores. On the other hand, blue pigments behave more like polyenes and show small wavelength shifts.

From the above discussion it seems clear that a careful study of cyanine dyes can give insight into the bond structure of conjugated chains and into the properties of π-electron systems, especially the visual pigments. In addition, dyes have been used extensively as

fluorescence probes of biological systems, most notably membranes, and a wealth of knowledge has come from those studies (for a general review, see Radda and Vanderkooi, 1972; Waggoner, 1976). An interesting prospect for the future would be to use non-fluorescent dyes as Raman probes of cell membranes as a complementary source of information. At any rate, many of the ideas used in analyzing the Raman spectra of cyanine dyes are directly applicable to the spectra of the visual pigments and hence a side-by-side study of the two systems is highly desirable.

SECTION II - Experimental

Photolability Problems and Solutions

Resonance Raman spectroscopy is an extremely useful analytical tool, especially in the study of the visual pigments and bacteriorhodopsin (see, for example, Callender and Honig, 1977). However, its use on the biological systems is not without a major complication. Since the exciting light is in resonance with a particular colored center, the sample is absorbing almost all of the light. For example, it has been reported that the Raman scattering cross-section of the most intense Raman line of rhodopsin (the C=C ethylenic mode) measured with the 568.2 nm line of the krypton laser is about 8×10^{-26} cm^2/mol-sr (Callender et al., 1976). This is more than eight orders of magnitude smaller than the absorption cross-section at the same wavelength. Thus, under typical conditions of a few milliwatts of laser light focused on the sample, each pigment complex absorbs a photon every millisecond or less, while the Raman measurements take several minutes to complete. Since light initiates a series of temperature-dependent transformations of the pigment (see Section I), the very attempt at taking a Raman spectrum of a pigment immediately causes replacement of the pigment with a quasi-photostationary mixture of several different species. Special techniques, therefore, must be used to permit Raman work on photolabile systems.

In general, the composition of the photosteady mixture produced by irradiation will depend in detail on the absorption cross-section, quantum yield, and kinetic lifetime of each component relative to the photon flux of the incident beam. At 80K, however, laser irradiation produces a photostationary state containing only rhodopsin, isorhodopsin, and bathorhodopsin (correspondingly, bacteriorhodopsin and K in the purple membrane) (Oseroff and Callender, 1974). The relative concentrations of the three components depend only on the wavelength of the incident illumination and are independent of other experimental factors, including photon flux.

Interpretation of resonance Raman scattering from a multiple component, photostationary system can be complex. The wavelength dependence of the resonance-enhanced Raman cross section of a molecule is not a simple function of its absorption profile. It may scale differently for each of the components of the photostationary state. One early attempt around this problem used an exciting laser wavelength far from λmax of the sample (rhodopsin) (Lewis et al., 1973). Unfortunately, the wavelength was sufficiently close to cause major light-induced changes. Although the sample was assayed in the experiment by measuring the bulk absorption before and after irradiation with laser light and both absorptions were identical, photoisomerization still occurred. Since the laser light was focused,

it could affect only the very small portion of the sample actually in the beam. Therefore, changes in the bulk absorption would not be expected even though the sample in the laser beam contained a mixture of photoproducts.

The first experiment to control the effect of photolability of visual pigments was that of Oseroff and Callender (1974) in their study of bovine rod outer segment vesicles at liquid nitrogen temperatures. Two laser beams were used simultaneously, one acting as a "pump" to modify the photostationary state of the sample and the second at a different wavelength and weaker in intensity acting as a "probe" to excite the Raman scattering. The exact sample composition of rhodopsin, isorhodopsin, and bathorhodopsin for each pump wavelength was assayed by using well-developed techniques of absorption spectroscopy. Thus, all factors, including the resonance enhancement factors for various Raman lines, were held constant, except, of course, for sample composition. They were then able to assign the Raman bands. This technique was used to obtain many of the Raman spectra in this work.

A second method which eliminates problems associated with photolability for samples in solution was independently developed by Mathies et al. (1976) and Callender et al. (1976). Briefly, it involves flowing a sample through a wide (with respect to the laser beam diameter) capillary at a rapid enough rate to prevent the vast majority of mol-

ecules of sample from isomerizing, and for those that do, from contributing to the Raman scattered intensity. The Raman measurements may be taken over a period of several hours with less than a controllable percentage of sample in a photoinduced intermediate state. One drawback of the flow technique is that it requires a substantial amount of sample in the system and hence this method was not used in these analog studies because of the small quantities of analog compounds available.

Methods and Materials

Resonance Raman spectra were obtained with a 1401 Spex double monochromator, a cooled RCA 31034 photomultiplier tube and photon counting electronic apparatus interfaced to a PDP-8e minicomputer. The entrance and exit slits on the monochromator were opened to 300 microns, giving a resolution of about 6 cm^{-1}, depending upon the exciting wavelength used. Absorption spectra were taken with a GCA McPherson UV-VIS spectrophotometer. The temperature in the cell holder of the spectrophotometer was controlled by a bath circulator Lauda Super K/2R and monitored by a thermometer. The spectrophotometer was also interfaced to the PDP-8e. Part of the computer's memory was reserved for data storage in discreet channels. More permanent storage was accomplished with a floppy-disk system and a PDP-10 computer, both interfaced to the minicomputer.

A Coherent Radiation model 52B krypton ion laser and a Spectra-Physics model 165 argon ion laser were used to produce the monochromatic excitation of the samples. The available wavelengths span the range from the UV (350.4 nm) to the red (647.1 nm). The laser beam was diffracted on a grating to separate the discharge lines and the first order diffracted beam was used to excite the sample. A right angle scattering geometry was used. Power levels were measured before the sample with a calibrated thermopile (Eppley Laboratories, Newport, R.I.). A schematic diagram of the Raman apparatus is shown in Figure 5.

Low temperature Raman spectra were taken using a home-built nitrogen cold finger dewar connected to the end of a flexible nitrogen/helium transfer line LT-3-110 (Air Products and Chemicals, Allentown, Pa.). The sample was deposited in a concave depression in a temperature-controlled copper sample holder arranged for 90° scattering from the surface of the sample. The holder was cooled by a continuous stream of nitrogen gas. Temperature in the holder could be set between $-190^{\circ}C$ and $0^{\circ}C$ and maintained within $.5^{\circ}C$ of the set temperature, which was monitored with a thermistor.

The monochromator was calibrated with the known Kr^{+} and Ar^{+} laser lines. Line assignments are accurate to within ± 3 cm^{-1}. All the spectra presented here consist of digitally pooled data from multiple runs and all iden-

Figure 5

Schematic diagram of a Raman apparatus. ν_L and ν_S are the frequencies of the exciting and scattering light, respectively. ν_o is the vibrational frequency of a simple normal mode.

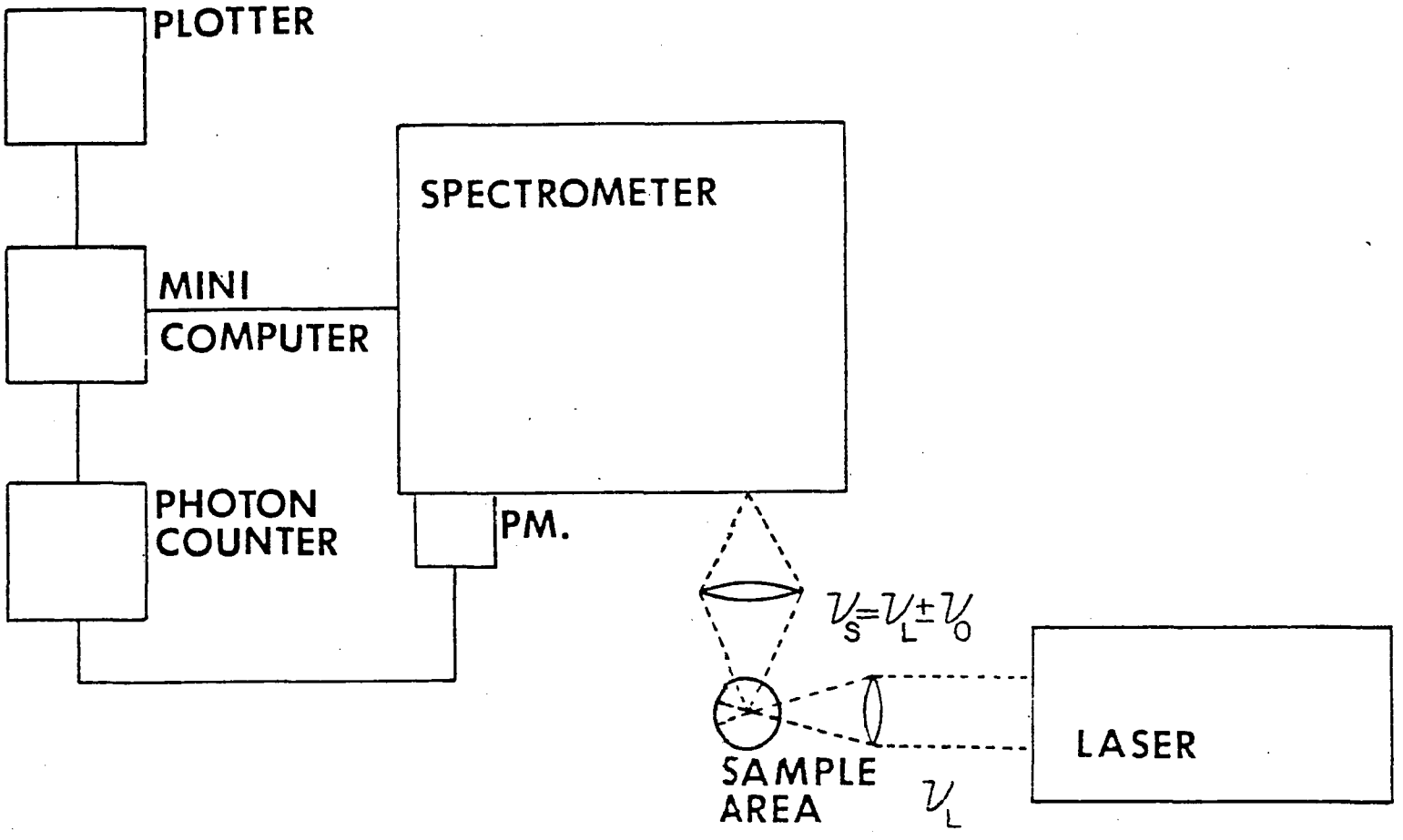
PLOTTER
SPECTROMETER
MINI
COMPUTER
PHOTON
COUNTER
PM.
$\nu_S = \nu_L \pm \nu_O$
LASER
SAMPLE
AREA
ν_L

tified lines have been observed in several separate measurements. A typical single scan consisted of a monochromator speed of 50 cm^{-1}/min. and a channel duel time of 2.2 sec. (an effective time constant of about 12 sec.) for a total of 512 channels, thus producing a span of 939 cm^{-1} for a scan.

Room temperature spectra were taken in a 3 x 3 mm x 2 cm quartz cuvette arranged for 90° scattering. Care was taken to have the laser beam enter the cell as close to the front face as possible, to reduce the amount of reabsorption of the Raman scattered light in the sample solution.

All work on the analogs and the visual pigments was carried out in the dark under dim red light.

In order to enhance the signal to noise ratio of the Raman spectra, numerous digitally-pooled runs were combined additively. The fluorescence background was computer subtracted by finding a polynomial curve that fit a number of background points. The values of 512 equidistant points on the curve were subsequently calculated and subtracted from the corresponding channels of the raw data.

Analogs

Retinals:

The four all-trans retinal analogs - 13-desmethyl, 10-methyl, 14-methyl, and 10,14 dimethyl - were the generous gift of Dr. Walter Waddell. The 13-desmethyl retinal was prepared by manganese dioxide oxidation of the

corresponding vitamin A analog (Waddell et al., 1978), which was synthesized according to the procedure of van den Tempel and Hiusman (1966). The all-trans isomers of 10-methyl, 14-methyl, and 10,14-dimethyl retinal were prepared according to the procedure of Tanis, Brown, and Nakanishi (1978). 5,6-dihydro retinal (all-trans) was a gift of Prof. Koji Nakanishi and the synthesis has been described elsewhere (Arnaboldi et al., 1979).The five analog compounds, drawn in Figure 6, were isolated and purified to greater than 99.5% isomer purity by HPLC methods and were characterized by nuclear magnetic resonance methods. The HPLC was performed on a Waters 6000 psi system equipped with a system injector, and a Laboratory Data Control 350 nm detector was used with one or two μ-poracil 1 ft x .25 in. column(s). The solvent system was 1 - 4% (v/v) ether/n-hexane and the flow rate was adjusted to 1-2 ml/min. NMR spectra for sample identification were recorded on an HF 250 MHz NMR Spectrometer.

Resonance Raman Spectra of the retinal analogs were taken at room temperature in a cuvette, with an exciting wavelength of 647.1 nm. The solvent used was either carbon tetrachloride or methanol, and any solvent lines were computer subtracted from the spectrum. Concentrations were typically 1 mM. The resonance Raman enhancement cross section drops off more slowly than the absorption cross section as the laser frequency moves away from the absorption band, and therefore the amount of light at 647.1 nm ab-

Figure 6

Conformations of the various analogs of retinal (R=O) and its protonated Schiff base ($R=NH^+$) used in this work. (a) 10,14-dimethyl; (b) 14-methyl; (c) 10-methyl; (d) 5,6-dihydro; (e) 13-desmethyl.

A.

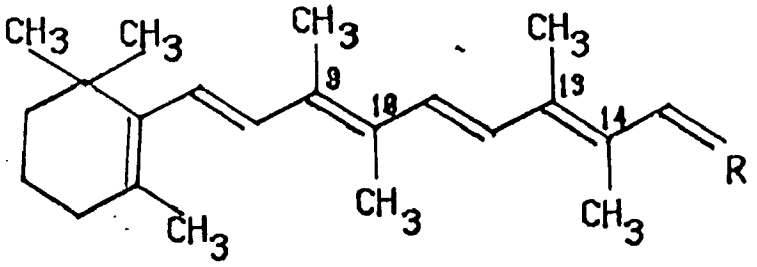

B.

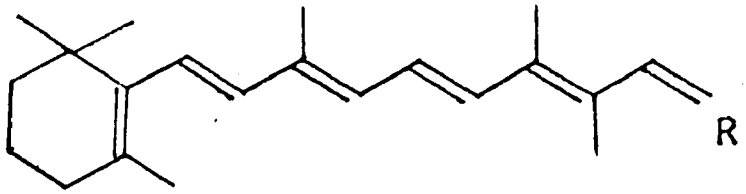

C.

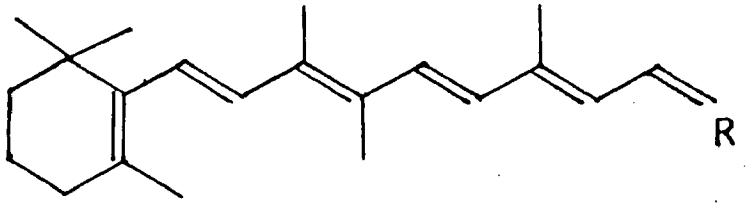

D.

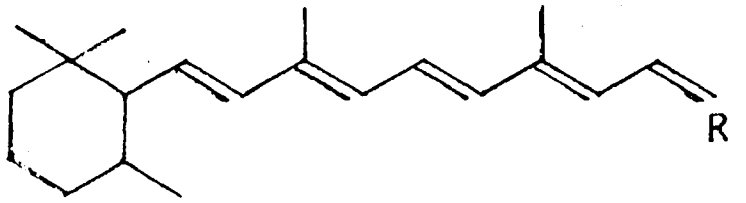

E.

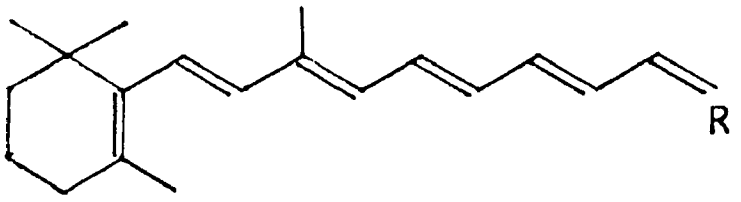

sorbed by the retinals was negligible, while the Raman enhancement was still appreciable. As a check, a spectrum of all-trans retinal was obtained under the same experimental conditions and it was identical with that taken using the flow technique, which has been shown to be pure (Callender et al., 1976). Additionally, the absorption spectrum of each retinal analog was taken before and after each Raman experiment and they were identical.

Protonated Schiff Bases

Retinal analog Schiff bases were prepared by adding an excess amount of n-butylamine to an n-hexane solution of the analog at $0^{o}C$. The solution was stirred for one hour under a stream of nitrogen. The completion of the reaction was determined by the appearance of a 10-20 nm blue shift in the absorption spectrum. The solution was then dried to completely remove the excess amine and the remaining powder was dissolved in methanol. Protonation of the Schiff base was accomplished by titrating the Schiff base compound with a methanol/hydrochloric acid mixture. The protonation was detected by the large red shift in the absorption maximum.

Raman measurements of the protonated Schiff base analogs were taken under the same conditions as the retinals, but the solvent in each case was methanol. Again, a measurement of all-trans retinal protonated Schiff base taken under the same conditions was identical with that obtained by the flow technique (Mathies et al., 1976), and

the absorption spectra of the analogs did not change as a result of the Raman experiment.

Bacteriorhodopsin Pigments

The five all-trans retinal analogs were regenerated with the apoprotein of bacteriorhodopsin by Prof. T. G. Ebrey and co-workers. Their procedure has been described in the literature (Tokunaga and Ebrey, 1978). Resonance Raman spectra were taken of the PM analogs at liquid nitrogen temperatures. In order to increase the concentrations of the samples (more concentrated samples are needed at low temperatures because light scatters off the sample surface only), the pigments were spun down at 10000 RPM for one hour and the resulting pellet was resuspended in a small volume of water to the desired concentration, usually about 4 OD/cm. The sample was then pipetted onto the cold finger system described previously and frozen down to 85 K, where the measurements were taken. For the deuterated samples, the centrifugation procedure was repeated three times with deuterium oxide instead of water and the final pellet was suspended in a small amount of D_2O.

At 85 K, a photostationary equilibrium exists between the parent pigment in bacteriorhodopsin and the first intermediate, K. The photoconversion of PM to K is much less efficient in bacteriorhodopsin than in the visual pigments, the quantum yield having been reported to be .3

in the bacterium (Becher and Ebrey, 1977) as opposed to .67 in rhodopsin (Hubbard and Kropf, 1958; Dartnall, 1972). In addition, one notices very little difference between the Raman spectrum of a 70% - 30% mixture of PM and K, and a Raman spectrum of 100% PM (see discussion of Fig. 15 in Section III). This is due to the small Raman cross section of K. Thus even though the sample may contain 30% K, the contribution of that intermediate to the Raman spectrum is closer to 10%. Moreover, Ebrey and coworkers have determined that in general, the photosensitivity of analog pigments is temperature dependent, decreasing with lowered temperature (Hurley et al., 1977; Tokunaga and Ebrey, 1978; Iwasa et al, 1980). Therefore, we estimate that the contribution of a first intermediate to the Raman spectra of these analogs at 85 K is negligible.

A serious concern in measuring Raman spectra of bacteriorhodopsin (or its analogs) is the possible presence of carotenoids in the sample. As measured by Rimai et al. (1973), these contaminants have strong Raman lines at 1154 and 1510 cm^{-1} (Rimai et al., 1973). It was pointed out by Lewis and coworkers that carotenoids can be eliminated from a BR sample by washing with a 10 mM solution of sodium deoxycholate (Lewis et al., 1974). The sample used in this work did not manifest any Raman intensity at 1154 and 1510 cm^{-1} indicating that the carotenoid

content, if any was present, was removed during the purification process.

Table 1 summarizes the experimental parameters used in the Raman study of the bacteriorhodopsin analogs. The exciting wavelength was chosen to be near the absorption peak of each pigment for resonance enhancement purposes. The energy interval between λmax and the exciting laser line frequency is roughly the same for each pigment to obtain approximately uniform excitation profiles for the various compounds.

K Photoproduct

Cultures of H. halobium were grown and the purple membrane purified according to the procedures of Becher and Cassim (1975). Samples were light adapted by irradiating with 568.2 nm light for one hour prior to the Raman measurement, and all work was done under normal room light. Verification of light adaptation was obtained by determining that the absorption maximum of the pigment was 568 nm.

Laser Raman spectra of K and deuterated K were acquired by use of the double beam technique at liquid nitrogen temperatures (Oseroff and Callender, 1974) combined with computer subtraction methods. Two laser beams were used simultaneously in the experiments, one at 647.1 nm acting as a pump beam, and the second at 488 nm acting as the Raman probe, with a pump/probe power ratio of 10. Care was taken to ensure that the two beams were coaxial

Table 1

EXPERIMENTAL CONDITIONS

Compound	λmax(nm)	Temperature	Laser Line
Bacteriorhodopsin	558	85 K	5208 Å
10-Methyl BR	575	85 K	5208 Å
13-Desmethyl BR	565	85 K	5208 Å
5,6-Dihydro BR	472	85 K	5208 Å
14-Methyl BR	425	85 K	4880 Å
10,14-Dimethyl BR	433	85 K	4880 Å
Retinals	360-380	R.T.	6471 Å
Protonated Schiff Bases	420-445	R.T.	6471 Å

and the relative and absolute beam powers were measured just before the sample using a calibrated Eppley thermopile. The Raman spectrum was measured repeatedly, with each successive run alternating between double beam irradiation and probe-only excitation. The pump beam drives the photostationary equilibrium between PM and K at 85 K toward the parent pigment, since its red color is much closer to the absorption peak of K (630 nm) than to PM (568 nm). Calculations based on quantum yields of the intermediates indicate that at a pump/probe ratio of 10:1, the dual beam spectrum is of 100% PM. Because the probe beam intensity is relatively weak, it does not affect the photocomposition at all. When the probe alone was used, a mixture of PM and K was present. Under the conditions described, this was measured to be 70% PM and 30% K (Becher and Ebrey, 1977). By alternating single and dual beam runs, the uniformity of the experimental conditions was assured. Increasing the pump/probe ratio to 25:1 did not cause any changes in the spectra. Numerous digitally pooled runs were combined additively for an enhanced signal to noise ratio. 70% of the resulting pure PM spectrum was computer subtracted from the mixture (single beam) spectrum to obtain the Raman spectrum of 100% K. Preparation of deuterated bacteriorhodopsin was the same as was described above for the BR analog pigments.

"Seven - Membered Ring"

The so-called "seven-membered ring" analog of retinal, drawn in Figure 7, was synthesized, purified, and regenerated with opsin by Prof. K. Nakanishi and coworkers and their methods have been described in detail elesewhere (Akita et al., 1980a). The room temperature Raman spectrum was measured with 6 mw of 476.2 nm light. The sample, dissolved in 2% octylglucoside (Calbiochem-Behring Corp.) was contained in a cuvette identical to the one used for the retinal analogs described above. All preparations and measurements were carried out in the dark under dim red light.

Cyanine Dyes

The homologous series of cyanine dyes used here (designated as diQ-C_n-(2m+1), where diQ refers to the two quinoline end groups, n is the number of carbons in the tail attached to the nitrogen on each ring, and 2m+1, m an integer, is the number of carbons in the polymethine chain connecting the end rings - see Figure 8) were the generous gift of Prof. Alan Waggoner of Amherst College. Their synthesis is described elsewhere (Hamer, 1964). Raman spectra were taken at room temperature, as described above. The samples were all dissolved in methanol, although changing the solvent polarity did not affect the results (West and Geddes, 1964). Laser lines at 530.8, 647.1, 482.5, 647.1 and 530.8 nm were used to irradiate

Figure 7

Conformation of the "seven-membered ring" analog of retinal, shown as a protonated Schiff base.

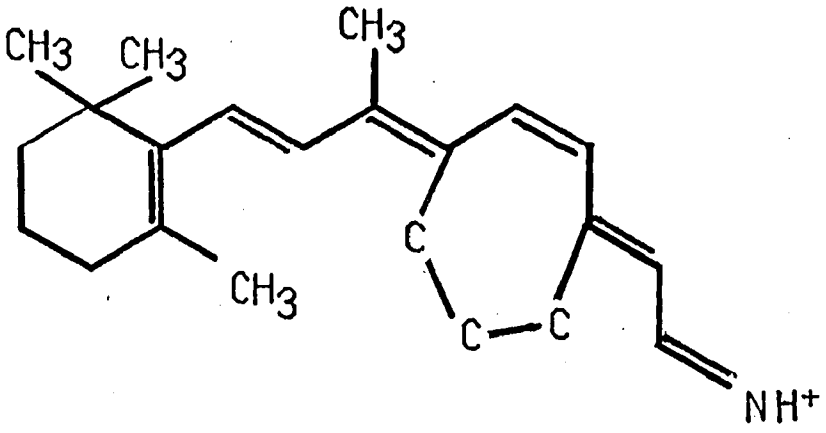
CH3
CH3
CH3
CH3
C
C
C
NH+

Figure 8

Structure of the cyanine dye series used in this work, known as diQ - C_n - (2m + 1) (see text). The counterion for dyes diQ -C_2 - (1), diQ - C_2 - (5), diQ - C_2 - (7), and diQ - C_4 - (3) is iodine, while for the dye diQ - C_2 - (3) it is chlorine.

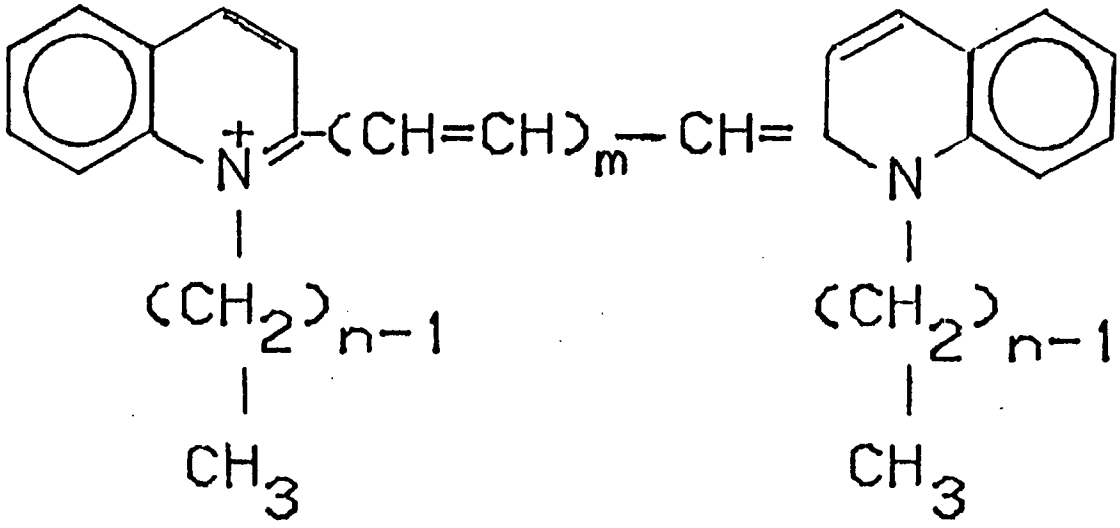

the C_2-(1), C_2-(3), C_2-(5), C_2-(7), and C_4-(3) dyes, respectively. The spectra did not change appreciably when other excitation wavelengths were used. As the cyanine dyes are not photosensitive, all work could be done in normal room light. Absorption spectra were taken of each dye before and after each Raman experiment to verify that no laser damage was done to them.

Rhodopsin Analogs

An attempt was made to obtain the resonance Raman spectrum of 9-cis ∝-retinal regenerated with bovine opsin, known as ∝-isorhodopsin. ∝-retinal differs from "natural" retinal in that the position of its ring's double bond is shifted to the 3-4 location from the usual 5-6 position. Bovine retina were purchased from Hormel (Austin, Mn.). ROS (rod outer segments) were prepared according to the procedures described in Hubbard et al. (1971). All procedures involving rhodopsin were carried out under dim red light.

The retina (usually 100 - 150 prepared at a time) were diluted with phosphate buffer (.067 M and PH 6.8) and poured several times through a cheesecloth to separate out the neural tissues, which were discarded. To the strained ROS suspension was added an 80% (W/V) sucrose solution of equal volume, resulting in a 40% sucrose concentration. This was then centrifuged (Sorvall, model RC2-B) for 30 minutes at 10000 RPM in a swinging bucket rotor. Black

pigment epithelium sedimented to the bottom of the centrifuge tube. The crude ROS were carefully removed with a pipet from the phosphate-sucrose interface and diluted to several times this volume with phosphate buffer. This was centrifuged at 10000 RPM for an hour to precipitate the ROS. The resulting pellet was suspended in phosphate buffer and delicately dropped on top of a stepwise sucrose gradient consisting of equal volumes of 41%, 31%, and 27% sucrose solution. After centrifugation in the swinging bucket rotor for 30 minutes at 10000 RPM, the purified ROS were collected with a pipet. Retinal tissue, floating at a lower level in the sucrose solution, was discarded. The ROS were then washed several times with phosphate buffer and centrifuged (10000 RPM, 20 minutes) to eliminate any water-soluble impurities.

The purified ROS thus obtained were resuspended in phosphate buffer. To determine the rhodopsin yield of the preparation, a small, measured fraction of the total volume was removed and dissolved in a .75% solution of Ammonyx-Lo (Onyx Chemical Co., Jersey City, N.J.) to extract the rhodopsin. The optical density of this sample at 500 nm was measured and the total OD of the ROS was calculated. One hundred retinas usually yielded about 50 OD of rhodopsin.

Fifteen to twenty OD of opsin were used to prepare a regenerated sample. About .1 mM of ethylinediamine tetraacetic acid (Calbiochem-Behring, Inc.) was added to the

ROS and the sample was bleached under argon in room light for 45 minutes. An equal OD of 9-cis α-retinal (a gift of Prof. Allen Kropf, Amherst College) was dissolved in a few drops of ethanol and injected violently with a syringe into the bleached opsin. The sample was then incubated at room temperature overnight. A small, measured amount was then removed and dissolved in Ammonyx-Lo and the absorption checked to determine the extent of regeneration. We usually found that 90% of the opsin recombined with the new chromophore. The pigment was then washed several times with phosphate buffer and .1 mM dithiothreitol (Sigma Co., St. Louis, Mo.) to prevent oxidation of the sulfhydryl groups. Extraction of the pigment was done with a solution of .01 M phosphate buffer, .1 mM dtt, and .75% Ammonyx-Lo. This was centrifuged (10000 RPM, 20 minutes) and the supernatant collected. The pellet was again extracted and the final residue was discarded.

Purification of the regenerated pigment from unregenerated components and from lipids was necessary to obtain a Raman signal. It was accomplished by pouring the sample on a 30 cm x 9 mm column (Pharmacia) packed with hydroxylapetite (BioRad) and equilibrated with the same extraction solution. After washing overnight at 0^0C with the extraction solution, the purified pigment was eluted with an exponential gradient of phosphate buffer (.01 M - .1 M) in 1 ml fractions. The Ammonyx-Lo and dtt concentrations were maintained throughout.

The purity of rhodopsin or its artificial analogs is determined by the ratio of absorption at the peak of the protein band (280 nm) to the peak of the visible band. The lower this ratio, the better the sample. The best preparations of rhodopsin reported in the literature cite a ratio of 1.6. We obtained ratios of 1.8 - 1.9. The purity of the sample is crucial in the Raman measurements since a relatively impure sample shows an increased fluorescent background which adversely affects the Raman signal to noise ratio.

The artificial pigment, absorbing at 476 nm, had to be concentrated to about 4 OD/ml to yield a Raman spectrum at 85 K with an appreciable signal to noise ratio. Several methods were tried, including vacuum dialysis, lyophilization, and dialysis followed by centrifugation (to pellet the sample). All these techniques resulted in the sample denaturing, as evidenced by the absorption spectrum.

A control experiment was performed wherein 11-cis retinal was regenerated with opsin by the above procedure and the Raman spectrum obtained was identical to the rhodopsin spectrum reported in the literature. (The 11-cis retinal was a gift from Hoffmann-LaRoche Co. and was used without further purification). Artificial chromophores other than α-retinal have been successfully regenerated with bovine opsin by the method described above and have been stable for long periods of time (G. Eyring, personal

communication). We conclude, therefore, that the 9-cis ∝-retinal pigment is an especially sensitive one and it became unstable in the lipid-free environment created by column purification.

SECTION III - Results and Discussion

Bacteriorhodopsin Analogs

The resonance Raman spectra of retinals, visual pigments, and bacteriorhodopsin have been the subject of a great deal of analysis in recent years, both theoretical and experimental (for recent reviews, see Warshel, 1977; Mathies, 1979; Stoeckenius et al., 1979). The region receiving the most attention is found between 750 and 1700 cm^{-1}, since no significant vibrational intensities have been observed outside this domain. Various general spectral assignments have been made and these divide the aforementioned region into subgroups:

(a) the region between 900 and 1450 cm^{-1}, which has been shown to be sensitive to the isomeric conformation of the molecule under examination (Callender and Honig, 1977). For example, the resonance Raman spectrum of 11-cis retinal shows significant changes in this region from the spectrum of all-trans retinal, while outside this region they are similar. This section of the spectrum is known as the fingerprint region because of its ability to distinguish among various isomers. The vibrations in this frequency range are primarily C-C single bond stretches (Warshel, 1977), C-C-H bends (Rimai et al., 1971), and methyl stretches (Rimai et al., 1973).

(b) the so-called "ethylenic" mode region, between 1500 and 1620 cm^{-1}. Vibrations here are due to C=C double bond stretches (an "ethyl" group) and are normally very intense in polyenes (Warshel and Karplus, 1974; Warshel, 1977).

(c) the terminal end group between 1600 and 1700 cm^{-1}. In aldehydes, this is a C=O stretch (typically 1670-1680 cm^{-1}), in the Schiff bases it is a C=N stretch (usually around 1630 cm^{-1}), and in the protonated Schiff bases as well as the pigments that are protonated, it is a $C=NH^{+}$ stretch mode (approximately 1650 cm^{-1}).

Fingerprint Region

A detailed understanding of frequencies and intensities of the Raman lines in this section of the spectrum would, in principle, lead to a good understanding of the specific isomeric conformation of the chromophore being studied and of the interactions of the chromophore with its environment. Unfortunately, no theory has yet been proposed that can adequately explain the line positions and intensities in this region. A typical approach that is used to unlock some of the secrets of the fingerprint vibrations in visual pigments and bacteriorhodopsin is to compare the bands in those pigments with those in model compounds such as protonated and unprotonated Schiff bases

of various retinal isomers in solution with the hope of assigning a particular isomeric conformation to a pigment's chromophore. This technique has met with a great deal of success for rhodopsin and the intermediates of its photocycle (see Callender and Honig, 1977). Chemical extraction and regeneration studies have shown that 11-cis and all-trans retinal are the only possible chromophores in those pigments (Hubbard and Kropf, 1958; Kropf and Hubbard, 1958; Wald, 1968) and comparisons of the Raman spectra of those chromophores as protonated and unprotonated Schiff bases with those of the various pigments revealed unambiguously that rhodopsin contained 11-cis retinal (Mathies et al., 1977) while metarhodopsins I and II both had all-trans retinal as a chromophore (Doukas et al., 1978b). Although the fingerprint lines of 11-cis retinal P.S.B. are not identical with those of rhodopsin, presumably because of chromophore-protein interactions in the latter, they are quite similar, and considerably different from those of any other isomer. In bacteriorhodopsin, however, this method has not been so informative. For example, chemical extraction and regeneration studies suggest that all-trans and 13-cis retinal are the only possibilities for the chromophore in bacteriorhodopsin (Sperling, et al., 1977; Ohno et al., 1977; Maeda et al., 1977). The fingerprint lines of light- and dark-adapted bacteriorhodopsin, however, show both similarities to, and differences

from, the lines in the all-trans and 13-cis retinal model compound spectra (Aton et al., 1977) - see Figure 9. In addition, the fingerprint spectra of the two model chromophores are quite similar to each other, which makes the assignment of one or the other as the chromophore of a particular pigment even more difficult. In this work, no attempt is made to identify the isomeric conformation of a particular BR (bacteriorhodopsin) analog's chromophore. Such a study using Raman spectroscopy would probably not lead to conclusive results, based on the native BR data. Moreover, the analysis would require the use of the 13-cis isomer of each retinal analog in addition to the all-trans, and these were not available for this work. We therefore restrict ourselves in this work to analyzing specific line patterns in the fingerprint region by comparing the all-trans model compound data and the pigment data for the analogs and for native BR. A particularly interesting line pattern that appears in the Raman data will now be discussed.

The fairly intense vibration in the vicinity of 1000 cm^{-1} found in the Raman spectra of visual pigments and bacteriorhodopsin has been assigned to vibrations of the methyl groups on the polyene chain (Rimai et al., 1973). Looking at the intensity of this line for the various analog pigments in Figure 10, one notices an interesting pattern. While the frequency of this vibration is relatively

Figure 9

Resonance Raman spectra of (A) PM558 dark-adapted purple membrane chromophore; (B) PM568 light-adapted purple membrane chromophore; (C) 13-cis retinal n-butylamine-HCl; (D) all-trans retinal n-butylamine-HCl. The spectrometer resolution is 7 cm^{-1}. (from Aton et al., 1979).

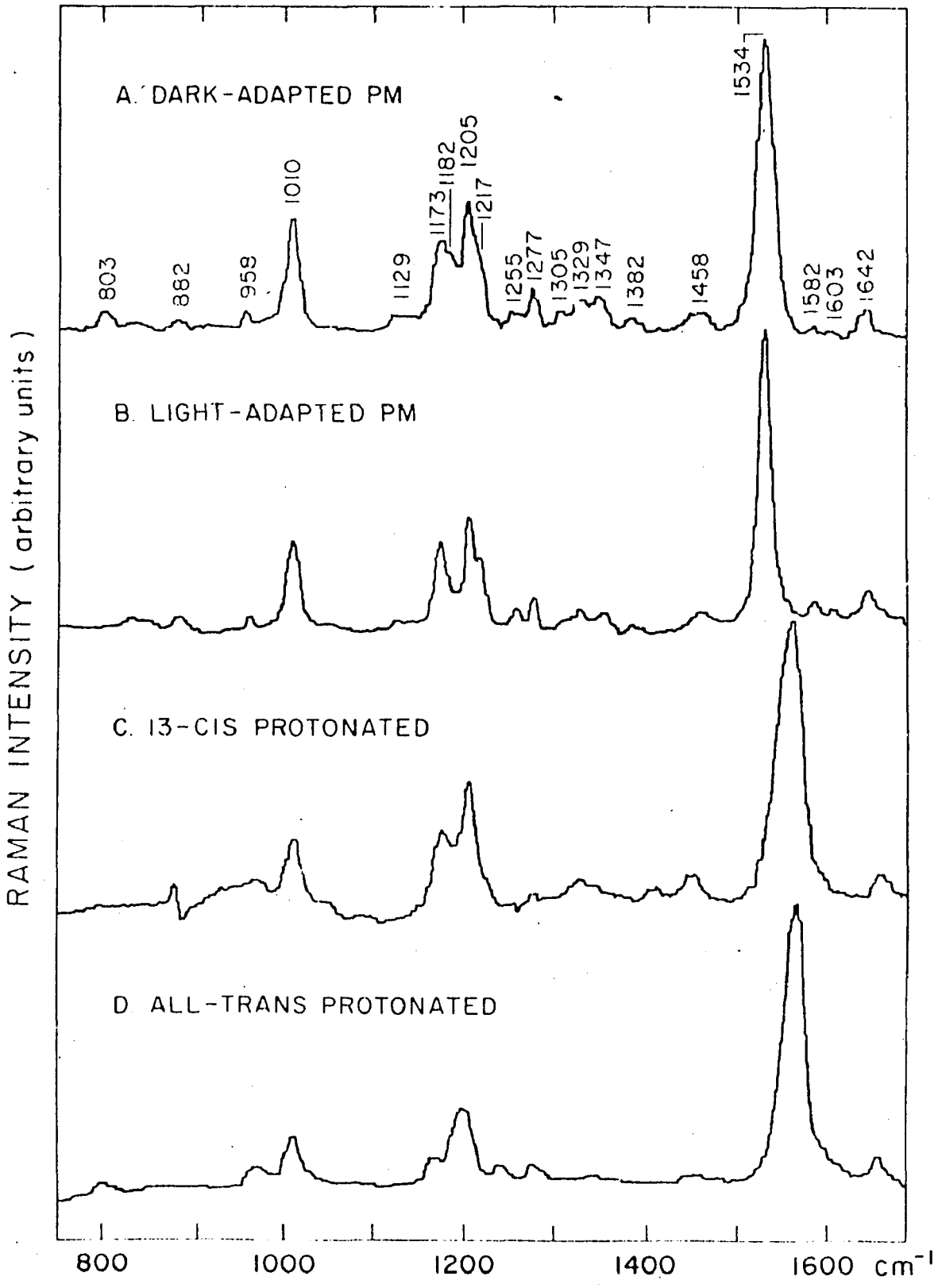
A. DARK-ADAPTED PM
B. LIGHT-ADAPTED PM
C. 13-CIS PROTONATED
D. ALL-TRANS PROTONATED
RAMAN INTENSITY (arbitrary units)
803
882
958
1010
1129
1173
1182
1205
1217
1255
1277
1305
1329
1347
1382
1458
1534
1582
1603
1642
800
1000
1200
1400
1600 cm⁻¹

Figure 10

Resonance Raman spectra of five bacteriorhodopsin analogs, taken at 85 K. The 10,14-dimethyl and 14-methyl spectra were taken with the 488.0 nm laser line, while the 10-methyl, 5,6-dihydro, and 13-desmethyl spectra were taken with the 520.8 nm laser line. All samples were suspended in water. The resolution in all cases is 7 cm^{-1}.

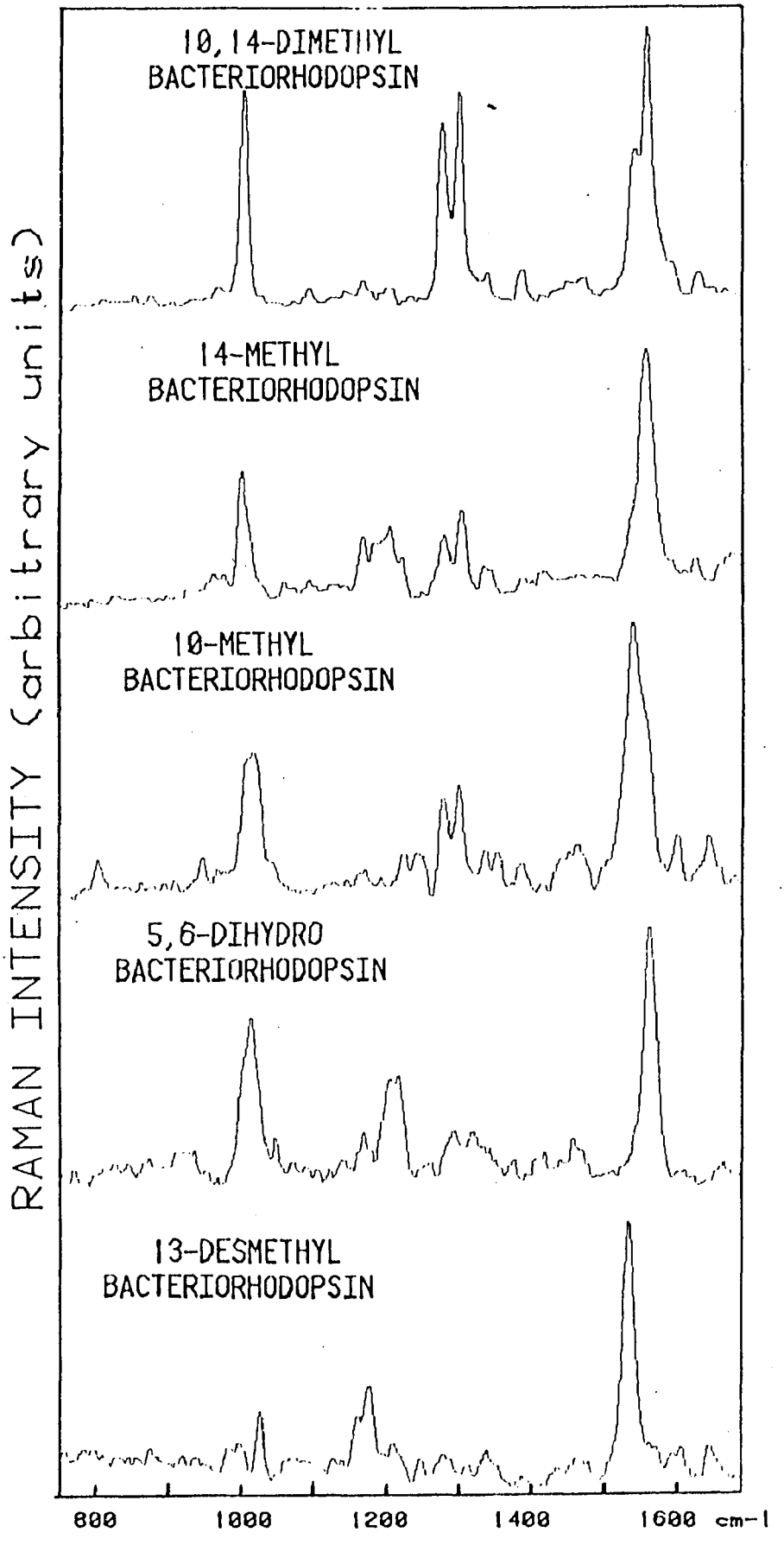
10,14-DIMETHYL
BACTERIORHODOPSIN
14-METHYL
BACTERIORHODOPSIN
10-METHYL
BACTERIORHODOPSIN
5,6-DIHYDRO
BACTERIORHODOPSIN
13-DESMETHYL
BACTERIORHODOPSIN
RAMAN INTENSITY (arbitrary units)
800
1000
1200
1400
1600
cm-1

unchanged for all the analogs, the relative intensity (all spectra are normalized to the intensity of the C=C stretch vibration) increases as the number of methyl groups on the polyene chain increases. Thus, 13-desmethyl BR, with the smallest number of methyls, has the weakest intensity for this line. Native BR has a larger peak, while 10-methyl and 14-methyl BR are larger still, and roughly equivalent. The most intense line at this frequency is in 10, 14-dimethyl BR, which has the greatest number of methyl groups. Moreover, the intensity of this line in the latter pigment is approximately equal to the sum of the intensities of the 10-methyl and 14-methyl pigments. These facts argue strongly for this line to be assigned to a methyl group vibration. The 5,6-dihydro pigment is excluded from this analysis because double bond effects alter the strength of its 1010 cm^{-1} line.

Figure 11 shows a plot of the linear relationship between the number of methyl groups in a chromophore versus the relative intensity of the 1010 cm^{-1} line. What should be noticed is that 13-desmethyl is assigned two methyl groups, BR is associated with three, 10-methyl and 14-methyl have four, and 10,14-dimethyl has five. The two methyl groups attached at the C_1 position have not been taken into account and the curve still goes through the origin, signifying that these two methyls do not contribute appreciably to the intensity of the 1010 cm^{-1}

Figure 11

A plot of the relative intensity of the 1010 cm^{-1} methyl stretch Raman line for the five BR analogs studied here versus the number of methyl groups in the chromophore of each analog.

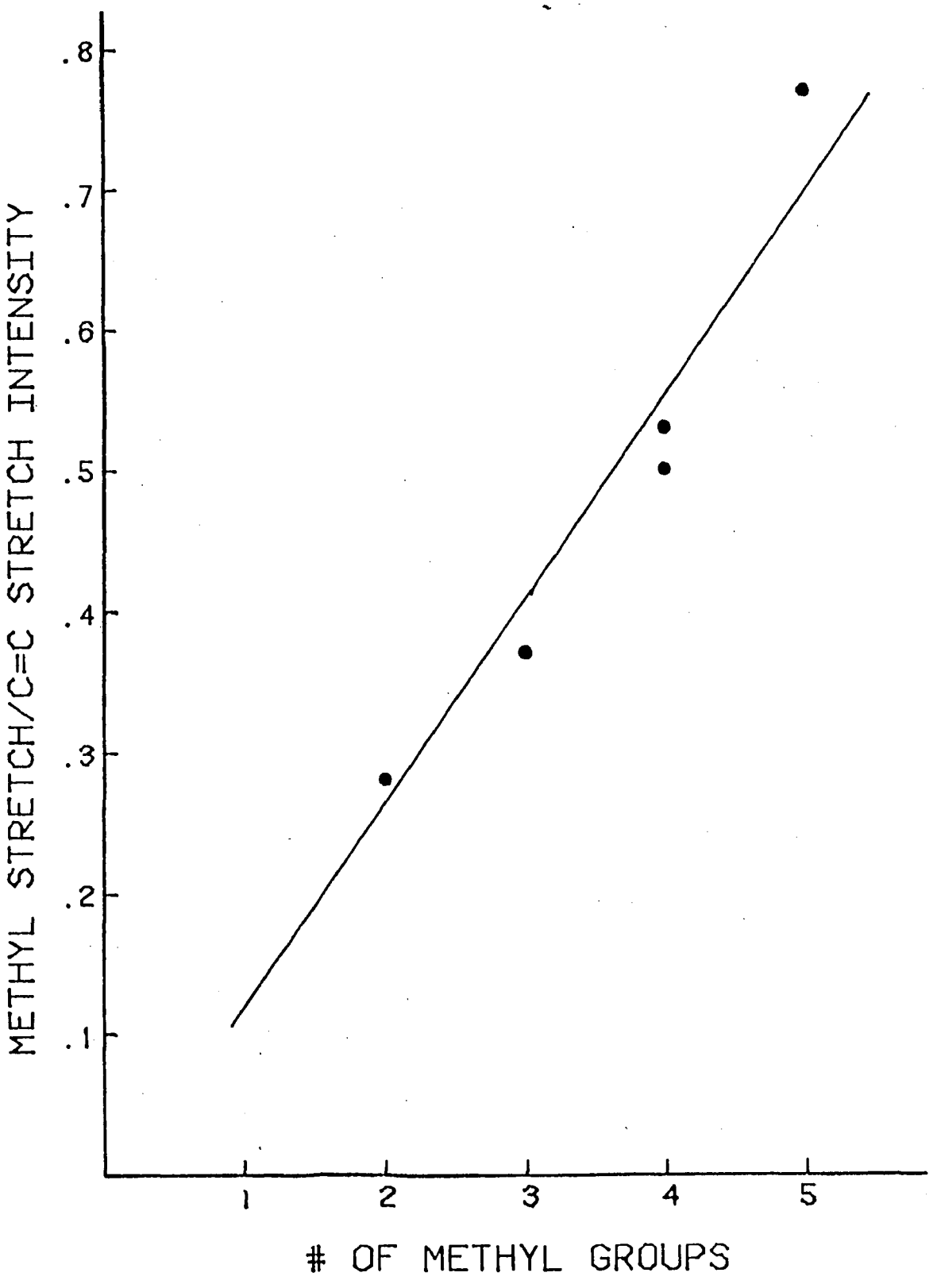
METHYL STRETCH/C=C STRETCH INTENSITY
.8
.7
.6
.5
.4
.3
.2
.1
1
2
3
4
5
OF METHYL GROUPS

vibrational mode. This is to be expected, since these methyls are not on the conjugated π-electron chain, and the $\pi-\pi^*$ transitions, which are the major contributors to the Raman intensities (Honig et al., 1976), are associated with that chain.

In the retinal analog spectra of Figure 12 and in the protonated Schiff base spectra of Figure 13 (note that 14-methyl and 10,14-dimethyl retinal do not form protonated Schiff bases, for reasons to be discussed later, and hence are not included in Fig. 13), the relative intensity of the 1010 cm^{-1} line is considerably less than in the corresponding pigment compounds. The implication of this may be understood by considering the A term expression for the Raman intensity (see Section I). The larger the Franck-Condon integrals in the numerator of that expression are, the more intense the Raman line will be. The Franck-Condon factors are proportional to the amount of distortion of the excited state, measured along the equilibrium nuclear coordinate of a particular mode, as compared to the ground state. It follows, then, that since the intensities of the 1010 cm^{-1} line are greater in the pigments than in the model compounds, that a greater distortion of the excited state along that mode's normal coordinate exists when the chromophore is in the protein binding site than when it is in solution, at least along the normal coordinate of the methyl vibration.

Figure 12

Resonance Raman spectra of five retinal analogs, taken at room temperature with the 647.1 nm laser line. All samples were suspended in methanol. The resolution is 8 cm^{-1}.

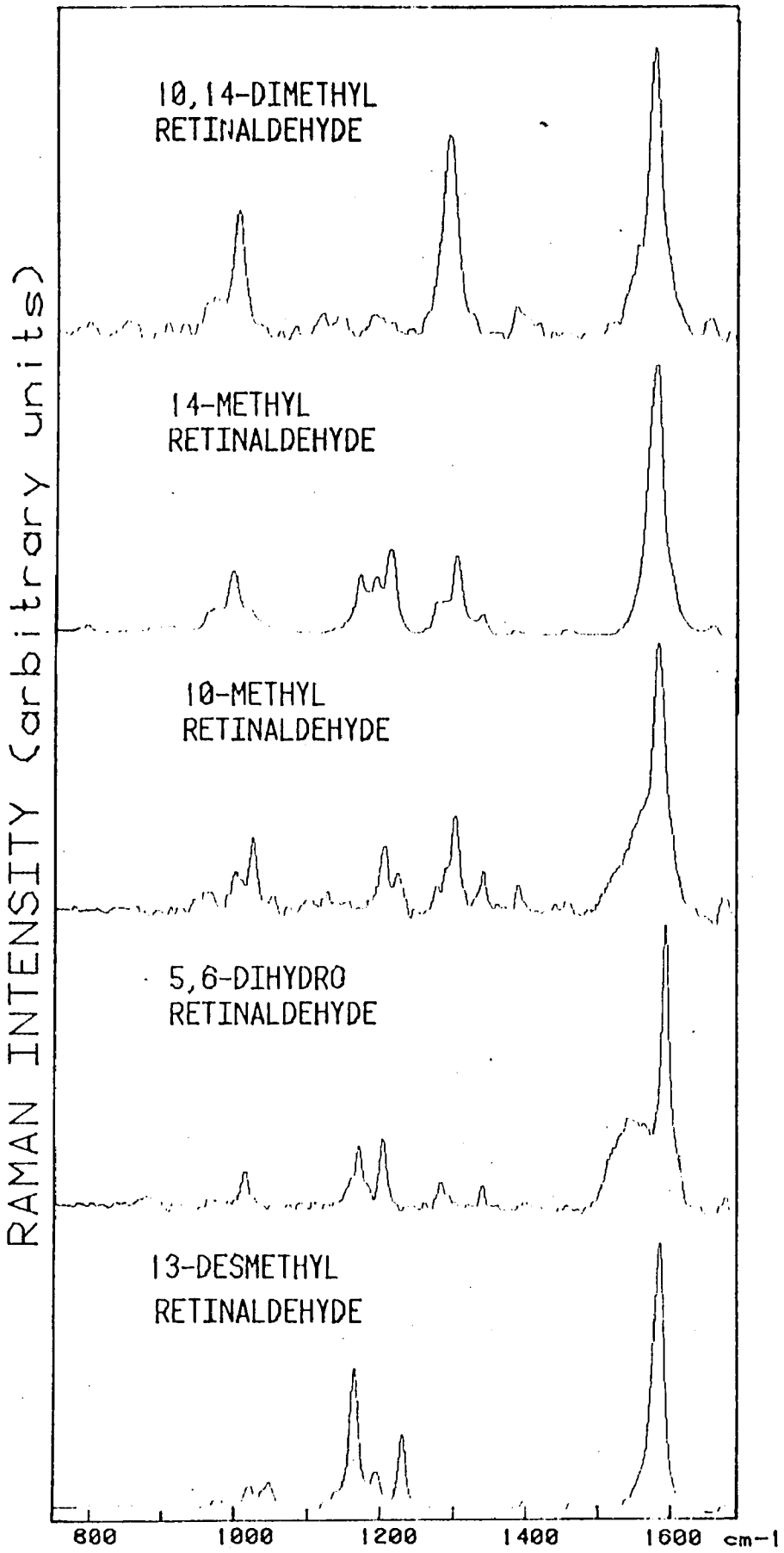
10,14-DIMETHYL
RETINALDEHYDE
14-METHYL
RETINALDEHYDE
10-METHYL
RETINALDEHYDE
5,6-DIHYDRO
RETINALDEHYDE
13-DESMETHYL
RETINALDEHYDE
RAMAN INTENSITY (arbitrary units)
800
1000
1200
1400
1600
cm-1

Figure 13

Resonance Raman spectra of three protonated Schiff base analogs of retinal, taken at room temperature with the 647.1 nm laser line. All samples are suspended in methanol. The resolution is 8 cm^{-1}.

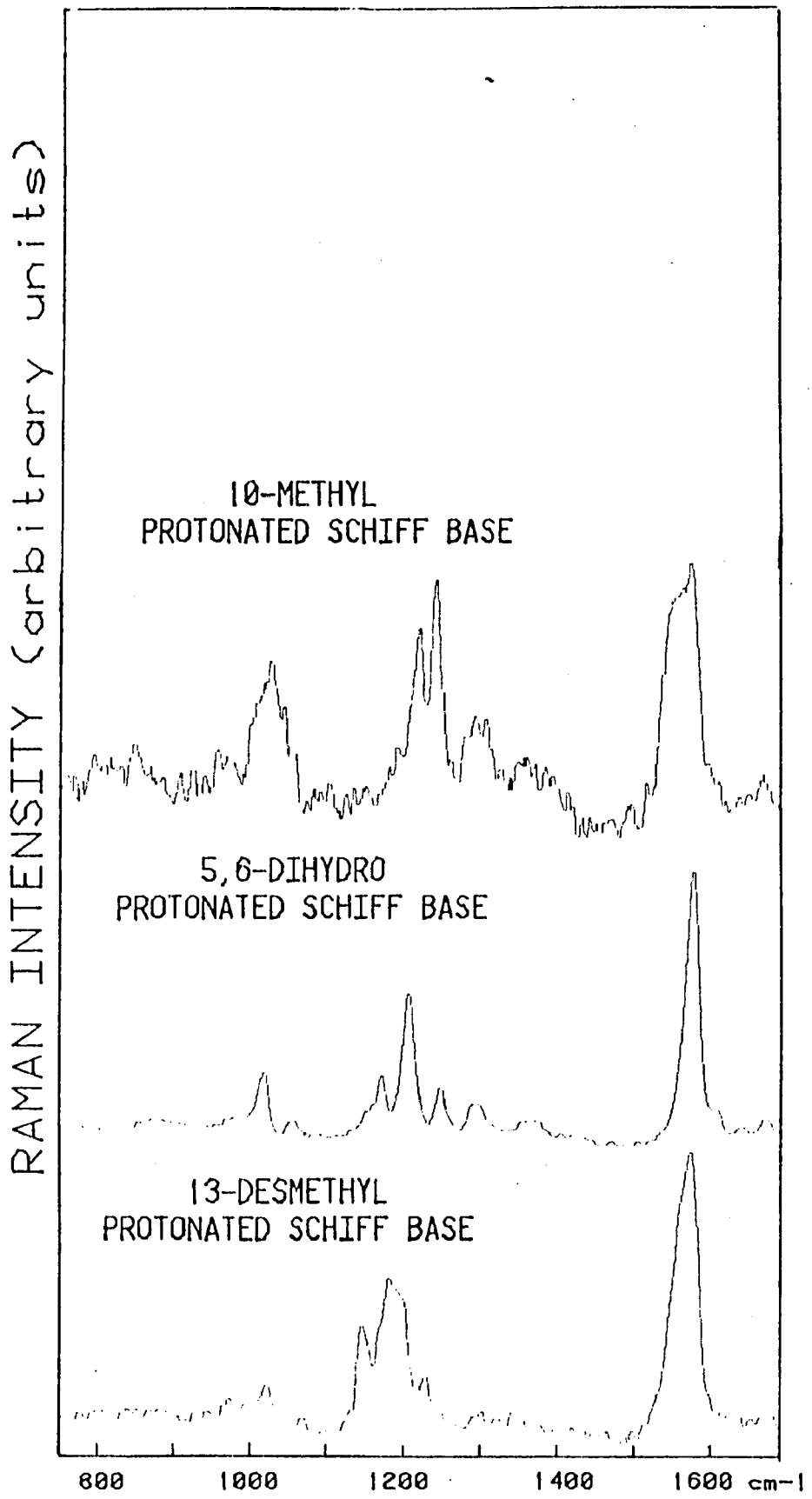
RAMAN INTENSITY (arbitrary units)
10-METHYL
PROTONATED SCHIFF BASE
5,6-DIHYDRO
PROTONATED SCHIFF BASE
13-DESMETHYL
PROTONATED SCHIFF BASE
800
1000
1200
1400
1600 cm-1

The line at 1300 cm^{-1} appears to exhibit the same additive intensity relationship for 10,14-dimethyl BR, 14-methyl BR, and 10-methyl BR as does the 1010 cm^{-1} line, but the correlation does not extend to the other pigments. One possible assignment for this mode is that of an interaction vibration of adjacent methyl groups - the 9- and 10-methyl groups, and the 13- and 14-methyl groups. The 10,14-dimethyl pigment, with two pairs of adjacent methyls, has a line at 1300 cm^{-1} with twice the intensity of that in the 10-methyl and 14-methyl pigments, each with one pair of adjacent methyl groups. In addition, the relative intensity of the line is the same in the pigment and solution spectra of each of the three analogs, unlike the 1010 cm^{-1} line. The local environment (whether solvent or protein) does not seem to have an effect on the 1300 cm^{-1} mode, which lends support to the assignment. Another possibility is that this line arises from a change in the normal mode structure of the polyene chain due to the added methyls. In this context, note that the 1300 cm^{-1} line seems to gain intensity at the expense of the 1205 cm^{-1} line, indicating that a shift in normal mode frequencies may be present.

A relatively strong line is seen in BR at 1205 cm^{-1}. This line appears again in the 5,6-dihydro BR spectrum with the same relative intensity. Apparently, divorcing the ring from the conjugated chain (which is the effect of sat-

urating the ring's double bond) has no effect on that mode, which implies that the 1205 cm^{-1} vibration is purely a chain mode, having no interactions with the ring. The same argument can be made for this line in the protonated Schiff base spectra of 5,6-dihydro retinal and all-trans and 13-cis retinals. When the intensities of this line in the pigment and solution spectra are compared for each retinal, one notices a sharp decrease in this mode's strength in the regenerated compounds compared to the model chromophores. In addition, this line is present in the 10-methyl retinal model compounds but is also reduced in intensity in the pigment. This pattern of decreased intensity of the 1205 cm^{-1} line in the regenerated form of these various chromophores suggests that a relaxation of the excited state of the molecule along this mode's normal coordinate occurs in the binding site of the protein which reduces the relative distortion between the ground and excited states in solution.

Ethylenic Mode Region

The C=C stretching mode vibrations, known as "ethylenic" modes, are by far the strongest in the resonance Raman spectra of bacteriorhodopsin, visual pigments, model compounds, and in all analogs of those molecules. Their intensity is due to large changes between the ground and excited state geometries, as measured along the equilibrium nuclear coordinate of this vibration, which increase the

values of the Franck-Condon factors and, in turn, of the A term in Albrecht's intensity expression (Callender and Honig, 1977). The number of possible lines that can appear in this region is equal to the number of C=C double bonds in the molecule. In most cases, however, most of the lines are degenerate or Raman silent and hence are not distinguishable. With the analogs, however, we can detect a lifting of the degeneracy. The 10,14-dimethyl pigment has three noticeable ethylenic lines, while the 10-methyl pigment has a strong shoulder which appears on the high frequency side of the main band. As will be shown further, a red-shifted intermediate would have a shoulder on the low frequency side of the intense band, and therefore it is clear that we are observing lines in the parent pigment only. The lifting of the degeneracy, which is also seen in 11-cis retinal crystals, may be due to the steric hindrance involved in fitting the extra methyl groups of the analogs into the protein binding site. A twisting of the bonds to relieve this hindrance would be a likely cause of the removal of the degeneracy. Alternatively, the extra mass on the polyene chain, or the changed electronic structure of the molecule, could also induce the same result. There is also a general broadening of the ethylenic lines in the model compound solution spectra compared with those in the pigment spectra. This is most probably caused by slight differences in the ground state vibrational levels of the

various chromophore molecules due to their random degree of exposure to the solvent molecules. In the pigments, however, the local environments of the chromophore molecules are the same due to protein shielding, and therefore the ground state vibrational levels for the retinal molecules are likely to be more uniform than in solution, causing sharper Raman peaks.

Let us now focus our attention on the factors that determine the frequency of the ethylenic mode vibration. Rimai and coworkers were the first to suggest a connection between the absorption maximum of one of the pigments and the position of its C=C mode in the Raman spectrum (Heyde et al., 1971). A cartesian plot of these two parameters for a large number of retinals, protonated Schiff bases, and pigments has revealed a linear relationship between the two. As the absorption peak shifts toward the red, the ethylenic frequency is lowered, and vice-versa. It has been suggested that the regulation of the color of the visual pigments is controlled by the extent of π-electron delocalization along the conjugated chain (see, for example, Callender and Honig, 1977). An increased delocalization lowers the energy of both the ground and first excited states. It has been shown, however, that the excited state is lowered in energy more than the ground state, causing a bathochromic shift in absorption (Honig and Ebrey, 1974). The delocalization, then, affects the

character of the bonds of the polyene chain, decreasing the electron density of the double bonds and increasing that of the single bonds. Consequently, if we think of the electron density as being proportional to the force constants of the vibration, the frequency is lowered by reducing the force constant. Thus the linear correlation of the absorption maximum with the ethylenic frequency is a confirmation of the fact that π-electron delocalization is the mechanism for color regulation in the visual pigments and bacteriorhodopsin. In Figure 14, this correlation is extended to the bacteriorhodopsin analogs. The slope of the curve is roughly the same as it is in other studies, about 4 nm for each cm^{-1} (Doukas et al., 1978b). The intercepts are also very close, making this curve virtually identical to the curve in Doukas et al. (1978b). Thus the position of the C=C band is a sensitive indicator of the extent of delocalization of the π-electrons.

We can explain the absorption shifts and the relative ethylenic position of the various analog model compounds and pigments on the basis of the arguments of the preceding paragraph. When the oxygen of the aldehyde form of the analogs is replaced by the less electronegative nitrogen, there is a tendency for the π-electrons to localize on the various atoms. Thus the absorption maximum is blue-shifted with respect to the aldehyde, roughly from 380 nm

Figure 14

Correlation of ethylenic (C=C) stretching frequency of bacteriorhodopsin and its analogs with their respective absorption maxima.

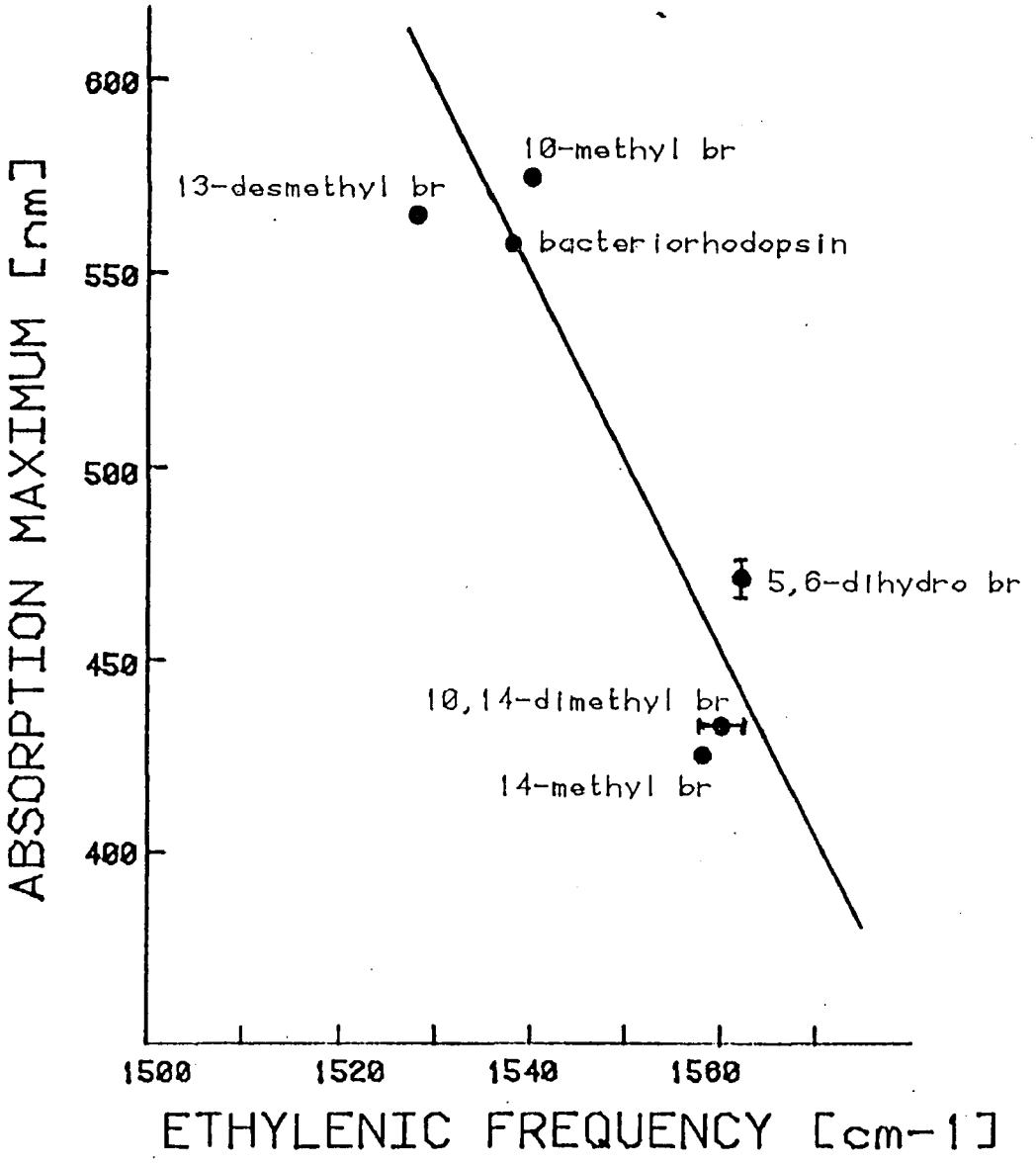
ABSORPTION MAXIMUM [nm]
600
550
500
450
400
10-methyl br
13-desmethyl br
bacteriorhodopsin
5,6-dihydro br
10,14-dimethyl br
14-methyl br
1500
1520
1540
1560
ETHYLENIC FREQUENCY [cm-1]

to 370 nm. Protonating the Schiff base pulls the π-electrons towards the proton and causes a large red shift in the absorption, to about 440 nm. X-ray studies of all-trans retinal and its unprotonated and protonated Schiff base forms in fact show a significant change of the bond alternation, especially between the latter two species (Hamanaka et al., 1972).

Absorption studies on model compounds, mostly protonated Schiff bases, have shown that their absorption maxima depend on the environment of the molecule (Erikson and Blatz, 1968; Irving et al., 1970; Blatz et al., 1972; Blatz, 1972; Blatz and Mohler, 1972). In addition, theoretical calculation has shown that negative or positive charges placed in appropriate positions in the proximity of the chromophore can induce significant wavelength shifts (Wiesenfeld and Abrahamson, 1968; Waleh and Ingraham, 1973; Suzuki et al., 1974; Honig et al., 1976). In fact, any mechanism that increases delocalization should induce bathochromic shifts in the absorption spectra. Thus, the protein, by controlling the micro-environment of the chromophore in the opsin matrix, can regulate the absorption spectra of the pigments. Figure 14 tends to indicate that a similar mechanism regulates the colors of the artificial bacteriorhodopsin.

The high degree of correlation among the various pigments and model chromophores also suggests that there is

little double bond twisting in the analog chromophores. A model based on double bond twisting has been advanced to explain color regulation (Kakitani and Kakitani, 1975). As has been pointed out by Doukas et al. (1978b), the model compound data arise from strain - free chromophores in solution. Thus, it would be quite accidental that chromophore electron density patterns arising from two quite different sources, electron delocalization in chromophores with strain-free double bonds in some cases and twisted double bonds in others, would all give the same correlation of absorption maximum with ethylenic stretching frequency.

Terminal End Group

The band around 1670 cm^{-1} in the retinal analogs as well as in the unmodified retinal compounds is assigned to a C=O stretching vibration. The frequency has been shown to be insensitive to the conformation of the isomer, but it is affected by the polarity of the solvent (see, for example, Heyde et al., 1971; Doukas, 1977). Polar solvents generally decrease the frequency of the C=O vibration. This effect may be due to hydrogen bonding of the solvent to the oxygen of the carbonyl group.

In the Schiff base form of various retinals, the line appearing between 1620 cm^{-1} and 1640 cm^{-1} has been labeled as a C=N stretching vibration. In all the retinals, protonation of the Schiff base not only red-shifts the absorption maximum, but also increases the frequency

of this end group vibration in the resonance Raman spectrum by roughly 30 cm^{-1}. This shift between the C=N and $C=NH^{+}$ modes was first noted by Rimai and coworkers (Heyde et al., 1971). To confirm that the frequency of this line was due to protonation, Oseroff and Callender (1974) exchanged the proton on the Schiff base for a deuteron and noticed a measurable decrease in the stretching frequency, from about 1655 cm^{-1} to 1630 cm^{-1}. Thus the position of this end group vibration has been used extensively to identify the state of protonation of a chromophore in its protein environment.

In the spectra of the bacteriorhodopsin analogs (Figure 10), we notice a line in the 10-methyl, 13-desmethyl, and 5,6 dihydro pigments in the 1640 - 1660 cm^{-1} range which shifts to lower frequencies upon deuteration (Figure 15). This clearly indicates that the chromophores of these analog pigments are linked to their respective binding sites by protonated Schiff bases. This, along with protein interaction effects, accounts for the absorption peaks of these molecules being considerably red-shifted from their non-regenerated counterparts.

Consideration of the 14-methyl and 10,14-dimethyl pigments, however, reveals that the end group mode has a frequency of only 1625 cm^{-1} and this line did not shift upon substituting deuterium oxide for water. These facts imply that these two pigments are connected to the protein

Figure 15

Resonance Raman spectra of five bacteriorhodopsin analogs suspended in deuterium oxide (D_2O) at 85 K. The 10,14-dimethyl and 14-methyl spectra were taken with the 488.0 nm laser line, while the 10-methyl, 5,6-dihydro, and 13-desmethyl spectra were taken with the 520.8 nm laser line. The resolution in all cases is 7 cm^{-1}.

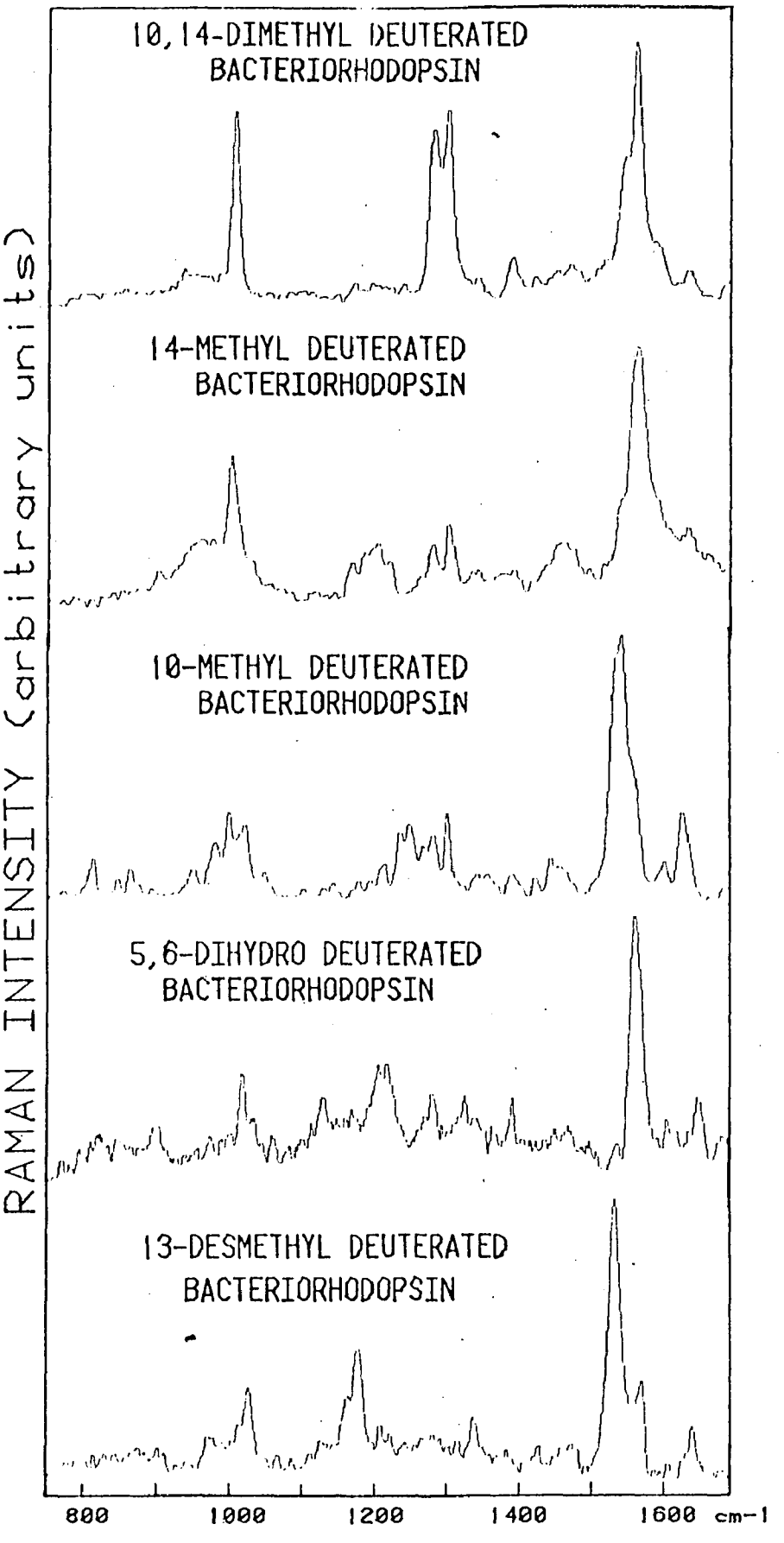
10,14-DIMETHYL DEUTERATED
BACTERIORHODOPSIN
14-METHYL DEUTERATED
BACTERIORHODOPSIN
10-METHYL DEUTERATED
BACTERIORHODOPSIN
5,6-DIHYDRO DEUTERATED
BACTERIORHODOPSIN
13-DESMETHYL DEUTERATED
BACTERIORHODOPSIN
RAMAN INTENSITY (arbitrary units)
800
1000
1200
1400
1600
cm-1

via unprotonated Schiff bases. This would be consistent with the blue-shifted λmax of these two analogs, compared with the other pigments (Table 1). Because the C=N bond is unprotonated, the extent of delocalization of the π-electrons is considerably less than in protonated chromophores, and hence the absorption peak is hypsochromically (blue-) shifted.

Schrekenbach et al. (1978) have proposed a scheme for the various steps in the combination of a retinal chromophore with bacterio-opsin to form a pigment. Initially, the chromophore binds non-covalently in the binding site, and the absorption shifts from 375 nm (all-trans retinal) to 400 nm when co-planarization of the ring and chain occurs. Further interaction with the protein moves to 430 nm and formation of the pigment is completed by a reaction mediated by a base, termed B_2, with a PK of 4.5. This last step is restricted to the all-trans and 13-cis isomers of retinal. Perhaps it is in this last step that the presence of a 14-methyl group on the retinal (in the 14-methyl and 10,14-dimethyl analogs) becomes critical. The protonation of the Schiff base may be blocked by the 14-methyl group. This is especially interesting in view of the fact that 14-methyl retinal has been regenerated with bovine opsin to form the artificial visual pigment 14-methyl rhodopsin, and this pigment did not exhibit any appreciable differences from native rhodopsin in its absorption or CD

spectra, or in its photosensitivity (Chan et al., 1974; Ebrey et al., 1975). This is another example, in addition to the variances as to which isomers are accommodated, of the differences that exist between the binding sites of bacteriorhodopsin and rhodopsin.

The absolute position of the end group vibration can be correlated with the absorption maximum for the various analog pigments and protonated Schiff bases, and this correlation can be extended to the native pigments and unmodified protonated Schiff bases as well. In Figure 16, the position of the $C=NH^+$ mode is plotted versus the ethylenic frequency (which, as was shown previously, is proportional to λmax) for each compound. For each molecule, the frequency of the terminal group's vibration shifts linearly with the C=C vibration. As in Figure 14, the increased π-electron delocalization of the pigment weakens the force constant between the oscillating carbon and nitrogen atoms and shifts the vibration to lower frequencies. The correlation exhibited by this graph supports the contention mentioned in the discussion of Fig. 14 that twisting of double bonds is an unlikely cause of color regulation, since both model chromophores, which are strain-free, and pigments fit nicely on the curve.

We must now turn our attention to considering the effect of the protein environment on the C=C and $C=NH^+$ stretching vibrations. It is of interest to consider the

Figure 16

Correlation of the protonated Schiff base ($C=NH^+$) stretching frequency with the ethylenic (C=C) stretching frequency for various protonated Schiff base retinal analogs, their corresponding BR pigments, and "natural" bacteriorhodopsin and some of its photoproducts. Abbreviations: 13-D R, 13-desmethyl retinal; 5,6-D R, 10-methyl retinal; A-T R, all-trans retinal; BRLA, light-adapted bacteriorhodopsin; BRDA, dark-adapted bacteriorhodopsin. The data on all-trans retinal (protonated Schiff base) and dark- and light-adapted BR were taken from Aton et al., 1979. Rhodopsin (RH) and bathorhodopsin (BATHO) data, taken from Aton et al., 1980, have been included for comparison.

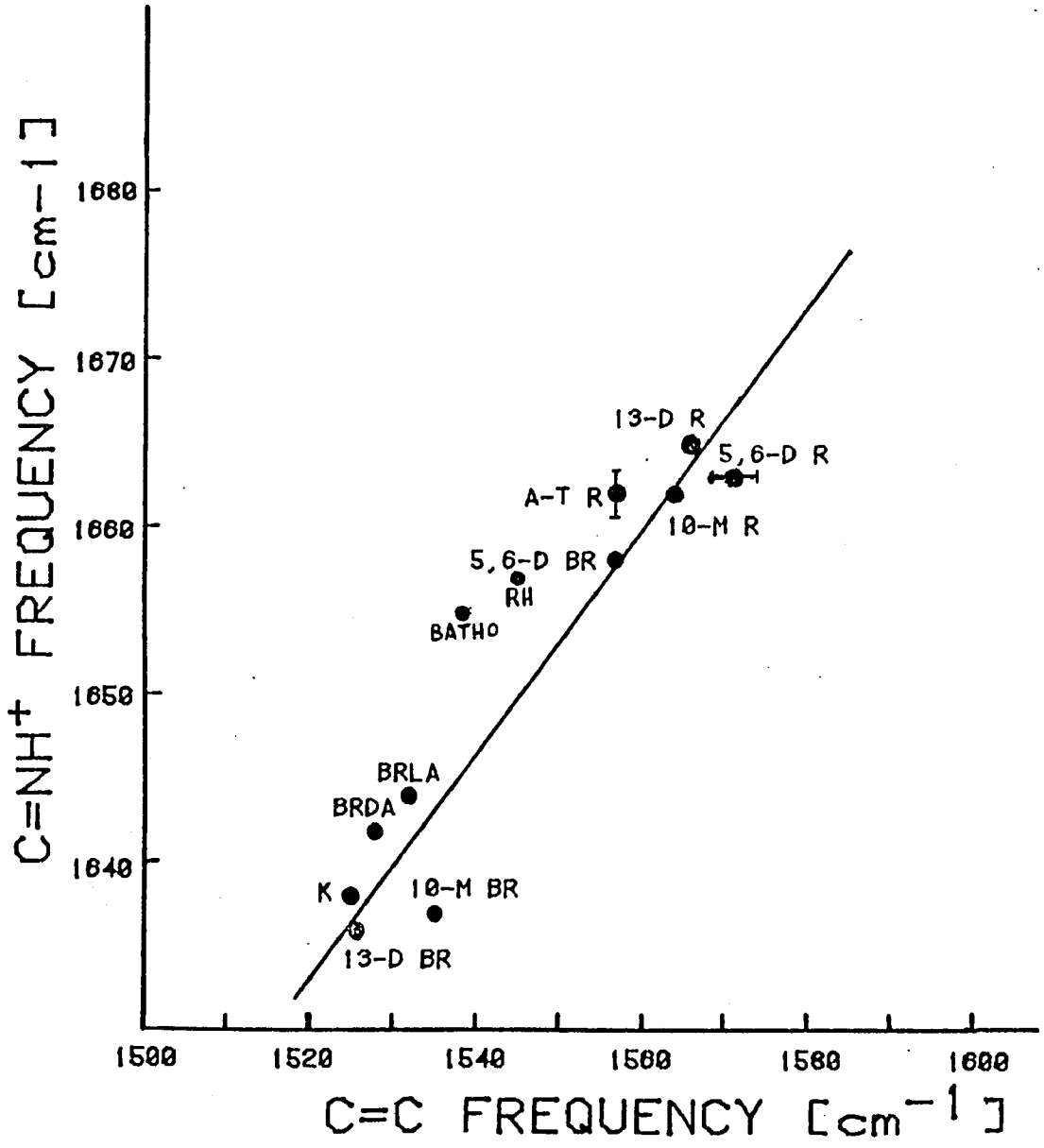
C=NH+ FREQUENCY [cm-1]
1680
1670
1660
1650
1640
13-D R
5,6-D R
A-T R
10-M R
5,6-D BR
RH
BATHO
BRLA
BRDA
K
10-M BR
13-D BR
1500
1520
1540
1560
1580
1600
C=C FREQUENCY [cm-1]

relative positions of these lines. The upper part of Table 2 lists, for the protonated Schiff bases of various retinals, the differences between the frequencies of these two bands (14-methyl and 10,14-dimethyl are omitted since they do not form protonated Schiff bases). The lower half of the table contains the same information for these retinals regenerated into pigments (all are dark-adapted for uniformity). We notice that for each chromophore, the increased delocalization of the protein environment over that of the solution ambience does not affect the relative positions of the two lines. For example, the difference between the two stretching frequencies in 10-methyl retinal P.S.B. is 98 cm^{-1} while in 10-methyl BR it is 102 cm^{-1}. Thus both the C=C stretch and the $C=NH^{+}$ stretch are influenced to the same extent by the change in π-electron delocalization. The table also indicates that various modifications in the chromophore structure do not disturb the energy difference between the two modes, both in solution and in the protein; the entries in the last column are very nearly the same in both the upper and lower halves of the table. In order to observe the impact of the chemical modifications of the retinals on the extent of the increase in π-electron delocalization caused by the protein, we have tabulated in Table 3 the shifts in frequency of the C=C stretch and $C=NH^{+}$ modes as the chromophore's environment changes from solution to protein. The last column of

Table 2

END GROUP AND ETHYLENIC FREQUENCIES

I. Protonated Schiff Bases

Chromophore	C=NH+	C=C	(C=NH+)-(C=C)
	(centimeters^{-1})		
All-Trans Retinal	1662	1557	105
10-Methyl Retinal	1662	1564	98
5,6-Dihydro Retinal	1663	1571	92
13-Desmethyl Retinal	1665	1566	99

II. Pigments

Bacteriorhodopsin	1642	1528	114
10-Methyl BR	1637	1535	102
5,6-Dihydro BR	1658	1557	101
13-Desmethyl BR	1636	1526	110

Table 3

FREQUENCY SHIFTS AMONG ANALOGS

I. C=C STRETCH

Chromophore	P.S.B.	Pigment	Difference
	(centimeters^{-1})		
All-Trans Retinal	1557	1528	29
10-Methyl Retinal	1564	1535	29
5,6-Dihydro Retinal	1571	1557	14
13-Desmethyl Retinal	1566	1526	40

II. C=NH+ STRETCH

All-Trans Retinal	1662	1642	20
10-Methyl Retinal	1662	1637	25
5,6-Dihydro Retinal	1663	1658	5
13-Desmethyl Retinal	1665	1636	29

Table 3 indicates that all-trans retinal, 10-methyl retinal, and 13-desmethyl retinal all experience the same degree of increased delocalization when inserted into the bacterio-opsin binding site,as evidenced by the nearly uniform shifts of the delocalization-sensitive vibrations (the C=C differences, for example, are all within 6 cm^{-1}, our resolution limit, of 35 cm^{-1}). The 5,6-dihydro moiety, however, exhibits a much smaller response to delocalization when bound to the protein - the C=C mode's frequency is reduced by only 14 cm^{-1}, and the $C=NH^{+}$ mode by only 5 cm^{-1}. Apparently, the binding site interactions with the chromophore are different for 5,6-dihydro Br than for the other three pigments.

These findings for the 5,6-dihydro compound are similar to those reported by Nakanishi, Honig, and co-workers using that analog and other dihydro retinals as protonated Schiff bases and regenerated with bacterio-opsin to form pigments (Nakanishi et al., 1980). On the basis of the protein's effect on the positions of the various absorption peaks of those compounds, they concluded that a counterion is located in the protein about 3.5 Å from the ionone ring in bacteriorhodopsin which, along with the counterion near the protonated Schiff base, controls the chromophore's color. The blue-shifted absorption of the 5,6-dihydro pigment (472 nm compared with 568 for BR), is then explained by the increased separation in this analog between the conjugated

polyene chain and the counterion near the ring. The data presented here support that model, and show that the extent of delocalization in 5,6-dihydro BR is not so great as it is in bacteriorhodopsin. The data also suggest that there is a minimal amount of perturbation in the degree of π-electron delocalization caused by the various methyl modifications studied here.

We have previously mentioned the deuteration effect upon the $C{=}NH^+$ vibration. It is of interest to consider the extent of the downshift in frequency for our set of analogs. Table 4 contains a summary of this information, taken from Figures 9, 10, and 15. In order to interpret the tabulated information, we must understand what the cause of the frequency reduction upon deuteration is.

As has been pointed out previously, it is generally the case that protonation increases the frequency of the C=N stretch. This seems to run counter, however, to our observation that protonation increases the extent of π-electron delocalization, and hence weakens the double bonds. Moreover, another factor, the increased effective mass of the nitrogen resulting from protonation, should also tend to decrease the vibrational frequency, based on a simple harmonic oscillator model. Clearly then, other factors are operative here in shifting the $C{=}NH^+$ vibration upward in frequency.

Table 4

END GROUP FREQUENCY SHIFTS

Pigment	C=NH+	C=ND+	(C=NH+)-(C=ND+)	C=C	(C=NH+)-(C=C)
		(cm^{-1})			
Bacteriorhodopsin	1642	1625	17	1534	114
10-Methyl BR	1637	1616	21	1535	102
5,6-Dihydro BR	1658	1636	22	1557	99
13-Desmethyl BR	1636	1632	4	1526	110

It has been proposed by Aton et al. (1980), on the basis of a computer model normal mode analysis, that protonated Schiff base C=N stretching frequencies are "pushed up" by interactions with the C=N-H bending mode (typically at 1250 cm^{-1}), which of course are absent in the unprotonated Schiff bases. Upon deuteration, the frequency of the C=N-H bending mode shifts down to 947 cm^{-1} (as a C=N-D bend), which reduces the extent of interaction with the C=N stretch because of the increased separation of the vibrational frequencies. Thus the downshift due to deuteration is not primarily a reduced mass effect, as was previously assumed, but rather because the C=N stretching mode is not being pushed up as much as in the protonated case. The suggestion of Aton et al. (1980), then, explains the direction of the shifts in the C=N vibration both upon protonation and deuteration. They also point out that coupling between the C=C stretch and the C=N stretch vibrations would generally increase the frequency of the latter mode. The last column in Table 4 gives the closeness in energy between the ethylenic and Schiff base stretching modes and may be used as a rough guide as to the relative extent of coupling between them. All the values listed are within 5% of an average value of 107 cm^{-1} and so indicate that the interaction of the two stretching modes is approximately the same for all the pigments considered here. Interestingly, native bacteriorhodopsin, 10-methyl BR, and 5,6-dihydro BR all exhibit the same deuteration downshift.

Based on the model of Aton et al. (1980), this is entirely reasonable, since adding a methyl group on the 10-carbon or saturating the ionone ring should not affect the interaction of the C=N-H bend with the C=N stretch. These data are not consistent, however, with a suggestion made by Lewis et al. (1978) and by Terner et al. (1979). They observed that for various intermediates of bacteriorhodopsin, the lower the $C=NH^+$ frequency, the smaller the deuteration shift, and they suggested that this was a general pattern in retinal pigments. They then constructed a theoretical explanation of this trend, based on the extent of hydrogen bonding between the Schiff base proton and the protein. The data in Table 4 show, however, that although the $C=NH^+$ frequency is 1658 cm^{-1} in 5,6-dihydro BR and only 1637 cm^{-1} in 10-methyl BR, the deuteration downshifts for these two pigments are the same, violating the Lewis model.

An extremely small deuteration shift is observed for the 13-desmethyl pigment. One possible explanation is that it is more difficult to deuterate this compound than any of the other pigments (the procedures for deuteration were identical for all the compounds, as explained in Section II). But careful scrutiny of the protonated and deuterated spectra of this analog in Figures 10 and 15 reveals that all the lines match with the exception of the Schiff base band and a band in the 960-980 cm^{-1} region.

This seems to indicate that deuteration has indeed occurred. Another possibility is that removing the 13-methyl group somehow has an impact on the interaction of the C=N-D bend and the C=N stretch. Alternatively, the absence of the 13-methyl group may enhance the extent of coupling of the C=C mode with the C=N stretching vibration. Further investigations to determine the cause of the small downshift in deuterated 13-desmethyl BR are warranted.

Primary Event

In order to determine whether trans-cis (or in the case of the visual pigments, cis-trans) isomerization is an accurate model for the primary event in bacteriorhodopsin and rhodopsin, a series of experiments which would test that model was performed. An isomerization event implies that a major change has occurred in the conformation of the chromophore, and this change should be detectable with resonance Raman scattering techniques. In addition, the main alternate model that has been proposed for the primary event - proton translocation - suggests that the initial photoproducts in the BR and rhodopsin photocycles, namely K and bathorhodopsin, respectively, are not linked to their respective proteins by protonated Schiff's bases, since this proton has tunnelled elsewhere (Applebury et al., 1978). Should the Raman spectra of these intermediates reveal that they are still attached by protonated Schiff bases, the case for the Schiff base's proton tunnelling

away in the first picoseconds after irradiation would be severely weakened.

We see in Figure 17 the resonance Raman spectrum of the K intermediate of bacteriorhodopsin. The intense ethylenic line is shifted towards lower frequencies as compared with the parent pigment, in accordance with the red-shifted absorption of K with respect to BR. Even though K is 30% of the mixture in part (a) of the figure, it does not exert much influence on the position of the ethylenic line in that spectrum, because of the low Raman cross-section of the first intermediate.

The fingerprint region in K exhibits marked differences from that of bacteriorhodopsin. Lines at 1159, 1193, and 1211 cm^{-1} appear in K that are absent in BR, while the 1205, 1217, and 1277 cm^{-1} lines of BR are missing in K. Since that section of the spectrum has been shown to be sensitive to the chromophore's isomeric conformation, we conclude that bacteriorhodopsin has undergone a trans-cis isomerization in forming K. Additionally, lines at 1638 cm^{-1} or 1623 cm^{-1} may be assigned to the protonated Schiff base vibration. To ensure that assignment, the sample was mixed with deuterium oxide and the spectrum is presented in Figure 18. We see that the line at 1638 cm^{-1} has disappeared, and a new line appears at 1607 cm^{-1}. Clearly, then, the chromophore K is linked to its protein via a protonated Schiff base. We also notice numerous

Figure 17

Resonance Raman spectra of bacteriorhodopsin at 77 K using single and double beam excitation. (a) 488.0 nm probe beam alone; (b) 647.1 nm pump beam simultaneous with 488.0 nm probe beam, with a pump/probe ratio of 10:1; (c) computer subtraction of 70% of (b) from (a). The resolution is 7 cm^{-1}.

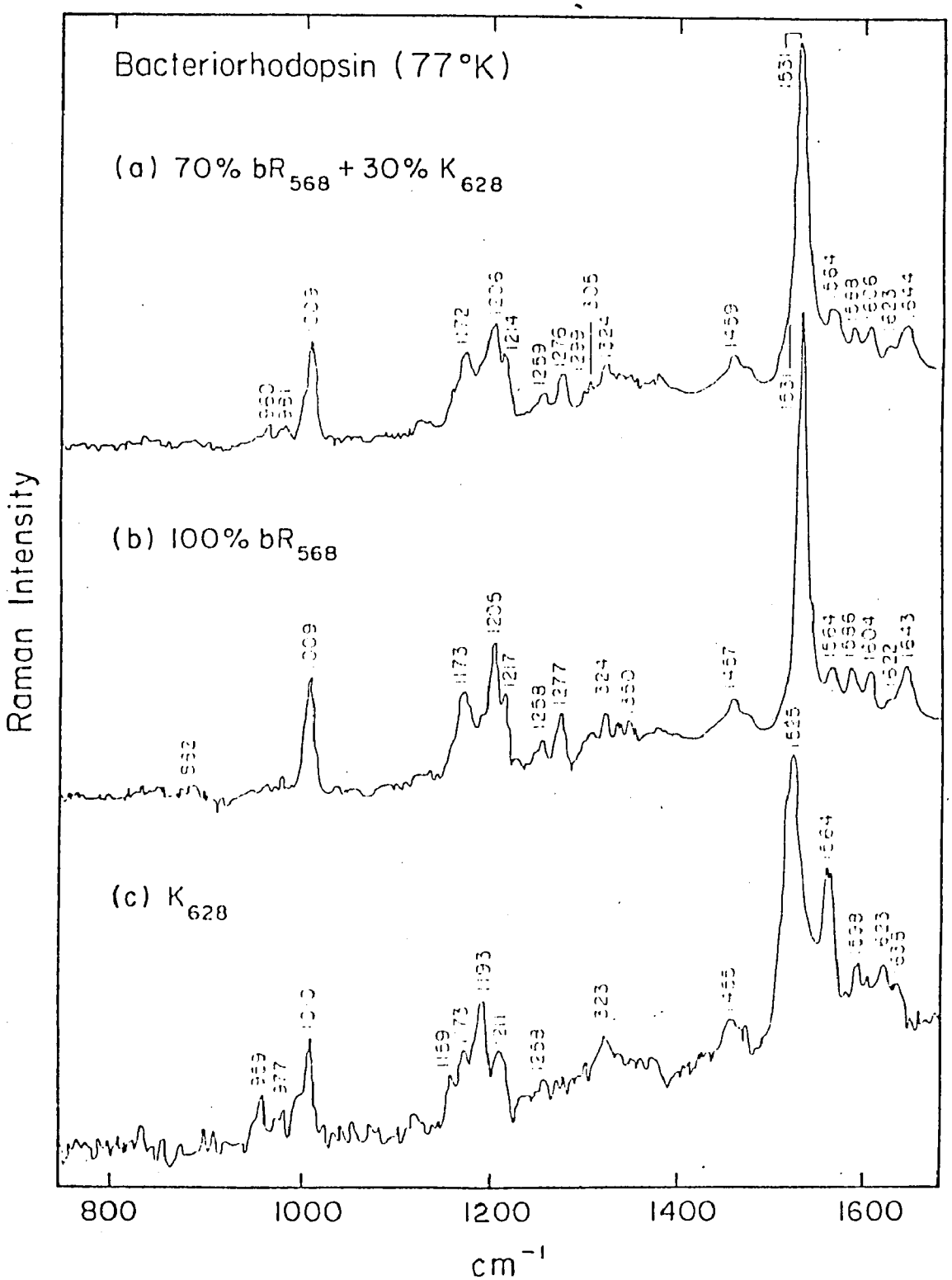
Bacteriorhodopsin (77°K)
(a) 70% bR568 + 30% K628
(b) 100% bR568
(c) K628
Raman Intensity
800
1000
1200
1400
1600
cm-1

Figure 18

Resonance Raman spectra of bacteriorhodopsin suspended in deuterium oxide (^2H_2O) using single and double beam excitation at 77 K. Descriptions of (a), (b), and (c) are identical with those of Figure 17.

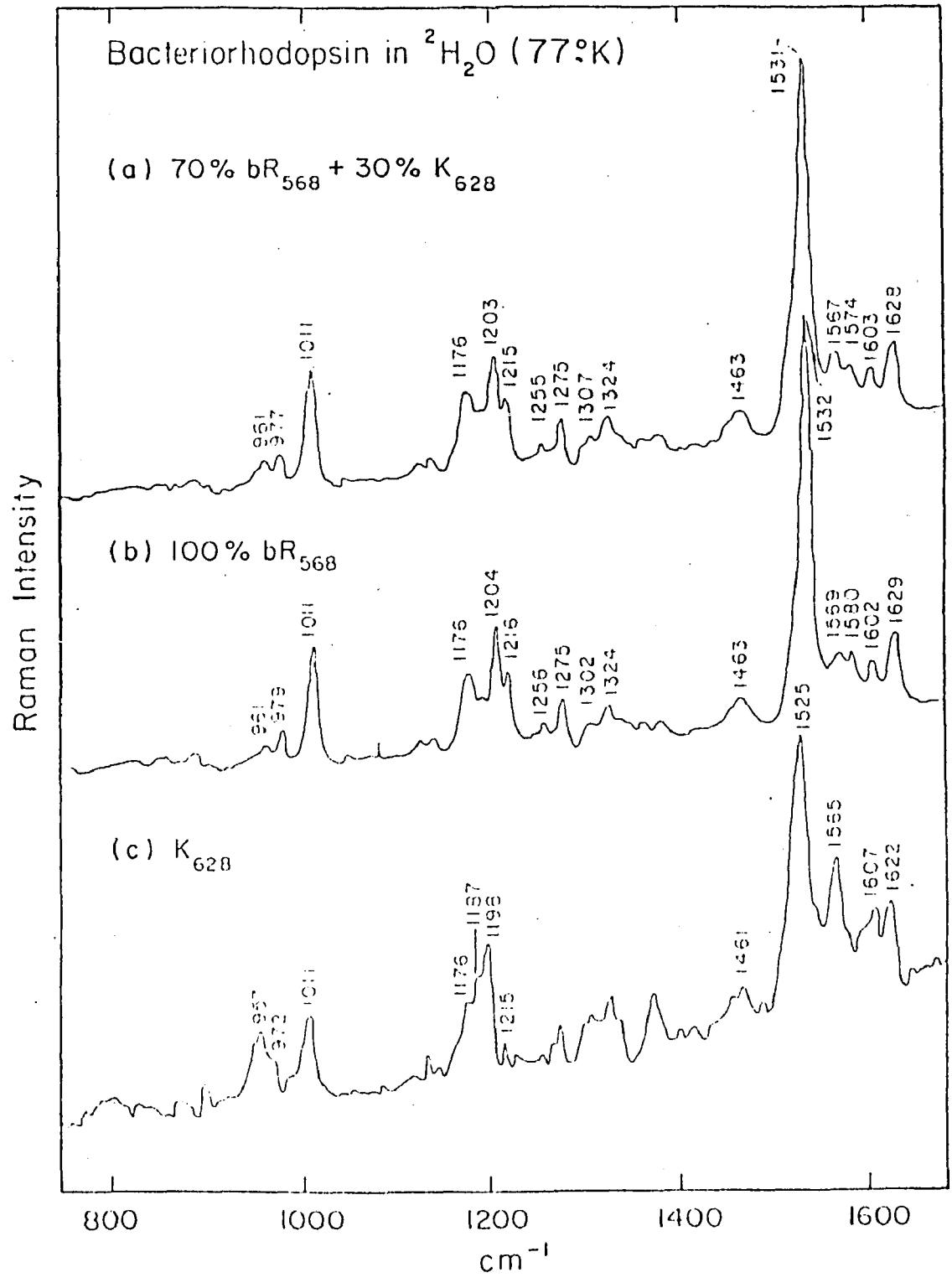
Bacteriorhodopsin in ^2H_2O (77°K)
(a) 70% bR_{568} + 30% K_{628}
(b) 100% bR_{568}
(c) K_{628}
Raman Intensity
800
1000
1200
1400
1600
cm^{-1}
951
977
1011
1176
1203
1215
1255
1275
1307
1324
1463
1531
1532
1567
1574
1603
1628
961
979
1011
1176
1204
1216
1256
1275
1302
1324
1463
1525
1559
1580
1602
1629
957
972
1011
1175
1187
1198
1215
1461
1555
1607
1622

changes in the fingerprint region of the deuterated spectrum of K as compared with its protonated spectrum, as opposed to bacteriorhodopsin, which has identical fingerprint regions in the protonated and deuterated spectra. Apparently, major changes have occurred in the BR to K transition, and a trans-cis isomerization is the most reasonable candidate for that change.

To further establish trans-cis (cis-trans) isomerization as the mechanism for the primary event in bacteriorhodopsin and rhodopsin, we have obtained from Prof. K. Nakanishi and coworkers a retinal analog, regenerated with bovine opsin, that does not isomerize in light. The structure is drawn in Figure 7. Because of the carbon chain bridging the C-10 and C-13 carbons, the molecule is "locked" into the 11-cis conformation. Figure 19b shows the room temperature Raman spectrum of the analog pigment. If this chromophore is photosensitive, then various intermediates should be contributing to the spectrum. We compared the fingerprint region of this spectrum with that of the model spectrum of the chromophore as a protonated Schiff base - see Figure 19a. The fingerprint regions are very similar, thus establishing that the chromophore in the pigment is situated in the protein binding site. We intend to measure the Raman spectrum of this pigment at liquid nitrogen temperatures. The photocycle is blocked at this temperature (Akita et al., 1980b). If that

Figure 19

Resonance Raman spectrum of the "seven-membered ring" analog, taken at room temperature. (a) The analog in methanol as a protonated Schiff base. (b) The analog regenerated with bovine opsin and dissolved in 2% octyl-glucoside. Excitation in both cases was with the 476.5 nm laser line. The resolution is 6 cm^{-1}.

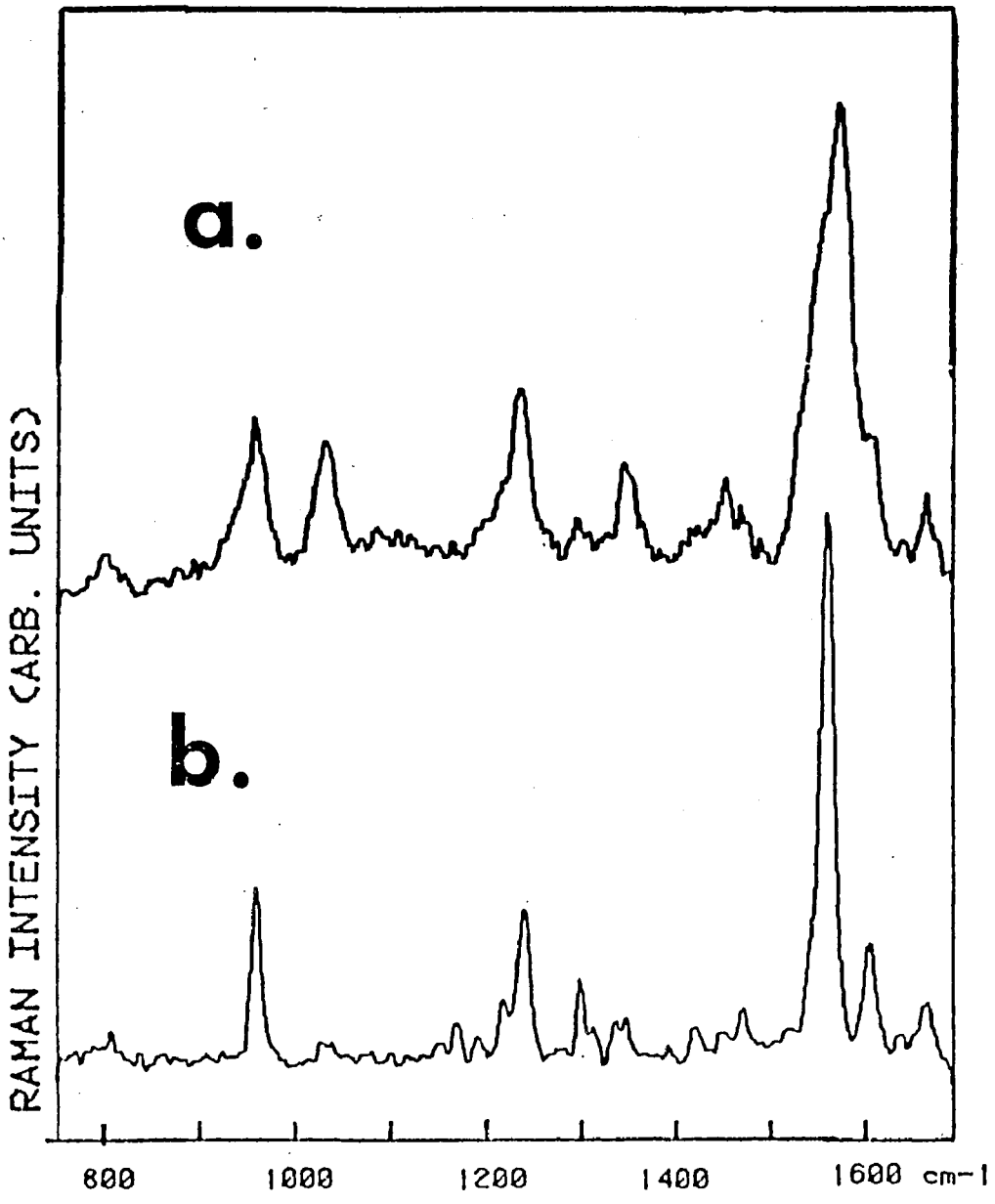
a.
b.
RAMAN INTENSITY (ARB. UNITS)
800
1000
1200
1400
1600 cm-1

spectrum is identical with the room temperature spectrum, and we strongly suspect that it will be, we will then have further proof that a cis-trans isomerization is necessary for the formation of the first photoproduct in the visual pigment - purple membrane systems.

Cyanine Dyes

In Figure 20 are the absorption spectra of a series of cyanine dyes of varying conjugated chain length. Part of the spectrum of diQ-C_2-(7) extends beyond the long wavelength limit of the spectrophotometer, but the main peak appears to occur slightly to the low energy side of 800 nm. The absorption maxima exhibit the large red-shifts with increasing chain length that are characteristic of highly delocalized π-electron systems (Brooker, 1942). The magnitude of the shifts appears to be constant for each added double bond, with the exception of the transition from the shortest chain length to the next higher one. The short molecule (C_2-1) seems to be red-shifted by about 20 nm from the position that would fit the constant linear pattern of increase. A possible explanation of this deviation will be offered below.

The cyanine dyes are highly delocalized in their ground state configurations. Thus, excitation to a higher energy level does not appreciably change the equilibrium nuclear configuration of the molecule and absorptions between the 0-0 bands occur with a high probability. This results in a small amount of vibrational progression and, consequently,

Figure 20

Absorption spectra of a homologous series of cyanine dyes. (a) diQ - C_2 - (7); (b) diQ - C_2 - (5); (c) diQ - C_2 - (3); (d) diQ - C_2 - (1). Spectrum (a) is near the long wavelength limit of the spectrophotometer and hence appears truncated. All dyes were suspended in methanol at the same concentration.

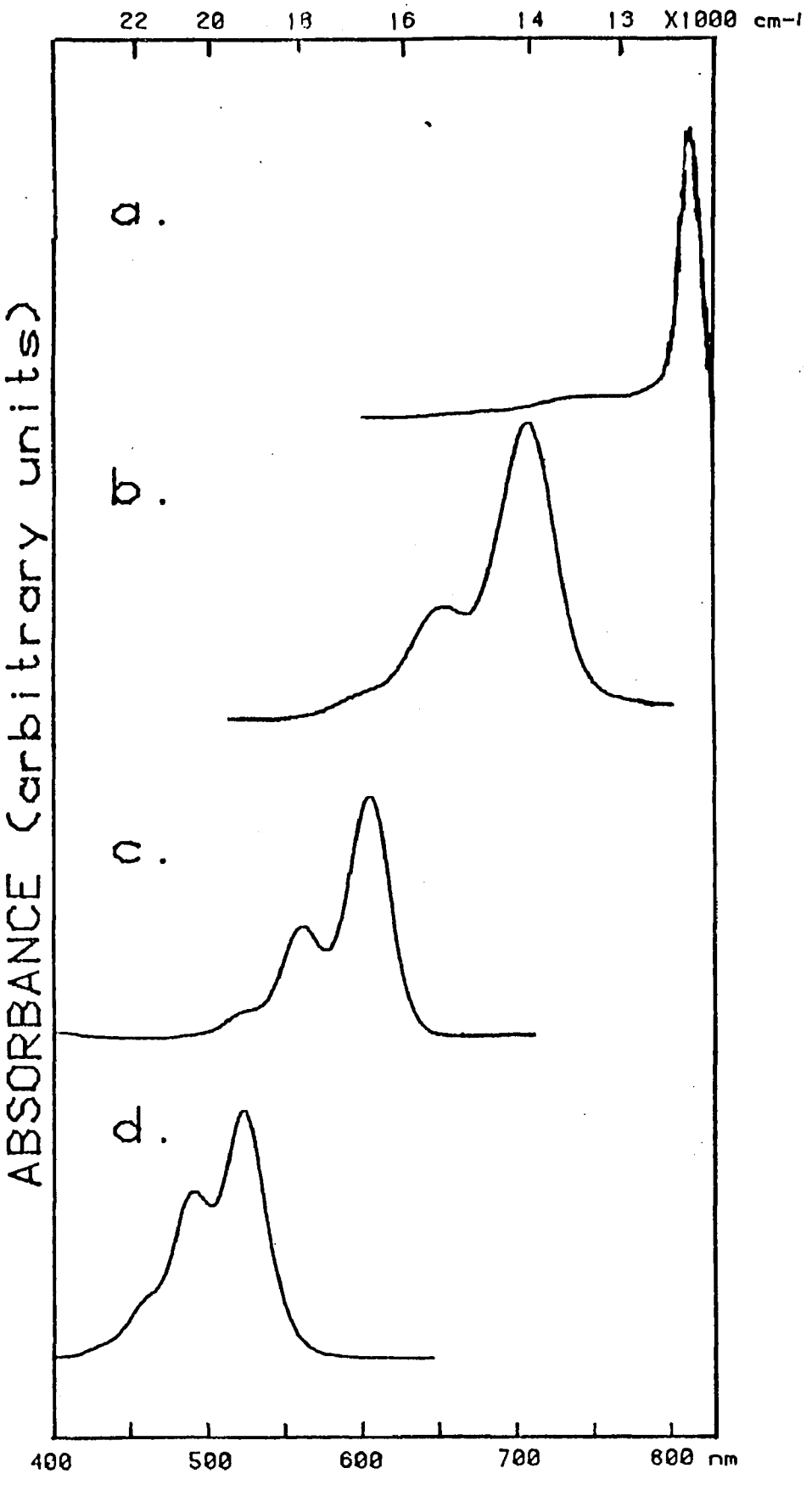
22
20
18
16
14
13
X1000 cm-1
a.
b.
c.
d.
ABSORBANCE (arbitrary units)
400
500
600
700
800 nm

a narrow absorption band (Suzuki, 1967). In Figure 20, we notice only two strong vibrational peaks in the main absorption band of each dye, and a third, weaker one towards higher energies. The secondary peak in each dye is displaced from the main band by the same amount of energy (measured in cm^{-1}). These facts imply that the extent of π-electron delocalization does not increase with chain length as it does for the visual pigments and bacteriorhodopsin (Blatz and Liebman, 1973; Greenberg et al., 1975). These latter molecules display a narrowing of their absorption bands with increasing chain length, caused by an increased π-electron delocalization which results in greater overlap of ground and excited state electronic potential curves and decreased vibrational progression in the absorption bands. Apparently, the cyanine dyes represent an extreme degree of delocalization because of the symmetry of their resonance structures, and increasing the length of the conjugated chain cannot delocalize the electrons any more. Moreover, the energy difference between the two main vibrational peaks is about 1250 cm^{-1} for each of the four dyes, confirming the extreme delocalization.

It has been observed that the absorption spectra of cyanine dyes are virtually insensitive to changes in solvent polarity (West and Geddes, 1964). Almost identical spectra were measured for this series of cyanine dyes

whether they were dissolved in water, methanol, or chloroform. Solvent effects become noticeable when a certain degree of polarity (high or low) favors one resonance structure over another. Because the resonance structures of the cyanine dyes are highly symmetrical, changes in polarity have no effect on the extent of one structure's contribution to the total wave function over another (Suzuki, 1967). Again, this is very different from the polyenes, where solvent effects have been measured (Heyde et al., 1971).

The resonance Raman spectra of these dyes are presented in Figure 21. Each spectrum is dominated by a strong line at 1360 cm^{-1}. We assign this mode to a C-C in-chain stretching vibration, since this is the mode that is most strongly coupled to the dominant $\pi - \pi^*$ transitions, by analogy with the retinals. The position of this mode between the frequencies of the C-C vibration (1200 cm^{-1}) and the C=C vibration (1600 cm^{-1}) seems to indicate that it is caused by chain vibrations of the highly hybridized single and double bonds. It should be pointed out that this line does not shift in frequency with increasing chain length and λmax, as opposed to the C=C mode of the visual pigments, which shifts considerably (see the discussion of BR analogs above). This is another indication that the π-electrons are fully delocalized. Apparently, these progressions do not change much for the various conjugated

Figure 21

Resonance Raman spectra of a homologous series of cyanine dyes, taken at room temperature. Laser lines at 530.8, 647.1, 482.5, and 647.1 nm were used to irradiate diQ - C_2 - (1), diQ - C_2 - (3), diQ - C_2 - (5), diQ - C_2 - (7), respectively. All samples were suspended in methanol at the same concentration.

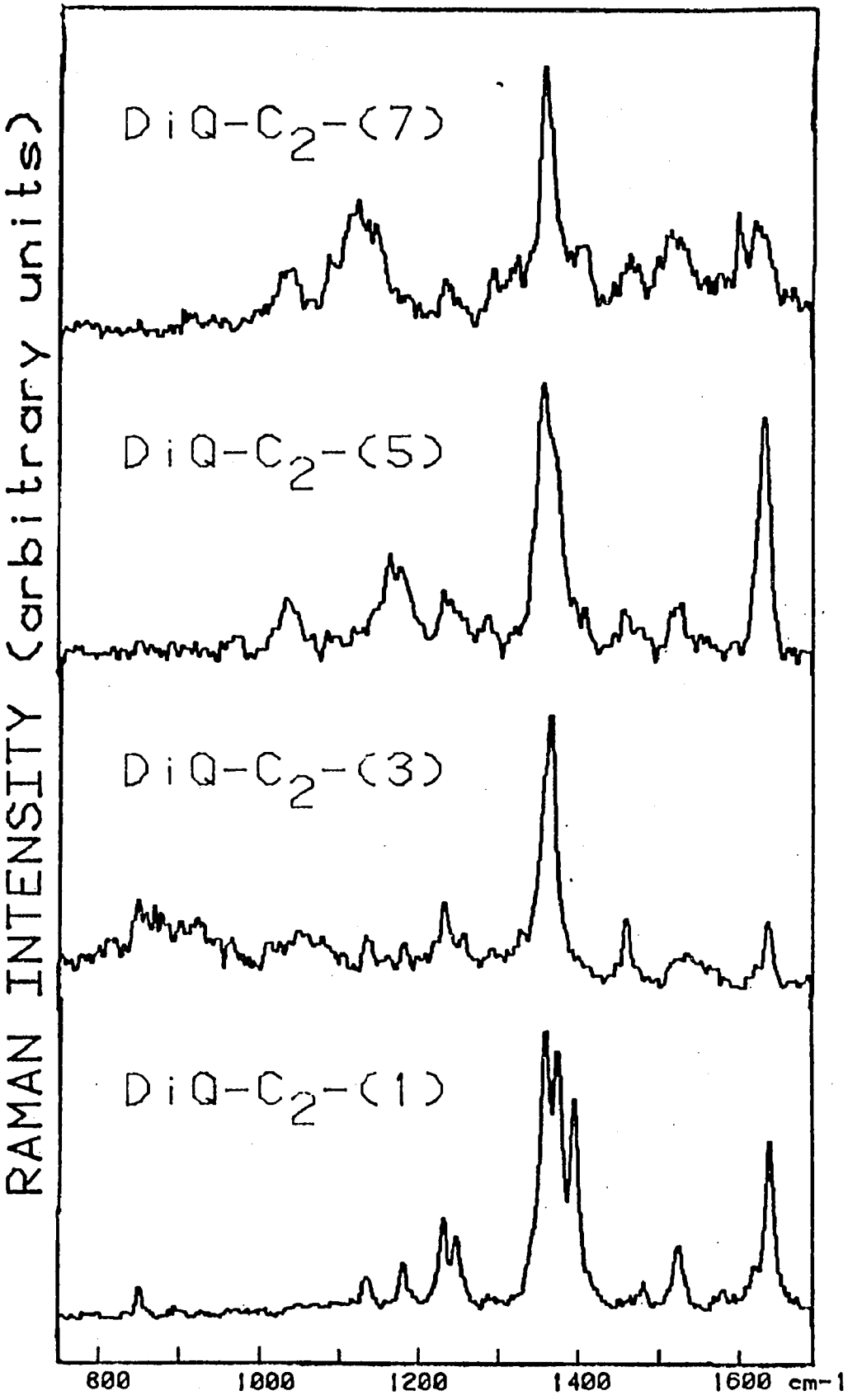
DiQ-C2-(7)
DiQ-C2-(5)
DiQ-C2-(3)
DiQ-C2-(1)
RAMAN INTENSITY (arbitrary units)
800
1000
1200
1400
1600 cm-1

chain lengths of the dyes, indicating that the degree of delocalization is not a function of the length of the polyene chain in the cyanines.

Curiously, there appears to be a splitting in the 1360 cm^{-1} line for dye C_2-(1) which is absent in the other members of the group. The closeness of the end group ring structures because of the short conjugated chain length of this dye may cause a steric hindrance to occur which is relieved by the molecule twisting about one of its bonds. This steric twisting would not only explain the splitting of the 1360 cm^{-1} line, but would also help us understand the anomalous red-shift of the λmax of this dye, alluded to above. Suzuki (1967) asserts that the twisting of a bond in a cyanine dye may very likely cause a bathochromic shift in absorption - in this case, about 20 nm. The steric effect would not occur in the other dyes because of the greater separation of the end groups.

In Fig. 22, the spectrum of C_2-(3) is compared with that of a molecule identical in all respects except that butyl groups are linked to the rings' nitrogens instead of ethyl moieties. All vibrational modes are exactly the same in both molecules, with the exception of one. The 1232 cm^{-1} line in C_2-(3) shifts down to 1218 cm^{-1} in C_4-(3). Although the counterion in each dye is different (Cl^- in C_2-(3) and I^- in C_4-(3)), this cannot be the cause of the shift because dyes C_2-(1), C_2-(5), and C_2-(7) all have an

Figure 22

Resonance Raman spectra of two homologous cyanine dyes, taken at room temperature. Laser lines at 647.1 and 530.8 nm were used to excite diQ - C_2 - (3) and diQ - C_4 - (3), respectively. Both samples were suspended in methanol at the same concentration.

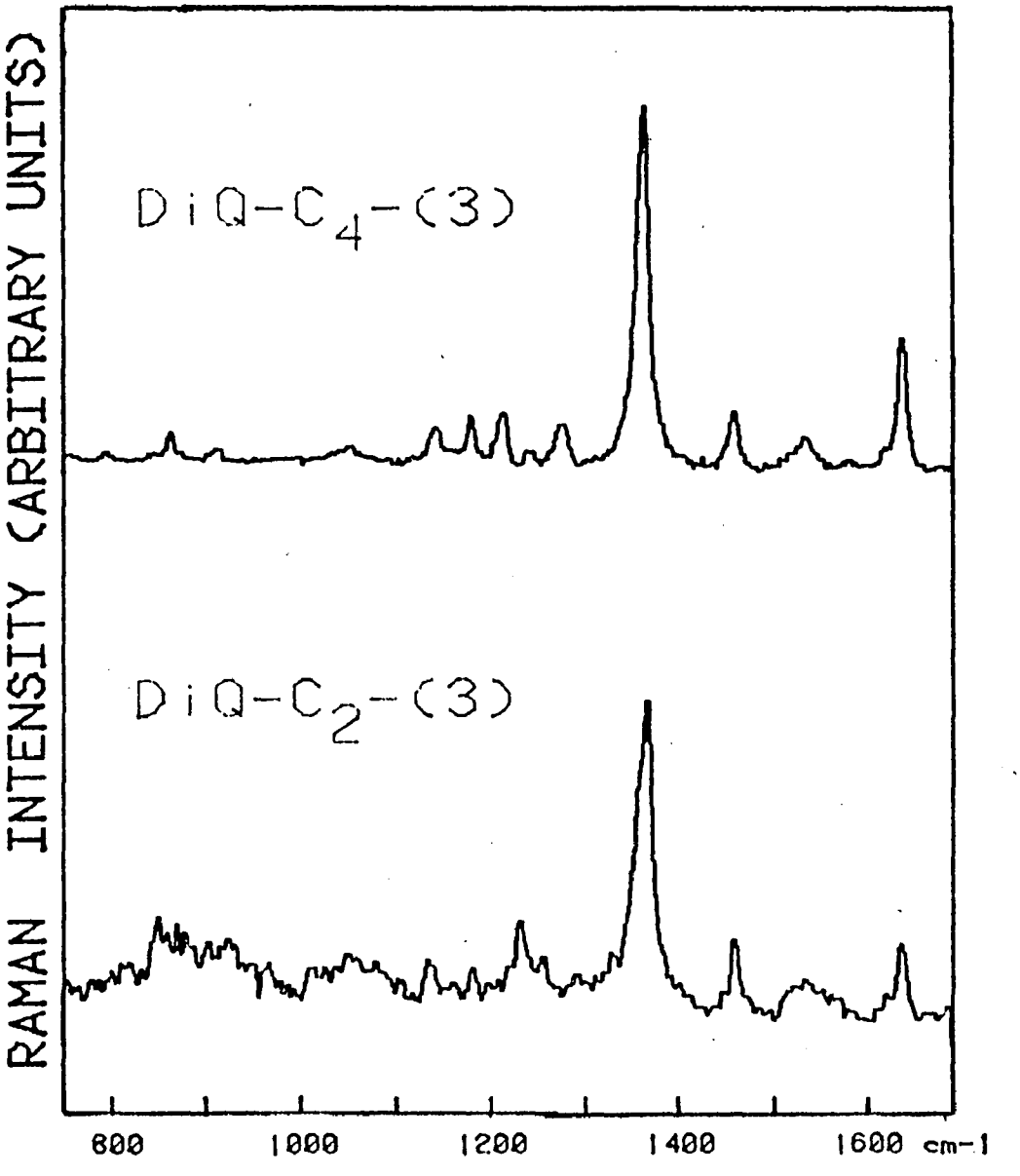
RAMAN INTENSITY (ARBITRARY UNITS)
DiQ-C4-(3)
DiQ-C2-(3)
800
1000
1200
1400
1600
cm-1

iodine counterion and all have a line at 1232 cm^{-1}. The only other possibility is that the increased mass of the butyl group of C_4-(3) affects the frequency of this band, moving it towards lower energies. This in turn suggests that a vibration associated with the ring and possibly coupled to the chain, gives rise to this mode.

The effect of the extent of π-electron delocalization on various normal modes in the resonance Raman spectrum, which can be obtained from a thorough analysis of cyanine dyes, can be incorporated into computer program models of polyene systems and enable a more accurate theoretical explanation of the vibrational frequencies of those molecules. This in turn will lead to a greater understanding of the physiological role that some of those molecules play in biological organisms.

Summary

This work has been concerned with exploring a new area-resonance Raman spectroscopy of retinal analogs and associated pigments - and the excursion has proved to be a fruitful one. The spectra of 13-desmethyl, 5,6-dihydro, 10-methyl, 10,14-dimethyl, and 14-methyl bacteriorhodopsin have been obtained and have been compared with those of their respective model compounds in solution, with that of "natural" bacteriorhodopsin, and with those of the deuterated analog pigments. We show here that π-electron delocalization is the mechanism for color regulation in these pigments. The same mechanism is responsible to a great degree for the frequency of the C=C stretch mode and the $C=NH^+$ vibration. Other influences on the latter Raman line have been discussed. The amount of shift of the protonated Schiff base vibration upon deuteration has been analyzed in terms of the results of that discussion. Theoretical work using computer models is now necessary to analyze more completely the above-mentioned results. Several line assignments in the Raman spectra of the analogs have been made and confirmation of a model which points to the existence of a counterion 3.5 Å from the ionone-ring in bacteriorhodopsin has been obtained.

The resonance Raman spectrum of the K intermediate of bacteriorhodopsin presented in this work was shown to support the hypothesis of a trans-cis isomerization as the

primary photochemical event in the purple membrane system. In addition, it was pointed out that the Schiff base of K was protonated, which would contradict a suggestion that that proton had tunneled away to form K. And an outline was presented of a Raman experiment on a rhodopsin analog that does not isomerize (the "7-membered ring analog") which would add greater weight to the isomerization model as the primary event in visual pigments.

Finally, a Raman study of a homologous series of cyanine dyes was included in this work and the relationship between the extent of π-electron delocalization and the positions of Raman bands and absorption maxima for these dyes was analyzed. The implications for polyene systems such as the visual pigments were pointed out. Further studies of cyanine dyes, both theoretical and experimental, are warranted to more fully understand the intricacies of π-electron systems.

In conclusion, it is hoped that this work has demonstrated the usefulness of analog compounds coupled with resonance Raman techniques for the study of bacteriorhodopsin and the visual pigments.

Appendix

It has been observed that the absorption maxima of cyanine dyes increase uniformly with increased length of the polymethine chain (Brooker, 1942). As will be shown here, this is a direct result of the extreme delocalization of the π-electrons on the chain, which is due to the symmetrical structure of the dyes.

In this calculation (Kuhn, 1949), we will consider the π-electron system as an electron gas. In addition, a few simplifying assumptions have to be made. First, we restrict the π-electrons so that they can move only in the direction of the chain. Secondly, we assume that the potential energy of an electron remains constant as it moves along the chain, and that the potential energy rises sharply to infinity as it comes to the ends of the chain. This means that we replace the π-electrons of the polymethine chain by electrons moving in a one-dimensional box of length L, where L is the length of the polymethine chain. In order to take the end effects of the rings attached to the chain into account, we will assume that L is measured by the length of the polymethine chain between the nitrogen atoms on the ends, plus one bond distance on either side. Use of a constant potential inside the box implies a lack of bond alternation along the chain.

With these assumptions, it is easy to solve the Schrodinger equation for the π-electrons, and to calculate the

energy values that a particular electron can assume. If we take the zero of potential energy as the constant potential energy inside the box, then Schrodinger's equation in one dimension becomes

$$-\frac{h^2}{2m}\frac{d^2\psi(x)}{dx^2} = E\,\psi(x) \qquad (1)$$

where $\psi(x)$ is the one-dimensional electronic wave function. A solution which fits the boundary conditions can easily be shown to be

$$\psi(x) = A \sin\frac{N\pi x}{L}\,, \qquad (2)$$

where N is an integer and L is the effective width of the box. The coefficient of x in the argument of the trigonometric function is related to the energy by the deBroglie equation, which yields

$$E_N = \frac{N^2 h^2}{8mL^2} \qquad (3)$$

where h is Planck's constant and m is the electron mass. Since, by the Pauli exclusion principle, at most two electrons can occupy each of the N energy levels, only the lowest N/2 levels are occupied in the ground state by N π-electrons. Absorption is associated with the jump of one electron from the highest occupied level, number N/2, to

the lowest free level, number (N/2)+1. For the energy difference between those two levels, we use Eq. (3) to obtain

$$\Delta E_1 = \frac{h^2}{8mL^2}(N+1) \tag{4}$$

To get the wavelength shift involved in such a jump we use

$$\lambda = hc/\Delta E \tag{5}$$

and obtain

$$\lambda_1 = \frac{8mc}{h}\frac{L^2}{N+1} \tag{6}$$

where C is the speed of light. For the case of a cyanine dye with j double bonds, we find that N, the number of π-electrons, is given by

$$N = 2j + 2, \tag{7}$$

since each carbon atom has one π-electron, and the two nitrogens contribute three (see Fig. 8). The effective chain length L is given by

$$L = (2j + 2)s, \tag{8}$$

where s is the length of a C-C bond with bond number 1.5.

According to Pauling, s equals 1.39×10^{-8} cm (L. Pauling, 1945). Thus for dye C_2-(3), for example, N = 8 and L = 8s. Inserting equations (7) and (8) into equation (6) and evaluating the constants yields

$$\lambda_1 = 63.7 \frac{(2j+2)^2}{2j+3} \quad \text{(nm)} \qquad (9)$$

Applying equ. (9) to the four cyanine dyes studied in this work, we obtain

C_2-(1), λmax = 329 nm

C_2-(3), λmax = 455 nm

C_2-(5), λmax = 581 nm

C_2-(7), λmax = 708 nm

These results, although quantitatively inaccurate, exhibit the constant increase in λmax with increased chain length which is experimentally observed. For a more accurate quantitative result, we must take into account the effects on the potential function of the heterogenous atoms of the chain (nitrogen and carbon).

Bibliography

Abrahamson, E. W., and Fager, R. S. (1973)
Curr. Top. Bioenerg. 5, 125.

Akita, H., Tanis, S. P., Adams, M., Balogh-Nair, V., and Nakanishi, K. (1980a)
J. Am. Chem. Soc. In press.

Akita. H., Balogh-Nair, V., Nakanishi, K., and Ebrey, T. (1980b)
J. Am. Chem. Soc. In press.

Albrecht, A.C. (1961)
J. Chem. Phys. 34, 1476.

Applebury, M. L., Peters, K. S., and Rentzepis, P. (1978)
Biophys. J. 23, 375.

Arnaboldi, M., Motto, M. G., Tsujimoto, K., Balogh-Nair, V., and Nakanishi, K. (1979)
J. Am. Chem. Soc. 101, 7082.

Aton, B., Doukas, A. G., Callender, R. H., Becher, B., and Ebrey, T. G. (1977)
Biochem. 16, 2995.

Aton, B., Callender, R. H., and Honig, B. (1978)
Nature 273, 784.

Aton, B., Doukas, A. G., Callender, R. H., Becher, B., and Ebrey, T. G. (1979)
Biochim. Biophys. Acta 576, 424.

Aton, B., Doukas, A. G., Narva, D., Callender, R. H., Dinur, U., and Honig, B. (1980)
Biophys. J. 29, 79.

Azuma, M., Azuma, K., and Kito, Y. (1973)
Biochem. Biophys. Acta. 295, 520.

Becher, B., and Cassim, Y. (1975)
Prep. Biochem. 5, 161.

Becher, B., and Ebrey, T. G. (1977)
Biophys. J. 17, 185.

Blasie, J. K., Dewey, M. M., Blaurock, A. E., and Worthington, C. R., (1965)
J. Mol. Biol. 14, 143.

Blasie, J. K., and Worthington, C. R. (1969)
J. Mol. Biol. 39, 417.

Blatz, P. E., Dewhurst, P. B., Balasubramaniyan, V., and Balasubramaniyan, P. (1968)
Nature 219, 169.

Blatz, P., Lin, M., Balasubramaniyan, P., Balasubramaniyan, V., and Dewhurst, P. B. (1969)
J. Am. Chem. Soc. 91, 5930.

Blatz, P., Dewhurst, P. B., Balasubramaniyan, V., Balasubramaniyan, P., and Lin, M. (1970)
Photochem. Photobiol 11, 1.

Blatz, P. E. (1972)
Photochem. Photobiol. 15, 1.

Blatz, P. E., and Mohler, J. H. (1972)
Biochem. 11, 3240.

Blatz, P. E., Mohler, J. H., and Navangul, H. V. (1972)
Biochem. 11, 848.

Blatz, P., and Liebman, P. (1973)
Exp. Eye Res. 17, 573.

Blaurock, A., and Stoeckenius, W. (1971)
Nature (New Biol.) 233, 152.

Bogomolni, R. A., Stubbs, L., and Lanyi, J. K. (1978)
Biochem. 17, 1037.

Bridges, C. D. B. (1970)
In Biochemistry of the Eye, pp. 563-644., Graymore, ed. Academic Press, London, N. Y.

Brooker, L. G. S. (1942)
Rev. Mod. Phys. 14, 275.

Brown, P. K. (1972)
Nature (New Biol.) 236, 35.

Busch, G. E., Applebury, M. L., Lamola, A. A., and Rentzepis, P. M. (1972)
Proc. Natl. Acad. Sci. (U.S.A.) 69, 2802.

Callender, R. H., Doukas, A., Crouch, R., and Nakanishi, K. (1976)
Biochem. 15, 1621.

Callender, R. H., and Honig, B. (1977)
Ann. Rev. Biophys. Bioeng., 6, 33.

Campion, A., El-Sayed, M. A., and Terner, J. (1977)
Biophys. J. 20, 369.

Cassim, J. Y. (1980)
Photochem. Photobiol. In press.

Chan, W. K., Nakanishi, K., Ebrey, T., and Honig, B. (1974)
J. Am. Chem. Soc. 96, 3642.

Cone, R. A. (1972)
Nature (New Biol.) 236, 39.

Cookingham, R., and Lewis, A. (1978)
J. Mol. Biol. 119, 569.

Danon, A., and Stoeckenius, W. (1974)
Proc. Natl. Acad. Sci. (U.S.A.) 71, 1234.

Dartnall, H. J. A. (1972)
In Handbook of Sensory Physiology, Vol. VII/1, 122-145.

Denny, M. and Liu, R. S. H. (1977)
J. Am. Chem. Soc. 99, 4865.

Doukas, A.G. (1977)
Ph.D. Thesis, City Univ. of N.Y.

Doukas, A.G., Aton, B., Callender, R.H., and Honig, B. (1978a)
Chem. Phys. Lett. 56, 248.

Doukas, A. G., Aton, B., Callender, R. H., and Ebrey, T. G. (1978b)
Biochem. 17, 2430.

Ebrey, T. G., Govindjee, R., Honig, B., Pollock, E., Chan, W., Crouch, R., Yudd, A., and Nakanishi, K. (1975)
Biochem. 14, 3933.

Ebrey, T., and Honig, B. (1977)
Vis. Res. 17, 147.

Erickson, J. O., and Blatz, P. E. (1968)
Vision Res. 8, 1367.

Eyring, G., and Mathies, R. (1979)
Proc. Natl. Acad. Sci. (U.S.A.) 76, 33.

Eyring, G., Curry, B., Mathies, R., Broek, A., and Lugtenberg, J. (1980)
J. Am. Chem. Soc., In press.

Eyring, G., Curry, B., Mathies, R., Fransen, R., Palings, I., and Lugtenburg, J. (1980)
Proc. Natl. Acad. Sci. (U.S.A.), In press.

Fransen, M. R., Luyten, W. C. M. M., van Thuijl, J., Lugtenburg, J., Jansen, P. A. A., van Breugel, P. J. G., and Daemen, F. J. M. (1976)
Nature 260, 726.

Green, B. H., Monger, T. G., Alfano, R. R., Aton, B., and Callender, R. H. (1977)
Nature 269, 179.

Greenberg, A. D., Honig, B., and Ebrey, T. G. (1975)
Nature 257, 823.

Hamanaka, T., Mitsui, T., Ashida, T., and Kakudo, M. (1972)
Acata Cryst B28, 214.

Hamer, F. M. (1964)
The Cyanine Dyes and Related Compounds, John Wiley and Sons, N.Y.

Henderson, R. (1975)
J. Mol. Biol. 93, 123.

Henderson, R., and Unwin, P.N.T. (1975)
Nature 257, 28.

Henderson, R. (1977)
Ann. Rev. Biophys. Bioeng. 6, 87.

Hess, B., and Kuschmitz, D. (1979)
FEBS. Lett. 100, 334.

Heyde, M. E., Gill, D., Kilponen, R. G., and Rimai, L. (1971)
J. Am. Chem. Soc. 93, 6776.

Honig, B., and Ebrey, T. G. (1974)
Ann. Rev. Biophys. Bioeng. 3, 151.

Honig, B., Greenberg, A. D., Dinur, U., and Ebrey, T. G. (1976)
Biochem. 15, 4593.

Honig, B., Ebrey, T., Callender, R. H., Dinur, U., and Ottolenghi, M. (1979)
Proc. Natl. Acad. Sci. (U.S.A.) 76, 2503.

Honig, B., and Ottolenghi, M. (1980)
Photochem. Photobiol. In press.

Hubbard, R., and Kropf, A. (1958)
Proc. Natl. Acad. Sci. (U.S.A.) 44, 130.

Hubbard, R., Brown, P. K., and Kropf, A. (1959)
Nature 183, 442.

Hubbard, R., and Kropf, A. (1965)
J. Gen. Physiol. 49, 381.

Hubbard, R., Bownds, D., and Yoshizawa, T. (1965)
Cold Spring Harbor Symposia on Quantitative Biology 30, 301.

Hubbard, R., Brown, P. K., and Bownds, D. (1971)
"Methodology of Vitamin A and Visual Pigments", in Methods in Enzymology, V. 18, Vitamins and Coenzymes, Part C, p. 615. McCormick and Wright, eds., Academic Press, N. Y.

Hurley, J., Ebrey, T., Honig, B., and Ottolenghi, M. (1977)
Nature 270, 540.

Hurley, J., Becker, B., and Ebrey, T. G. (1978)
Nature 272, 87.

Inagaki, F., Tasumi, M., and Miyazawa, T. (1974)
J. Mol. Spectry. 50, 286.

Ippen, E. P., Shank, C. V., Lewis, A., and Marcus, M. A. (1978)
Science 200, 1279.

Irving, C. S., Byers, G. W., and Leermakers, P. A. (1970)
Biochem. 9, 858.

Iwasa, T., Tokunaga, F., Yoshizawa, T., and Ebrey, T. G. (1980)
Photochem. Photobiol. 31, 83.

Kakitani, T., and Kakitani, H. (1975)
J. Phys. Soc. (Japan) 38, 1455.

Kelly, M., and Liaaen-Jensen, S. (1967)
Acta Chem. Scand. 21, 2578.

Khorana, H.G., Gerber, G.E., Herlihy, W.C., Grey, C.P., Anderegg, R.J., Nihei, K., and Biemann, K. (1979)
Proc. Natl. Acad. Sci. (U.S.A.) 76, 5046.

Kropf, A., and Hubbard, R. (1958)
Ann. N. Y. Acad. Sci. 74, 226.

Kropf, A., Whittenberger, B. P., Goff, S. P., and Waggoner, A. S. (1973)
Exp. Eye Res. 17, 591.

Kuhn, H. (1969)
J. Chem. Phys. 17, 1198.

Lanyi, J. (1980)
Photochem. Photobiol. In press.

Larsen, H. (1967)
Adv. Microbiol., 1, 97.

Lewin, D. R., and Thomson, J. N. (1967)
Biochem. J. 103, 36P.

Lewis, A., Fager, R. S., and Abrahamson, E. W. (1973)
J. Raman Spectr. 1, 145.

Lewis, A., Spoonhower, J., Bogolmolni, R. A., Lozier, R. H., and Stoeckenius, W. (1974)
Proc. Natl. Acad. Sci. (U.S.A.) 71, 4462.

Lewis, A. (1978)
Proc. Natl. Acad. Sci. (U.S.A.) 75, 549.

Lewis, A., Marcus, M.A., Ehrenberg, B., and Crespi, H. (1978)
Proc. Natl. Acad. Sci. (U.S.A.) 75, 4642.

Lindley, E. V., and MacDonald, R. E. (1979)
Biochem. Biophys. Res. Comm. 88, 491.

Lozier, R. H., Bogomolni, R. A., and Stoeckenius, W. (1975)
Biophys. J. 15, 955.

Maeda, A., Iwasa, T., and Yoshizawa, T. (1977)
J. Biochem. 82, 1599.

Maeda, A., Iwasa, T., and Yoshizawa, T. (1980)
Photochem. Photobiol. In press.

Mao, B., Ebrey, T. G., and Crouch, R. (1980)
Biophys. J. 29, 247.

Marcus, M. A., and Lewis, A. (1977)
Science 195, 1328.

Mathies, R., Oseroff, A. R., and Stryer, L. (1976)
Proc. Natl. Acad. Sci. (U.S.A.) 73, 1.

Mathies, R., Freedman, T. B., Stryer, L. (1977)
J. Mol. Biol. 109, 367.

Mathies, R. (1979)
In Chemical and Biological Applications of Lasers, C. B. Moore, ed., vol. IV, p. 55, Academic Press, N. Y.

Matsumoto, H., and Yoshizawa, T. (1975)
Nature 258, 523.

Mendelsohn, R. (1976)
Biochim. Biophys. Acta 427, 295.

Monger, T. G., Alfano, R. R., and Callender, R. H. (1979)
Biophys. J. 27, 105.

Muccio, D. D., and Cassim, J. Y. (1979)
Biophys. J. 26, 427.

Nakanishi, K., Balogh-Nair, V., Gawinowicz, M. A., Motto, M., and Honig, B. (1979)
Photochem. Photobiol. 29, 657.

Nakanishi, K., Balogh-Nair, V., Arnaboldi, M., Sujimoto, K., and Honig, B. (1980)
J. Am. Chem. Soc., In press.

Narva, D., and Callender, R. H. (1980)
Photochem. Photobiol., In press.

Nelson, R., deRiel, J. K., and Kropf, A. (1970)
Proc. Natl. Acad. Sci. (U.S.A.) 66, 531.

Oesterhelt, D. (1971)
Abst. Comm. 7th meet. Eur. Biochem. Soc. #517.

Oesterhelt, D., and Stoeckenius, W. (1971)
Nature (New Biol.) 233, 149.

Oesterhelt, D. (1972)
Hoppe-Seyler's Z. Physiol. Chem. 353, 1554.

Oesterhelt, D., and Hess, B. (1973)
Eur. J. Biochem. 37, 316.

Oesterhelt, D., Meentzen, M., and Schuhmann, L. (1973)
Eur. J. Biochem. 40, 453.

Oesterhelt, D., and Stoeckenius, W. (1973)
Proc. Natl. Acad. Sci. (U.S.A.) 70, 2853.

Oesterhelt, D., and Schuhmann, L. (1974)
FEBS. Lett. 44, 262.

Oesterhelt, D., Schuhmann, L., and Gruber, H. (1974)
FEBS. Lett. 44, 257.

Oesterhelt, D., and Stoeckenius, W. (1974)
Methods Enzymol. 31, 667.

Ohno, K., Takeuchi, Y., and Yoshida, M. (1977)
Biochim. Biophys. Acta 462, 575.

Oseroff, A. R., and Callender, R. H. (1974)
Biochem. 13, 4243.

Ovchinnikov, Yu. A., Abdulaev, N. G., Feigina, Yu. M.,
Kisiler, A. V., and Lobanov, N. A. (1977)
FEBS Lett. 84, 1.

Ovchinnikov, Yu. A., Abdulaev, N. G., Feigina, Yu. M.,
Kisiler, A. V., and Lobanov, N. A. (1979)
FEBS Lett. 97, 15.

Ovchinnikov, Yu. A., Abdulaev, N. G., Feigina, Yu. M.,
Kisiler, A. V., and Lobanov, N. A. (1979)
FEBS Lett. 100, 219.

Papermaster, D. S., and Dryer, W. J. (1974)
Biochem. 13, 2438.

Parson, W., and Ort, D. (1980)
Photochem. Photobiol. In press.

Patel, D. (1969)
Nature 221, 825.

Pauling, L. (1945)
The Nature of the Chemical Bond, Cornell Univ. Press,
Ithaca, N.Y., second edition.

Peters, K., Applebury, M., and Rentzepis, P. (1977)
Proc. Natl. Acad. Sci. (U.S.A.) 74, 3119.

Peticolas, W.L., Nafie, L., Stein, R., and Fanconi, B.
(1970)
J. Chem. Phys. 52, 1576.

Pettei, M. J., Yudd, A. P., Nakanishi, K., Henselman, R., and Stoeckenius, W. (1977)
Biochem. 16, 1955.

Placzek, G. (1934)
Handbach der Radiologie, E. Marx, ed. Vol. 2, pages 309-374. "Rayleigh and Raman Scattering" UCRL translation #526L.

Poo, M., and Cone, R. A. (1974)
Nature 247, 438.

Radda, G. K., and Vanderkooi, J. (1972)
Biochim. Biophys. Acta 265, 509.

Raman, C.V., and Krishnan, K.S. (1928)
Nature 121, 501.

Rimai, L., Gill, D., and Parsons, J. L. (1971)
J. Am. Chem. Soc. 93, 1353.

Rimai, L., Heyde, M. E., and Gill, D. (1973)
J. Am. Chem. Soc. 95, 4493.

Robertson, J. D. (1966)
N. Y. Ann. Sci. 137, 421.

Rosenfeld, T., Honig, B., Ottolenghi, M., Hurley, J., Ebrey, T. G. (1977)
Pure Appl. Chem. 49, 341.

Salem, L. (1966)
Molecular Orbital Theory of Conjugated Systems, W. A. Benjamin, Inc., Reading, Mass., Chapter 8.

Schreckenbach, T., Walckhoff, B., and Oesterhelt, D. (1978)
J. Am. Chem. Soc. 17, 5353.

Schulten, K., and Schulten, Z. (1980)
Photochem. Photobiol. In press.

Smekal, A. (1923)
Naturwissenschaften 11, 873.

Sperling, W. Carl, P., Rafferty, Ch. N., and Dencher, N. A. (1977)
Biophys. Struct. Mech. 3, 79.

Stoeckenius, W., and Kunau, W.H. (1968)
J. Cell Biol. 38, 337.

Stoeckenius, W., Lozier, R.H., and Bogomolni, R.A. (1979)
Biochim. Biophys. Acta 505, 215.

Stoeckenius, W., Casadio, R., and Hwang, S. -B. (1980)
Photochem. Photobiol. In press.

Suzuki, H. (1967)
Electronic Absorption Spectra and Geometry of Organic Molecules, Academic Press, N.Y., Chapters 12 and 17.

Suzuki, H., Komatsu, T., and Kitajima, H. (1974)
J. Phys. Soc. (Japan) 37, 177.

Tang, J., and Albrecht, A.C. (1970)
in Raman Spectroscopy, vol. II, pp. 33-68, H.A. Szymanski, ed., Plenum Press N.Y.

Tanis, S. P., Brown, R. H., and Nakanishi, K. (1978)
Tetrahedron Lett. 10, 869.

Terner, J., Hsieh, C.-L., Burns, A.R., and El-Sayed, M.A. (1979)
Proc. Natl. Acad. Sci. (U.S.A.) 76, 3046.

Tokunaga, F., Govindjee, R., Ebrey, T. G., Crouch, R. (1977)
Biophys. J. 19, 191.

Tokunaga, F., and Ebrey, T. (1978)
Biochem 17, 1915.

Tokunaga, F., Ebrey, T., and Crouch, R. (1980)
Photochem. Photobiol. In press.

Tsuda, M., Glaccum, M., Nelson, B., and Ebrey, T. G. (1980)
Photochem. Photobiol. In press.

Tsuda, M. and Ebrey, T. G. (1980)
Biophys. J. 30, 149.

Van den Tempel, P. J., and Huisman, H. O. (1966)
Tetrahedron 22, 293.

Van Vleck, J.H. (1929)
Proc. Natl. Acad. Sci. (U.S.A.) 15, 754.

Waddell, W. H., Uemura, M., and West, J. L. (1978)
Tetrahedron Lett. 35, 3223.

Waggoner, A. (1976)
J. Membrane Biol. 27, 317.

Wald, G. (1968)
Science 162, 230.

Waleh, A., and Ingraham, L. L. (1973)
Arch. Biochem. Biophys. 156, 261.

Warshel, A., and Karplus, M. (1972)
J. Am. Chem. Soc. 94, 5612.

Warshel, A. (1973)
Israel J. Chem. 11, 709.

Warshel, A., and Karplus, M. (1974)
J. Am. Chem. Soc. 96, 5677.

Warshel, A. (1976)
Nature 260, 679.

Warshel, A. (1977)
Ann. Rev. Biophys. Bioeng. 6, 273.

West, W., and Geddes, A. L. (1964)
J. Phys. Chem. 68, 837.

Wiesenfeld, J. R., and Abrahamson, E. W. (1968)
Photochem. Photobiol. 8, 487.

Worthington, C. R. (1974)
Ann. Rev. Biophys. Bioeng. 3, 53.

Wu, C. W., and Stryer, L. (1972)
Proc. Natl. Acad. Sci. (U.S.A.) 69, 1104.

Yoshizawa, T., and Wald, G. (1963)
Nature 197, 1279.